

Universität für Bodenkultur Wien
University of Natural Resources and Life Sciences, Vienna

Department of Water, Atmosphere and Environment
Institute of Sanitary Engineering and Water Pollution Control



Assessment of the water quality by means of fouling indexes.

**Master thesis
In partial fulfilment of the requirements
for the degree, of
Diplomingenieur**

Submitted by:
ERDENE, NOMUNDARI

Supervisor: Ao.Univ. Prof.Dipl.-Ing. Dr. Fürhacker, Maria
Co-Supervisor: Ing. Ph.D. Svehla, Pavel

Student number 1541839

Acknowledgements.

This master thesis was accomplished at the Institute of Sanitary Engineering and Water Pollution Control, University of Natural Resources and Life Sciences, Vienna, under the supervision of Ao.Univ.Prof. Dipl.-Ing. Dr. Maria Fürhacker and co-supervision of Ing. Pavel Švehla, Ph. D.

Foremost, I would like to express my sincere gratitude to Prof. Fürhacker for her profound support throughout the whole thesis process, for her patience and motivation. She encouraged me to be creative, but she was always available for guiding me in the right direction when I needed to be. Thanks to her, I have had learned the most, throughout my whole master's study.

I would like to thank WTG and Mr. Ramharter for the support and the supply of the equipment and materials. I have had very comfortable environment to work on.

Also, USF and Mr. Walter Lintner for contributing with the possibility to work on INSPECTOR apparatus.

Lastly, I would like to thank the whole staff of the Institute of Sanitary Engineering and Water Pollution Control and the technical hall of the University.

Table of contents

1. Introduction.....3

2. Objective.....5

3. Fundamentals and literature review.....5

 3.1 Reverse osmosis membrane system literature review.....5

 3.1.1 General attributes of membrane separation system.....5

 3.1.2 Principles of reverse osmosis system.....5

 3.1.3 Pesticide filtration by means of membrane system.....11

 3.2 Fouling types and their characteristics.....19

 3.3.1 Standard measurement of SDI and MFI.....24

 3.3.2 Parameters affecting the MFI and SDI values.....28

 3.3.3 Alternative indexes that have derived from SDI and MFI.30

4. Materials and methods.....35

 4.1 Reverse osmosis pilot plant unit.....35

 4.2 Microcontroller Arduino.....37

 4.3 SDI and MFI measurement.....41

 4.3.1 INSPECTOR apparatus from Convergence Ltd.....44

 4.4 Sample preparation.....47

 4.4.1 SDI and MFI measurement.....47

 4.4.2 Reverse osmosis trial samples.....49

5. Statistics and calculation.....53

6. Results and discussion.....56

 6.1 Calculation of MFI.....56

 6.2 Dilution series.....58

 6.3 SDI15 and MFI values.....60

 6.3.2 SDI2, SDI5, SDI10, SDI15 and MFI.....62

 6.3.3 Values obtained from the filters with different pore sizes.....64

 6.3.4 Relations of the indexes with the water quality parameters.....66

 6.3.5 INSPECTOR apparatus results.....69

6.3.6 Comparison of INSPECTOR and BOKU Instrument values.....	72
6.4 Reverse osmosis membrane experiments.....	79
6.4.1 Reverse osmosis water trial without pressure modification.....	79
6.4.2 Deviation of the pressure valve.....	81
6.4.3 Samples with different concentration.....	84
6.4.3 Rejection of pesticide, fertilizers and heavy metal.....	91
6.4.5 Experiment with the biocide.....	96
7. Conclusion and outlook.....	99
7.1 MFI and SDI.....	99
7.2 Reverse osmosis membrane system experiment.....	100
8. Summary.....	101
9. List of Tables.....	105
10. List of Figures.....	106
11. Literature.....	107
12. Appendix.....	111
13. Curriculum Vitae.....	133
14. Affirmation.....	134

Abstract

Silt density index and modified fouling index are extensively employed as a fouling indication in membrane systems. However, there are several disadvantages in terms of reliability and accuracy. The exact relation between two indexes and other water quality parameters is still uncertain. The results from different measuring instruments show incomparable results. Lastly, it is under question whether the indexes can accurately predict the membrane system performance. The objective of this master thesis is to compare the MFI and SDI values with each other and with other water quality parameters and to assess performance and the chemical removal rates in a reverse osmosis pilot plant.

For this a reverse osmosis membrane pilot plant was constructed to run experiments with different water matrices, where pollutant removal rates are examined for Zn, Cu, diurone, atrazine and nitrate. In addition, experiments were conducted with a biocide. SDI and MFI measuring unit was arranged at BOKU and compared with the INSPECTOR apparatus.

Calculation of the MFI from the BOKU instrument, show that the system requires at least 45 seconds to reach the cake filtration. SDI15 values are on average 1.7 times higher than the MFI values. Experiments with filters with different pore sizes approve that the main mechanism of the filtration process is size exclusion. SDI and MFI have high correlation to turbidity, conductivity and TDS. The comparison of MFI generated from 2 different instruments show statistically significant differences ($p=0.28$). The removal rate of the pollutants is not lower than 87%. Rejection rate is highest for the heavy metals ($>98.9\%$). The biocide efficiency depends on the fouling of the membrane. The new membrane has higher efficiency (99.5%) than old membrane (88%) in terms of live microbial cells.

Kurzfassung

Silt-Density-Index und Modified-Fouling-Index werden in Membransystemen häufig als Verschmutzungsindikatoren eingesetzt. Sie weisen jedoch einige Nachteile hinsichtlich der Zuverlässigkeit und Genauigkeit auf. Die genaue Beziehung zwischen den zwei Indizes und anderen Wasserqualitätsparametern ist unsicher. Die Ergebnisse aus verschiedenen Quellen zeigen nicht vergleichbare Ergebnisse. Es ist fraglich, ob die Indizes die Leistungsfähigkeit des Membransystems genau vorhersagen können. Ziel dieser Masterarbeit ist es, SDI und MFI miteinander und mit anderen Wasserqualitätsparametern zu vergleichen und die Performance und chemische Entfernungsraten der Membranen zu bewerten.

Dafür wurden Experimente mit einer Umkehrosiose-Pilotanlage mit verschiedenen Wassermatrizen durchgeführt, in dem die Schadstoffentfernungsraten für Zn, Cu, Diuron, Atrazin und Nitrat und der Einfluss eines Biozids untersucht wurden. Zusätzlich wurde eine Messeinheit für die SDI und MFI-Messung von der BOKU aufgebaut und mit dem INSPECTOR verglichen. Es wurden auch Versuche mit Filtern unterschiedlicher Porengröße durchgeführt.

Die Berechnung des MFI durch das BOKU-Instrument zeigt, dass das System mindestens 45 s benötigt, um die Kuchenfiltration zu erreichen. Im Durchschnitt sind die SDI15-Werte 1,7-fach höher als die MFI-Werte. Die Experimente mit Filtern mit unterschiedlichen Porengrößen zeigen, dass der Hauptmechanismus des Filtrationsprozesses der Größenausschluss ist. Verschmutzungsindizes weisen eine hohe Korrelation zu Trübung, Leitfähigkeit und TDS auf. Der Vergleich des MFI aus zwei verschiedenen Instrumenten zeigt einen statistisch signifikanten Unterschied ($p=0,28$). Die Schadstoffentfernungsraten lag über 87%. Die Rückweisungsrate war bei den Schwermetallen am höchsten ($>98,9\%$). Die Biozideffizienz hängt von der Verschmutzung der Membran ab. Die neue Membran hat eine höhere Effizienz (99,5%) als die alte Membran (88%) in Bezug auf lebende mikrobielle Zellen.

1. Introduction

With its simple procedural concept and high production efficiency, filtration systems, such as reverse osmosis (RO), are one of the best options for production of clean water. Further applications include an industrial process such as high concentration syrup production. The very first commercially available RO membranes were introduced by Film Tec Corp. in mid-1970's with flow rate production of 4000 gallons per day (gpd) and a salt rejection of 99.4% (Nguyen et al, 2018). High demand for utilization imposes a need for a constant improvement of the system in terms of design and technology. Reverse osmosis membrane is expensive and energy intensive technology, in which improvements had to be done not only in terms of cost efficiency but also in reduction of carbon footprints. Ever since number of fundamental developments have been implemented throughout the evolution of RO membranes, such as full automation and material improvements. The latest break-through in the development of the membrane technology is introduction of measurement technique of the elasticity and stiffness of the membrane. Despite these improvements, the biggest hindrance to the efficiency of the RO systems remain fouling phenomena of the membrane.

Fouling can be categorized as scaling with inorganic compounds, colloidal fouling, organic fouling and biofouling with microbial cells and extracellular polymeric substances. Each fouling type has its own distinctive characteristics of formation and deterioration of the membrane surface. Fouling causes decrease in recovery rates and the increase of osmotic pressure. As a result, the flow pattern gets disturbed. To keep the constant flux, the operation requires higher pressure. Moreover, deposition of the particles, colloids and organic substances create an optimal environment for the microorganisms to grow and develop biofouling. The acidic by-products of microbial nutrient exchange accumulate at the membrane surface, as a result it causes the membrane to biodegrade, making biofouling the most difficult fouling type to be removed.

Predicting the fouling potential of the feed would save much money and time since it will help to identify/specify the maximum permissible quality of the feed also pretreatment and membrane types to use for specific feed. For the prediction of the fouling potential, silt density index (SDI) was introduced by Du Pont in 1970's with intention to tackle the problem of only colloidal and particulate fouling. The procedure of measuring the SDI is straightforward and cheap. However, there are several drawbacks for this index: there is no correction for the inlet temperature, it is not based on the filtration mechanism, the membrane permeability has too much effect on the generated values, and most importantly there is no linear correlation to the particle concentration present in test water. The filtration mechanism was found out to be much more complex.

Modified fouling index (MFI) was introduced to overcome the SDI disadvantages. MFI is based on the filtration mechanism, takes into account temperature (viscosity) and filter surface diameter corrections and it has a linear correlation to the particulate matter present in test water.

The fouling indexes, especially MFI is a very sensitive index, in which the pressure and the duration of the filtration has to be documented precisely. Smallest inaccuracy results in often erratic results. Moreover, studies show that the indexes generated from different sources deviate resulting in incomparable values. There are constant improvements in the precision of the calculation and derivation of the values, however the standardization of the calculation is still needing to be updated.

Introduction

Moreover, clear correlation of MFI and SDI to the water quality parameters, such as conductivity, turbidity and salinity etc., are still one of the biggest questions. Lastly, the standard methodology/technique to derive MFI and SDI does not fully reflect the membrane filtration mechanism, thus it is uncertain in which extent the indexes would accurately predict the fouling.

2. Objective

The objective of this master thesis is to cover above-mentioned issues. In order to do so, the MFI and SDI measurement unit was arranged (in which the INSPECTOR apparatus was introduced in the end of the experiment, in order to compare the index values from different sources), apart from reverse osmosis pilot plant construction.

Following the objectives are specified:

- Specification of the calculation methodology of MFI derived from the instrument from the BOKU technical hall and investigate which parameters have the highest effect on the deviation of MFI values.
- Comparison of standard SDI and MFI values (MFI and SDI to be calculated in succession to American Society for Testing and Materials).
- Comparison of fouling indexes derived from filters with different pore sizes.
- Determination of the relations of the water quality parameters and fouling indexes.
- Comparison of the fouling indexes derived from the BOKU measurement equipment and INSPECTOR apparatus.
- Determination of the parameters, which are causing the difference in the fouling index values derived from different sources.
- Assess whether the fouling indexes depict the reverse osmosis operation flux decline rate.
- Investigation of the chemical removal efficiency of the reverse osmosis membrane.

3. Fundamentals and literature review

3.1 Reverse osmosis membrane system literature studies

This section will provide the study of the key processes that regulate the reverse osmosis filtration system, which cover the chemical, physical and hydrodynamic characteristics. Moreover, literature study comparison of recent experimental studies of reverse osmosis membrane under variety of water matrices will also be covered. As nutrients, heavy metals and pesticides inlets were investigated in this master thesis work, the overview is covering the studies with above mentioned chemicals.

3.1.1 General attributes of the membrane separation system

Reverse osmosis membrane technologies can be dated back to late 1700's. French physicist Jean-Antoine Nollet used pig bladder to illustrate the process. However, the method was almost forgotten until 1950's when University of California studied the desalination efficiency of the semi-permeable membranes (Glatter, 1998). The system was not commercially available until the 1970's.

Membrane modules can be recognized in two basic configurations: self-contained and open immersed. Most commonly utilized type is self-contained where the membrane is placed inside the housing. This module can be categorized as: pleated flat sheet membrane (microfiltration system), spiral wound flat sheet membrane, tubular membrane and, hollow fiber membrane (reverse osmosis membrane and ultrafiltration systems). Open immersed modules are inserted into the feed with the membrane being exposed to the feed.

Tubular and pleated flat sheet membranes are largely replaced because of their high cost of the operation. Hollow fiber membranes are mostly used for the ultrafiltration and microfiltration systems. Spiral wound flat sheet membranes are most accepted membrane module for the reverse osmosis system as it has a high packing density, easily replaceable and commercially widely available. However, it had disadvantage of not being easily cleaned by hydraulic, chemical procedures. Also, due to its small flow channels the procedure is highly susceptible to fouling.

Materials for the construction can be divided into 2 classes: organic and inorganic. Organic membrane materials include: cellulose acetate, thin film composite, polypropylene, polyamide, polyacrylonitrile (PAN) etc. Inorganic membrane materials available in the market are: ceramic, stainless steel, zirconium oxide. Organic membranes are commercially largely available and has a low maintenance cost. However, relative to inorganic materials it has a disadvantage of having limited range of pH and temperature for cleaning (Bodzek & Konieczny, 1998).

3.1.2 Principles of reverse osmosis system

Reverse osmosis membrane system utilizes pump that supplies high pressure in order to filter the feed water through the semi-permeable membrane. Separation of the feed of the system results in two streams: permeate stream with no (low) salinity and the second stream, retentate with high salinity (Fig. 1).

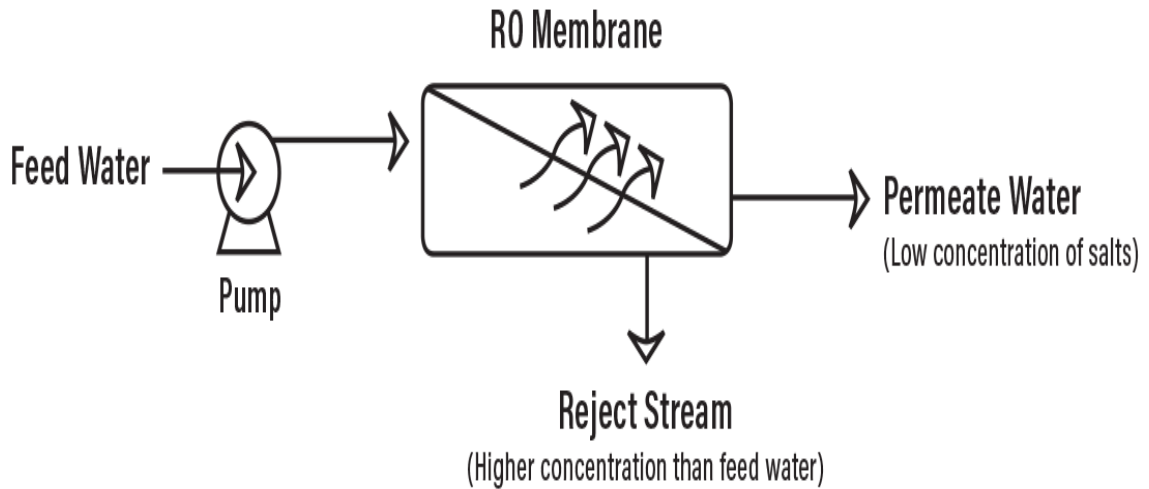


Figure 1. Reverse osmosis membrane separation system diagram. (www.puretecwater.com).

The RO is designed to employ a cross flow filtration mechanism which allows turbulent flow, in order to minimize the contaminant, build up. However, the dissolved ions accumulate with the operation time. This then causes the concentration polarization on the surface of the membrane, which is the primary reason for the formation of the fouling and scaling. However, due to concentration polarization, fouling and scaling the rejection decreases. This section will cover the principles of the reverse osmosis system with corresponding equations.

The most important attributes of the reverse osmosis system are flow rate and the salt rejection. Water passing through a semipermeable membrane has a linear relationship with membrane surface area (A), permeability constant of the membrane (K_w) and to the differential pressure feed-permeate (ΔP), as follows:

$$Q_w = dV/dt = (\Delta P - \Delta \pi) * K_w * A \quad (1)$$

where:

- Q_w - permeate flow (m^3/h)
- V - total filtered water volume (m^3 or L)
- t - the time of the filtration (h, min, sec)
- ΔP - hydraulic pressure difference of the feed and permeate (bar)
- $\Delta \pi$ - osmotic pressure difference of the feed and permeate (bar)
- K_w - the hydraulic permeability constant ($m^3/m^2/s/bar$)
- A - membrane surface (m^2)
- $(\Delta P - \Delta \pi)$ - the net driving pressure (bar)

Hydraulic permeability constant is a character of the membrane and is dependent on the porosity, membrane thickness, and temperature. Osmotic pressure is defined as the minimum pressure to overcome the backflow that is coming from the semi-permeable membrane, hence the applied pressure or the hydraulic pressure has to be higher than the osmotic pressure in order to complete the filtration.

Permeability is the normalized permeate flow rate for which the area is 1 m² and net transmembrane pressure is 1 bar, as follows:

$$P_w = \frac{Qp}{A * (\Delta p - \Delta \pi)} \quad (2)$$

where:

- P_w - permeability (m³/m²/s/bar)
- Qp - permeate flow (m³/h)
- A - membrane surface (m²)
- $(\Delta P - \Delta \pi)$ - the net driving pressure (bar)

Osmotic pressure is proportional to the total dissolved salt of the feed. In practice, it is accepted that brackish water with a salinity of 1000 mg/L has osmotic pressure around 0.7 bar whereas the seawater with a salinity of 35 000 mg/L has osmotic pressure around 25 bar. Hence the osmotic pressures (π) can be calculated by the rule of thumb, as follows:

$$\pi = 0.7 * 10^{-3} * TDS \quad (3)$$

where:

- π - osmotic pressure (bar)
- TDS - total dissolved salt (mg/L)

More accurate calculations can be obtained from the equation of Van't Hoff (Huang & Xie, 2010):

$$\pi_f = 8.308 * \varphi * (T_f + 273.15) * \sum m_i \quad (4)$$

where:

- π_f - osmotic pressure (bar)
- φ - osmotic coefficient
- T_f - the temperature of the feed (°C)
- $\sum m_i$ - summation of the molar concentration (mol/L)

The ration of the permeate flow and the surface area is defined as a flux and it is intended to be constant throughout the duration of the filtration. Flux can be determined as:

$$J_w = \frac{Q_w}{A} = \frac{1}{A} * \frac{dV}{dt} = (NDP) * K_w = (\Delta P - \Delta \pi) * K_w \quad (5)$$

where:

- J_w - water flux (L/m²/h)

- Q_w - permeate flow (m^3/h)
 V - total filtered water (m^3 or L)
 t - time of the filtration (h, min, sec)
 ΔP - hydraulic pressure difference of the feed and permeate (bar)
 $\Delta \pi$ - osmotic pressure difference of the feed and permeate (bar)
 K_w - the hydraulic permeability constant ($m^3/m^2/s/bar$)
 A -membrane surface (m^2)

($\Delta P - \Delta \pi$) - net driving pressure (bar)

Net driving pressure (NDP) is the actual pressure present to filter the water through the membrane and can be referred as the difference between the feed pressure or hydraulic pressure and osmotic pressure.

$$NDP = \Delta P - \Delta \pi \quad (6)$$

where:

- NDP - net driving pressure (bar)
 ΔP - differential hydraulic pressure (pressure feed – pressure permeate) (bar)
 $\Delta \pi$ - differential osmotic pressure (osmotic pressure feed – osmotic pressure permeate) (bar)

Given all the other parameters of the feed water as a constant, net driving pressure has a linear relationship with the flux, meaning as the net driving pressure increases, the flux increases proportionally.

The second important attribute of the reverse osmosis system as was mentioned is salt rejection. Salt rejection (SR) can be expressed as the ratio of the salt concentration of the feed and permeate over the salt concentration of the feed:

$$SR = \frac{C_p}{C_f} * 100 \quad (7)$$

where:

- SR - salt rejection (mg/L)
 C_f - salt concentration in the feed water (mg/L)
 C_p - salt concentration in the product water (mg/L)

Also, the salt rejection can be calculated with total dissolved (TDS) salt values:

$$SR = (TDS Product) / (TDS Feed) * 100 \quad (8)$$

where:

- SR - salt rejection (mg/L)
TDS - total dissolved salt (mg/L)

Salt passage (SP) can be calculated with salt rejection:

$$SP = 100 - SR \quad (9)$$

where:

SP- salt passage (mg/L)
SR- salt rejection (mg/L)

Salts can pass through the membrane at a small rate. Diffusion is the key mechanism of the salt to pass through the membrane. Diffusion is a tendency of salt ions to move from high concentration side to low concentration side. The salt concentration in the product water is a function of water flow and the salt transport and can be expressed as follows:

$$C_p = Q_s/Q_w \quad (13)$$

where:

C_p- salt concentration in permeate (mg/L)
Q_s- salt transport (m³/h)
Q_w- water flow (m³/h)

Q_s or the salt transport can be calculated by the following equation:

$$Q_s = \Delta C * K_s * A \quad (14)$$

where:

$$\Delta C = C_f - C_p \quad (15)$$

Q_s -flow rate of salt through the membrane (m³/h)
ΔC - salt concentration differential across the membrane (mg/L)
K_s -salt permeability of the membrane (m³/m²*s)
A - membrane area (m²)

Recovery (R) or the conversion is the percentage of the permeate related to the feed water.

$$R = Q_p/Q_f * 100 \quad (16)$$

where:

R - recovery (%)
Q_p- product water flow rate (m³/h)
Q_f- Feed water flow rate (m³/h)

Recovery is directly proportional to the salt concentration on the feed side, salt transport and permeates salinity (Burn & Gray, 2015).

Salt rejection triggers the concentration of the salt at the surface of the membrane to gradually increase. This then results in a diffusive flow back of the feed. After certain period of time the salt flow to the surface of the membrane is balanced by the diffusive flow back and the concentration on the membrane surface. At this the steady state, the concentration on the membrane surface is constant. This concentration accumulation is called concentration polarization. In the end, the bulk feed is less concentrated than the membrane surface. The mechanism of concentration polarization is illustrated in Figure 2.

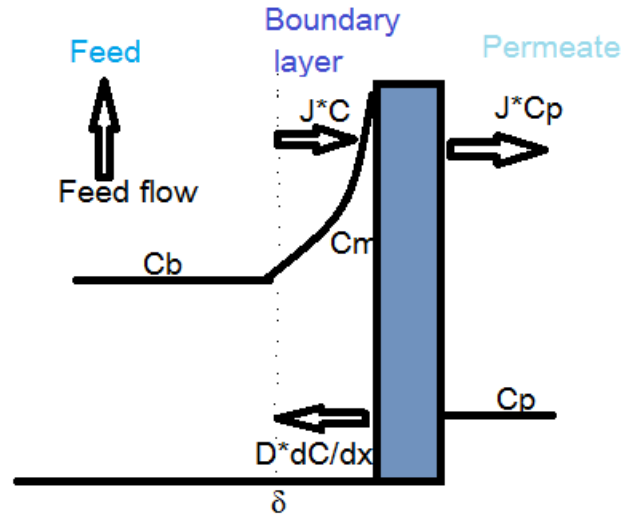


Figure 2. Concentration polarization (Wang, Z. et al., 2016).

where:

- C_b – concentration at the bulk (mg/L)
- C_p - concentration in the permeate (mg/L)
- C_m - concentration at the membrane (mg/L)
- D - diffusion coefficient (m^2/s)
- δ – the thickness of the boundary layer

The convective transport of the salt to the membrane ($J*C_p$) can be calculated as follows:

$$J*C_p = D*dC/dX + J*C \quad (17)$$

where:

- J - solute flux (m/s)
- C_p - permeate salt concentration (mg/L)
- D - diffusion coefficient (m^2/s)
- X - distance normal to membrane (m)

Mass transfer coefficient (K) can be determined by the ratio of the diffusion coefficient and the thickness of the boundary layer.

$$K = D/(\delta) \quad (18)$$

where:

- K - mass transfer coefficient (m/s)
- D - diffusion coefficient (m^2/s)
- δ – the thickness of the boundary layer

With the ratio of the concentration in permeate over the concentration at the membrane, derivation of the intrinsic retention (R_{int}) of the membrane is possible:

$$R_{int} = 1 - C_p/C_m \quad (19)$$

where:

R int - intrinsic retention of the membrane (%)

C_p- concentration at the permeate (mg/L)

C_m- concentration at the membrane (mg/L)

Concentration polarization factor is a ratio of the concentration at the membrane over concentration in the bulk/feed. Concentration polarization factor has a linear relationship with the flux, intrinsic retention and not proportional to the mass transfer coefficient (k).

The concentration polarization results in several negative consequences. It causes the osmotic pressure to increase, requiring higher feed pressure as the net driving pressure decreases. Salt rejection decreases with increased salt transport because of the higher salt concentration at the membrane. This then can result in a membrane surface scaling and fouling. Thus, controlling and managing concentration polarization is important effort to apply for the efficient filtration. There are several ways to reduce the concentration polarization:

Mass transfer coefficient is proportional to the flow velocity and the diffusivity. Diffusivity can be altered with the temperature. Increasing the velocity can increase the mass transfer coefficient.

The more water pass through the membrane the more salt will retain thus decreasing the flux is one way to control the concentration polarization.

One of the most important parameters in the filtration system is the temperature of the feed. It has a linear relationship on the water permeability (K_w). In practice, it is considered every 1 °C increase result in 3% increase in water permeability. Also, it has a crucial effect on the viscosity of the water. Thus, it is important to have temperature correction factor (TCF).

$$TCF = 1.03(t^{\circ}C-25) \quad (20)$$

where:

TCF- temperature correction factor

t°C- temperature of the feed (°C)

Permeability is corrected, as follows:

$$K_w = K_{25^{\circ}C} * 1.03(t-25) \quad (21)$$

where:

t – temperature in °C

K_w – membrane permeability at given temperature (m³/m²*s).

K_{25°C} - membrane permeability at 25°C (Burn & Gray, 2015).

3.1.3 Pesticide filtration by means of membrane separation systems

EU Drinking Water Directive (2015/1787 of 6 October 2015) issued a guideline for the permissible level of the pesticides as of 0.1 µg/L for each individual pesticide and sum of all the pesticide present in the drinking water not to be more than 0.5 µg/L.

Although in the EU it is restricted to use diurone, triazine class herbicides (atrazine and simazine) as a plant protection product (775/2005 EC and 1376/07 EC), due to an intensive application in the last two decades and its high potency to remain in the water bodies, the bulk and the residues of the pesticides are frequently found throughout the European Union

countries. For example, in a study where 164 individual ground-water samples from 23 European Countries were collected and analysed for 59 selected organic compounds. From which, atrazine was detected with 56% frequency (above the European groundwater quality standard) with maximum concentration of 253 ng/L, simazine 43% and maximum concentration 127 ng/L. Whereas, diuron inspections showed frequency of detection of 29% with 279 ng/L concentration as a maximum concentration. Atrazine and simazine are endocrine disrupting compounds and diuron has a high risk for the water ecosystem and is carcinogenic, thus removal of these pesticides is of high importance (Loos et al., 2015).

Chemical properties of pesticides:

Diurone.

Molecular formula: $C_9H_{10}Cl_2N_2O$
Molecular weight: 233.1 g/mol
IUPAC name: 3-(3,4-Dichlorophenyl)-1,1-dimethyl-2-hydroxyethanimine
Log K_{ow} = 2.68

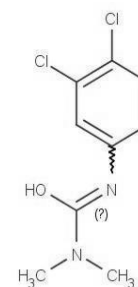


Figure 3. Molecular structure of Diurone

Atrazine.

Molecular formula: $C_8H_{14}ClN_5$
Molecular weight: 215.7 g/mol
IUPAC name: 6-chloro-4-N-ethyl-2,4-diamino-1,3,5-triazine

-propan-2-yl-1,3,5-triazine-2,4-diamine
Log K_{ow} = 2.61

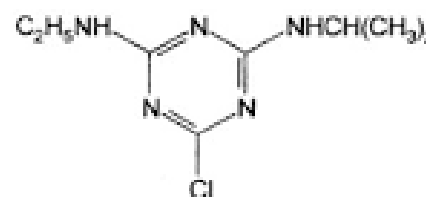


Figure 4. Molecular structure of Atrazine

Simazine.

Molecular formula: $C_7H_{12}ClN_5$
Molecular weight: 201.6 g/mol
IUPAC name: 6-chloro-2,4-diethyl-1,3,5-triazine

diamine. Log K_{ow} = 2.18

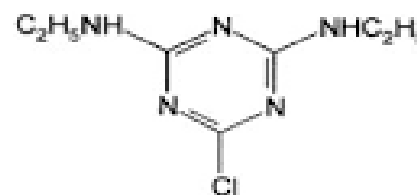


Figure 5. Molecular structure of Simazine

The exact mechanism or the combination of the mechanisms, to take action during the filtration will depend on the membrane characteristics, feed quality and solution properties. This chapter will give the general overview of the mechanisms that are taking place during the filtration process.

Membrane characteristics that affect the pesticide removal rate

Depending on the physicochemical characteristics of the pollutant and membrane, separation can be done by different mechanisms. Physical separation process includes size exclusion, steric

hindrance and charge repulsion. Chemical activities that take place during separation are chemical bonding, hydrophobic and hydrophilic interaction. Pesticide removal is complicated process, and it is still target of extensive research, however it is proven to be mainly coordinated by the size exclusion mechanism (Drazevic et al., 2002). It will be discussed about the membrane attributes such as molecular weight cut off and salt rejection, as well as the pesticide characteristics that influence the filtration processes.

Molecular weight cut off

Molecular weight cut-off (MWCO) is unitized in Daltons (Da) and it is referred as a minimum molecular weight of a solute in which 90% of the solute is retained by the membrane. For the standard experimental method proteins, dextran, polyethylene of 0.1 % are filtered with the transmembrane pressure of 100 kPa, at the temperature of 25 °C. The lower the molecular weight cut-off, the smaller the pore sizes of the membrane.

For the removal of pesticides, MWCO of 200- 400 Da is considered appropriate. TFC-3013-400 membrane has approximately 100 Da MWCO. Although it is expected to assume that the lower the pore sizes of the membrane better will be the rejection, the MWCO does not fully represent the efficiency. Studies showed that the membrane with lower MWCO performed worse than the membrane with higher MWCO, in terms of rejection rate (Van der Bruggen et al., 2006). This proves that the rejection is not fully dependent on the size exclusion; sieving mechanism; the physicochemical interactions of a membrane material and a solute also play an important role.

Porosity

Pore size distribution, minimum pore size, pore density and effective number of pores are more reliable information to predict the rejection capability. Methods for determining the pore size distribution is labor intensive and complicated, such as bubble gas transport method, mercury intrusion porosimetry, adsorption-desorption method etc. Thus, the information about porosity is usually not provided by the manufacturer. It was proven that the rejection rate is positively correlated with membrane porosity (Kosutic et al., 2002).

Salt rejection

Researchers generally agree that membrane's degree of desalination gives more reliable information about the separation capacity. Moreover, salt rejection parameter positively correlates with pesticide rejection rate. Meaning, rejection is highest for the membrane with greatest salt rejection capacity (Kiso et al., 2000).

Membrane charge and polarity

Reverse osmosis membranes are typically cellulose acetate or polysulfone coated with aromatic polyamide. Among the physicochemical interactions playing crucial role in rejection of pesticides, polarity of the membrane materials is regarded as a backbone of the interaction.

Most commonly found pollutants in the feed stream are charged negatively, thus most thin film composite (TFC) membranes are designed and manufactured to be negatively charged. The electrostatic repulsion of the pesticides on the surface of the membrane contributes to the rejection efficiency. This makes the foulants to be less adsorbed thus providing higher flux. Non-polar polyamide membranes have far better performance than cellulose acetate membranes (Karabelas & Plakas, 2012).

Pesticide properties, affecting the removal rate:

Pesticide molecular weight

In pilot plant study comparing the rejection of 11 different pesticides on the membrane with MWCO 200 Da, determined the positive correlation between rejection and the pesticide molecular weight. The higher the molecular weight the better the rejection which also supports the theory that the main mechanism of the pesticide retention is the size exclusion mechanism. Atrazine has a molecular weight of 215.68 g/mol, whereas diuron has a molecular weight of 233.1 g/mol and simazine 201.6 g/mol (<https://pubchem.ncbi.nlm.nih.gov/compound>). Also, it is worth mentioning that the molecular width and length play a significant role in the rejection of the pesticide. The strong difference in rejection rate was observed within the pesticide, depending on the nature, chemical bonding of the pesticide.

Pesticide relation to the water

Hydrocarbon part of the pesticide interacts with membrane via hydrophobic bonding, which adsorbs the pesticide to the membrane polymer. On the other hand, organic parts of the pesticide bond with hydrophilic groups of the membrane, also allowing it to adsorb to the membrane polymer. Thus, hydrophilic and hydrophobic interactions take place independently or simultaneously, depending on the nature of the pesticide, membrane material and feed characteristics. The first stage of the rejection process is a hydrophobic interaction, which proves that the rejection rate is higher when hydrophobic interactions are common.

Adsorption can be miscalculated as high rate of rejection thus in order to carefully determine the real rejection rate, it is recommended to saturate the membrane with compound, prior the evaluation. It is also worth noting that the retention and rejection represent the same meaning while adsorption refers to compound bounding with the membrane material, thus is not fully represent the retention/ rejection rate.

The hydrophobicity/hydrophilicity of a solute is measured in unitless octanol or water partition coefficient (log Kow). The octanol value of diuron is equal to log Kow= 2.87 (Hladik, 2012), whereas atrazine has log Kow= 2.28, and simazine has log Kow= 2.18 (Omatuyo, 2005). It is considered that the solutes with octanol value lower than 10, has relatively hydrophilic characteristics, having a tendency to have higher water solubility.

Polarity

The polarity of the pesticides and its retention rate has a negative correlation. The more polar the pesticide the lower the retention. This can be explained by the dipole formation, directed on the surface of the membrane, making the pesticide accessible to permeate the membrane. Phenyl-urea derivative pesticide such as diuron has lower retention rate relative to the triazine compounds such as atrazine and simazine; dipole moments of atrazine= 2.8 coulomb-meter and diuron = 5.77 coulomb-meter (Van der Bruggen, 2003).

Feed water parameters, affecting the retention rate of pesticide:

pH

pH affects the retention of the pesticide, mainly due to the deformation of the membrane material polymers and the interaction that is taking place on the membrane surface.

The rejection rate of atrazine was relatively constant in the pH ranging from 3 to 7. But when the pH reached 8, the sharp decline in rejection rate was inspected (Berg et al., 2007). The high pH level of the feed increases the OH⁻ ion adsorption, making the pesticide move in a more preferential way. That results in increased attraction, increased permeation, and lower retention.

Pesticide concentration

Based on the previous research works, it has been concluded that the concentration variation of the pesticide does not have a significant effect on the retention rate of the pesticide. Increase in pesticide concentration by 70 times higher than the prior concentration, reduced the retention rate only by 13% (Plakas, 2008).

Presence of inorganic solutes in the feed water

Ionic concentration present in the feed water causes the reduction of electrostatic forces, resulting in a reduction of the pore size of the membrane, which means an increase in rejection and decrease in fluxes. However, this theory is only applicable for porous membranes without taking into account the charge of the membrane. Calcium ions had a negative effect on the retention rate when was filtered by relatively dense and neutrally charged NF membrane. Whereas same calcium salts were tested for the negatively charged RO membrane, no significant difference was obtained. (Plakas, 2008).

Presence of organic solutes in the feed water

It is essential to know the effect of the organic matter content on the retention rate as the pesticides present in the groundwater or in the soil matrices are usually bound with the natural organic matter such as humic acid, fulvic acid, polysaccharides etc. These different organic matter types are bound to other compounds such as amino acids etc., which makes it hard for simulation for the laboratory assessment.

Relative to the salt content, organic matter concentrations have a significant effect on the retention rate. In general, natural organic matter in the feed increase the rejection rate, but the efficiency level is dependent on which type of organic matter, membrane characteristics and also the solute for the removal. Research work conducted with nanofiltration membrane with triazine pesticides (including atrazine and simazine) combined with a humic acid,

showed that the interaction of pesticide and humic acid resulted in forming a complex compound which in turn hindered the diffusion, increasing the retention rate.

Temperature

The temperature of the inlet has a crucial effect on the efficiency. As the temperature raises the viscosity decreases, which makes the water pass through the membrane more easily. Also, temperature effect the ion mobility and its dissolvability, thus it has a direct relation to the conductivity. 1 °C increase causes conductivity to increase by 2-4%. The general rule of thumb is that salt passage increases by 6% with every 1 °C increase.

3.1.4 Heavy metal removal by means of membrane separation system

Heavy metals are the essential part of many industrial processes. The effluent of these processes without proper treatment can affect negatively the ecosystem and human health. Standard adopted by the European Union Council for drinking water, in 2015, state permissible values for the copper as 2 mg/L, and no information about the zinc (EU Drinking Water Directive, 2015/1787). Whereas standard from the WHO (1993) state copper limit as 2 mg/L and no health-based guideline was proposed for zinc in drinking water (WHO, 2011) .

Reverse osmosis and nanofiltration systems are the most efficient membrane filtration systems in terms of heavy metals removal. However, it is generally considered bivalent heavy metals are rejected better by nanofiltration. Moreover, while both systems show off high flux and efficiency, the economic evaluation results in higher cost (initial and maintenance cost) for reverse osmosis system.

Among the reverse osmosis membrane studies, thin film composite polyamide membranes show better results than any other membrane materials available in the market. Unlike the pesticide study, heavy metal removal depends mainly on the solution-diffusion mechanism, in which the solution pH and membrane charge play the dominant role.

Feed water parameters

Effect of co-ions in the feed

Study on the effect of the co-ions (e.g. calcium, cadmium, potassium) concentration variables on the removal of the zinc by means of reverse osmosis, showed that there was no effect on the rejection rate when potassium and magnesium were introduced in the experiments. On the contrary increase of cadmium and calcium concentration in the feed, decreased the rejection rate of zinc by 2% (4 bars, temperature 25±2°C, pH 5.5, Zn 10 ppm) (Kagramanov et al., 2010).

Heavy metals concentration

Earlier studies show that concentration variations have a significant impact on the overall system. Low concentration of the heavy metals induced a sharp decline in the flux whereas high concentration of heavy metals caused a linear drop in the flux. Meaning, low concentrations of heavy metals result in higher rejection rates (Bakalar et al., 2009).

pH

Increase in pH level in the effluent accelerates the scaling process reducing the flux. Specifically, increase in pH causes heavy metals to co-precipitate with other ions present in the medium. Also, fouling rate increased with the higher pH, which can influence the retention rate positively. The removal rate of heavy metals increased from 99.1% to 100 % when pH increased from 5 to 9.5 (Mirghaberi et al., 2014). As noted before, whether the foulant/scalant formed in front of the membrane work as a double barrier or hindrance to the filtration, depends on many aspects.

Filtration operation parameters affecting the rejection of heavy metals

Pressure variations

Heavy metals removal rate can be slightly influenced by the pressure adjustment. Increasing the inlet pressure from 5 to 11 bars showed that the removal rate of the iron decreased slightly from 99.5% to 98.6% (Nader, 2016). TDS removal rate also has decreased from 83.3% to 61.3%. In this experiment, the heavy metals were in nitrate form ($Zn(NO_3)_2 \cdot 6H_2O$, $Fe(NO_3)_3 \cdot 9H_2O$, except for copper which was present in the form of $CuCl_2 \cdot 2H_2O$). The feed was simulated as a steel manufacturing wastewater and had been run through two-stage treatment before the reverse osmosis filtration.

On the other hand, another study concluded that the addition of pressure on the inlet causes heavy metals concentration to decrease in the permeate. Also, the addition of the concentration of the heavy metals in the inlet increases the concentration of the permeate (Hegazi, 2013). The difference in results might be due to the different experimental conditions, procedures, and methodology.

Recovery rate

Increase in recovery rate causes salt concentration and osmotic pressure to increase resulting in permeate flux decline. Additionally, membrane fouling formation rate is higher in higher recovery rate.

3.1.5 Separation of the fertilizer by means of membrane systems

Whether it is the result of excessive agricultural practice or industrial activity, nitrogen and phosphorus compounds and related residues are still present in soil and water bodies. WHO standard for the drinking water states as follows: nitrate 50 mg/L and nitrite 3 mg/L. No health-based guidelines were proposed for ammonia, only odour threshold of 1.5 mg/L at alkaline pH (WHO, 2011). Whereas standard from the EU guideline state nitrate 50 mg/L, nitrite 0.5 mg/L, ammonia 0.50 mg/L as permissible values (EU Drinking Water Directive, 2015/1787).

Generally, as nitrate is monovalent ion it is considered not suitable for reverse osmosis system (Reinsel, 2014). But still, reverse osmosis system studies result in high efficiency. For example, nitrogen separation from domestic wastewater by reverse osmosis experiment showed separation efficiency of 95% for total nitrogen (Bilstad, 1995). A study on the treatment of slurry showed that phosphorus elimination ($P-PO_4$) was higher (100%) than of total nitrogen (99.6%) and ammonia removal (99.6%) (Kwiencinska, 2012).

Ammonium nitrate is used widely as a nitrogen fertilizer. Experiment on nitrogen recovery by means of reverse osmosis shows that the rejection rate was dependent on the concentration of the ammonium, in this case increasing with the concentration increase. Also, the decrease in pH value from 5.5 to 3.7 had no effect on the permeability.

Experiment on the ammonium nitrate with TFC reverse osmosis membrane shows that pH has a negative correlation to the retention rate. On the other hand, presence of metals in the feed increased the retention rate. This can be explained as the ammonium had reacted with the metals and formed a compound which is larger than of the ammonium ion (Koyunku, 2002).

Urea is also commonly used as fertilizer. Unlike ammonium nitrate, urea is more hydrophilic and uncharged, which makes the removal by reverse osmosis quite difficult. Initial concentration for the urea was higher than of the other two trials, the flux decrease was lower. This is because the final concentration was lowest for the urea trial. Moreover, it was noted that the pH increases from 3.5 to 7.5 resulted in the increase of the rejection, however, pH higher than 8 was negatively affecting the rejection (Yoon & Lueptow, 2005).

When the pH of the feed increases, membrane becomes more negatively charged, this triggers the electrostatic repulsion between the inorganic ions. But in case of the urea, the rejection rate was changing but no trend. It is also worth mentioning that it was also concluded that the organic molecules rejection rates were much lower than of the inorganic molecules.

3.2 Fouling types and their characteristics

The fouling process was discovered to be much more complex than what have DuPont assumed back in 1960's, when they were developing the SDI. The fouling processes can be categorized as particulate fouling, scaling, organic fouling, and biofouling (Potts, 1981). They differ not only by their state but also by the fouling mechanism, effect on the membrane operation and removal method. In this section, the fouling types and their distinct characteristics will be discussed.

Regardless of the fouling type, the fouling itself is a complicated process. Although, the researchers still argue exact mechanism of the fouling, there are four major cases of the fouling:

1. When the adsorption takes place, particles plug the smaller pores and narrow the larger pores. This case has the most effect on the flux decrease. But will have the least effect on the retention.
2. When there is no evident sign of adsorption, particles can plug small pores and big pores are narrowed. This case has the least effect on the flux decrease.
3. Gel/cake formation. The fouling is irreversible.
4. Selective plugging. Big pores are blocked, and the small ones are narrowed (Belfort, 1980).

Further when there is a layer developed in front of the membrane, two distinct cases must be considered. First, if the membrane has a higher retention potential than the deposited layer in front of the membrane, then the layer in front of the membrane will increase the polarization resulting in reduced rejection. Second, if the layer deposited in front of the membrane has a higher retention potential than the membrane (by adsorbing the solute). Then the rejection rate will increase, but only for the certain period as at some point due to the membrane polarization the rejection rate will decrease.

Whether it is a first case or second case, will depend on many parameters such as the solute chemical properties and its interaction with the decomposed layer (scalant, foulant or biofoulant). In addition, the relation between the membrane and foulant also needs to be considered. Parameters of the foulant, membrane material and the characteristics of the feed water and the interactions of these three will decide whether the retention rate will shortly increase or decrease.

3.2.1 Scaling.

During the filtration operation, membrane draws up the salts present in the feed due to membrane polarization. Water-insoluble salts such as calcium carbonate, calcium sulfate etc., become oversaturated which causes the precipitation. This then forms a scaling. Samples from the scalant of the membrane show calcium (Ca^{2+}) and sodium (Na^+) are the most commonly occurring ions. Compared to sodium, calcium has a more damaging effect. This was proven in the experiment where two identical membranes were saturated with calcium and sodium separately, after which the membranes were chemically cleaned. The recovery rate was lowest when the membrane was saturated with calcium compared to virgin state and when saturation was done with sodium (Liu, 2016).

There are two major mechanisms for the scaling: heterogeneous (surface) crystallization and homogeneous (bulk) crystallization. Bulk crystallization takes place after the surface crystallization, when the surface of the membrane is oversaturated and fully covered with the salt. Scaling process depends not only on the concentration in the feed water but also on the nature of the feed water together with the operational characteristics.

In terms of the operational characteristics affecting the scaling formation, pressure and flow rate must be mentioned. The addition of the pressure into the system will increase the flux flow, recovery rate and polarization on the membrane. The polarization of the membrane is formed due to the increase of the salt concentration.

Feed parameters that play crucial role in scaling formation would be pH, ionic strength, and presence of other substances such as organic matters. High pH values cause CaCO_3 and the MgCO_3 to precipitate. In addition, high pH value causes the pores of the membrane to shrink due to the ionic strength.

Ionic strength of the feed has a relative effect on the fouling/scaling formation. Experimental work by Van der Brink and colleagues, showed that ionic strength increase alone does not have high influence on the fouling formation. However, when calcium was introduced with alginate as a source of polysaccharide, the fouling rate drastically increased. It was concluded that calcium not only main constituent of the scaling formation but also it plays a crucial role in fouling formation by bridging the polysaccharides and membrane surface (Van der Brink et al., 2009). On the other hand, the flux decreased drastically when ionic strength was increased whilst the presence of the particles of silica (Elzo et al., 1998). These indicate the complexity of the effect of the ionic strength on the permeate flux and fouling.

However, in the presence of higher salt contents, it was concluded that the higher ionic strength result in higher fouling and scaling when it was increased (by addition of the concentration), as the solubility of the solution decreases which enhances the crystal growth (Scheikholeslami, 2003).

3.2.2 Colloidal fouling.

Colloids are ubiquitous in all process waters and may include clays, iron oxide, colloidal silica, large organic macromolecules, organic colloids and suspended matter, and calcium carbonate precipitates (Stumm et al., 1992). Membrane autopsies show that more than 70% of the deposits are constituents of oxides of iron, aluminum silica, and organic deposits (Schaffer et al., 2000).

Colloidal fouling was proved to be reversible, meaning that the pore blockage is not the main mechanism of colloidal fouling. It is mainly controlled by the particle-surface and particle-retained particle interaction.

The opposite charge of the membrane surface and the colloidal foulant will form a layer at the surface. When the surface is covered with the colloids, the particles start to interact with the previously retained particles. There will be a strong double layer repulsion of the particles that accelerate the accumulation of the particles. Simultaneously, there will be permeation drag force which is directly proportional to the permeate flux velocity. When the permeation flux increases, the dragging force is higher than the repulsion thus increasing the fouling formation process. And when the permeation drag increases until the repulsion force is zero, it dominates the whole fouling formation (Gomez, 2007).

Moreover, gravitational and inertial lift, Van der Waals forces act in the transport of the particles. It is the interplay between these transport mechanisms. Also, Brownian deposition is of higher importance. Inertial lift occurs when the particles not larger than the Brownian size, are dragged away from the membrane surface.

Presence of the dissolved organic matters such as humic substances accelerate the fouling by co-precipitation. Electrostatic attraction between the negatively charged functional groups of humic macromolecules and positively charged sites of the colloidal particles are the reason for the co-precipitation.

3.2.3 Organic fouling.

Fouling of the organic matter on the membrane surface is largely influenced by the presence of the cations, for example calcium. Positive charge of the calcium reacts as a bridge between negatively charged organic matter and the membrane surface. Moreover, sodium and calcium ions actively interact with the organic matter, which in turn causes the rejection rate of these two ions to decrease, leading to higher scaling rate. Co-precipitation of the organic and salt ions take place when the pH is above 9 or when the organic matters are absorbed into the calcite scale on the surface of the membrane.

3.2.4 Biofilm and biofouling.

Biofilms are a conglomeration of microorganisms, attached to the surface of an object. Biofilms generate extracellular polymeric substances (EPS), which consists mainly of polysaccharides, proteins, lipids, and DNA. The EPS is the primary reason for the higher survival rates of the microorganisms present in the biofilms. Microorganisms in the biofilms can resist at certain extent pH differences, temperature deviations as well as biocides, nutrient stress, and toxic substances.

Biofilms cause biofouling at the surface of the membranes as it is a favorable location, because of the abundant availability of the nutrients at the surface, due to concentration

polarization. Biofouling includes live/active cells, dead cells, and EPS. But it is considered dead cells and EPS as the major components of the biofouling. Bacterial cells are responsible for the increase of transmembrane pressure on the membrane whereas the EPS triggers the elevation of the hydraulic resistance. This then leads to the reduction of the flux, and salt rejection, deteriorating the quality of the permeate. Moreover, studies suggest that there is a direct biodegradation of the membrane material by the biofouling. For example, cellulose acetate RO membrane was examined before and after biofouling, in which the hydroxyl groups that were initially present were gone, instead amin groups have been identified (Beverly, 2000).

Researchers can calculate and predict the scaling processes so that the antiscalants are used in the most efficient way possible, however, for the biofilms, there are no models or calculation techniques for the prediction. The biggest disadvantage to the membrane system is that the membrane itself does not tolerate the oxidizing biocides, thus the appropriate choice of the biocide is of high importance.

Biofouling formation

The very first step for the biofouling formation is when the suspended bacterial cells interact with a membrane surface and form a bacterial cell-surface bond, in which the hydrophobic and non-polar surfaces play a crucial role. The interaction happens due to fimbriae attachment mechanism. Then the bacterial cells start to feed on and “take up” the surrounding macromolecules, which accelerates the growth pace.

The attachment process is largely dependent on the hydrodynamics, feed solution characters such as pH, temperature, nutrient level etc. But the important part is the bacterial cells themselves. The cells must go through a mutation (e.g. cell lipopolysaccharides) that enhances the cell roughness, which protects the electrostatic repulsion. This mechanism supports the hydrophobic bond. Moreover, flagellar motility of the cells is necessary to overcome the repulsive forces (Vanysacker et al, 2013). Further, the biofilm grows by microcolony formation.

Disinfection methods against the biofouling

Disinfection methods can be generally categorized into two classes: physical and chemical. Physical disinfection methods include UV, pretreatment methods such as sand and carbon filtration. Easy installation and maintenance of the UV have an advantage of oxidizing the organic matters also. However, there is a high chance of scale formation.

Membrane pretreatment method is not cost effective but higher quality is obtained as a result. Sand filtrations have low installation and operation costs however the bacterial removal rates are the lowest.

The application of ozone, ClO_2 , NH_2Cl , HOCl , and OCl are sole chemical disinfection methods. They have higher efficiency rate, however, higher risks of membrane corrosion and degradation, and formation of toxic compounds such as trihalomethane, halo-acetic acid, chlorite toxicity and bromate (during the treatment of feed containing bromide) (Kim et al., 2009, Tynan et al, 1993).

Critical parameters influencing the formation of the biofouling

The intensity of the growth of the biofilm solely depends on the operational parameters and feed content. For example, spiral wound membrane system functions with the laminar flow which reduces the shear forces allowing the biofilm to grow without internal physical boundaries.

The biofilm growth rate follows the same trend as the other fouling types, such as scaling, meaning the higher permeate the higher the fouling. When operating with the recovery rate of 50%, bacterial levels should multiply by factor 2 from RO inlets to RO system.

The optimum water quality parameters for the biofouling growth would be optimum for the bacterial growth, such as pH ranging from 6.5-7.5, temperature ranging from 15-40° C etc. The nutrient availability is highly important, especially cations.

Effect of the cations present in the feed is crucial. For instance, the trivalent cation lanthanum causes to reduce the electrostatic repulsion between the dead cells and membrane surface, which leads to a formation of a cell cake layer (Herzberg, 2007).

3.3 MFI and SDI theoretical overview

Due to extensive industrialization, rapid population growth and climate change, drinking water is in high demand as never. Water shortage is one of the most important and critical issues of the 21st century. For instance, due to extreme drought and miss management of water resources, Cape Town is the first major city to limit the water utilization (Brown & Magoba, 2009). Moreover, the occurrences of the contaminants of drinking water with micropollutants such as heavy metal, medical compounds, organic pollutants etc., are becoming far more frequent. For example, the results of the investigation done in Berlin, Germany showed that the residues of the medical compounds are in high concentration in tap water samples (Wilhelm et al, 2010). Acetaminophen found to be reaching up to 29,000 ng/L in the surface water in Spain (Gómez et al., 2007). Hence, long-term strategic plan for the management, improvement of the water reuse technique, introduction of new drinking water production systems and advancement of the current water cleaning methods are required.

Desalination is an artificial method to produce fresh water and is largely used in the Arabian Gulf regions since there the major water source is sea water. Desalination capacity is rising each year, for instance in the first half of 2017 the capacity raised by 14% in a six-month period. Apart from the thermal method, membrane technologies are dominating in the desalination market. The annual capacity of membrane technology is 2.2 million m³/d, whereas thermal processes produce only 0.1 million m³/d (IDA Desalination Yearbook, 2017-2018). Ninety of the desalination capacity uses reverse osmosis membrane systems (DesalData, 2018). Intensive studies and research works have been done to advance the reverse osmosis system and it is transforming into the most efficient method (in terms of energy recovery, pretreatment options, low risk to the environment etc.). However, the biggest impediment to the reverse osmosis processes is still the fouling phenomena.

Fouling of the membrane has a very harmful effect as the performance of the membrane decreases (low production and low quality of the permeate), the frequency of the chemical cleaning increases, which leads to the deterioration of the membrane material itself. This leads to unpredictable costs of the operation and maintenance. Identification of the fouling potential to select the most appropriate pretreatment procedure is a crucial step to meet robust reverse osmosis operation. Pretreatment methods have diversified in recent years, introducing low-pressure membrane processes, such as ultrafiltration (UF) and nanofiltration (NF) (Lund and Baeckaskog, 2017).

Estimation of the fouling potential of the feed water is required to maintain high-efficiency operation. It is a prior necessity for every membrane operation.

Silt density index and modified fouling index are widely accepted methods for the estimation of the fouling potential of the feed water. Guidelines formulated by ASTM (American Society of Technology and Material) (D4189-07(2014)) suggest filtering an inlet in a dead end-mode for the duration of 15 minutes, under a constant pressure of 207 kPa using a cellulose acetate filter with pore size of 0.45 μm . The obtained values of the volume of filtrate and the amount of time, further go through a calculation.

One of the biggest concerns of these two indexes is the fact that the standard method for determination of SDI and MFI neglect the mechanisms and processes that are taking place inside the filtration of the membrane systems. SDI and MFI values are generated in a dead-end mode where most of the membrane filtration systems are based on cross-flow mode, meaning the hydrodynamics of cross-flow mode is completely neglected (turbulence promoting spacers etc.). Moreover, it was later proven that the particles smaller than 0.45 μm are the primary reason for the foulant formation and growth. This means that the standard measurement also neglects these small particles as the filters that are suggested to use are with the pore size of 0.45 μm . Thus, the results are generally indicating less fouling than it actually is in practice. Also, the standard procedure runs under the constant pressure whereas the reverse osmosis operates to support the constant flux, under deviating pressures. Thus, improvements of the index measurement technique, covering the membrane filtration mechanisms or at least reflecting it, are in high demand.

This section will provide the theoretical overview of the SDI and MFI with comparison of the studies done on the different parameters that affect the index values. Also, fouling types with their characteristics and alternative fouling indexes will be discussed.

3.3.1 Standard measurement of SDI and MFI

SDI

Back in 1960's, America's renowned DuPont/Permasep Product Company launched their very first hollow fine fiber RO permeators. Due to its frequent malfunction, caused by fouling, Silt Density Index was introduced at the request of the U.S Bureau of Reclamation. Initially, it was regarded as the main fouling was attributed to the particulate fouling. Thus, the silt density index is designed for the prediction for only particulate fouling (Schipper, 2014).

The experiment of SDI is based on measuring the time that is necessary to plug the filter with pore size of 0.45 μm under the constant pressure of 207 kPa. The time required to filter the first 500 milliliters is noted following the notation of the time that is required to filter second 500 milliliters after 15 minutes. And the values are used in the equation to generate the index. The index is expressed as percent flux decline per minute. It is apparent that the procedure for the measurement is easy and cost-effective and for these reasons, SDI was used for many years all around the world.

SDI less than 1 means that the operation will be running without cleaning for years, SDI less than 3 suggest for cleaning several months in between. SDI more than 5 means additional pretreatment is necessary. However, the limit values are different depending on the

type of the membrane system and manufacturers of the membrane. In Table 1, the pretreatment options for the SDI values are provided.

Table 1. Pretreatment methods for specific SDI and Nephelometric Turbidity Unit (NTU). (Yiantios, 2003).

SDI and NTU	Pretreatment types
SDI>5	Media Filtration
SDI>4, >1 NTU	Coagulation-Flocculation, Microfiltration
For spiral wound modules	
SDI>3	Cartridge microfiltration
SDI>5, >0.2 NTU	Precoat filters, UF, Cartridge filtration, Screen prefilters, Lime softening
For hollow fiber modules	
SDI>5	Ion exchange softening
SDI>3	
SDI>4, >1 NTU	

However, correction of the temperature was necessary because the results were having erratic, too variable relationship as feed temperature changes. But most importantly there was no linear correlation between SDI and colloidal/suspended matter, meaning that the feed appeared to be less fouling than it is. Moreover, the SDI does not reflect the actual practice. As mentioned before, SDI 3 indicates the necessity for cleaning the membrane every 6-7 months, however, SDI=3 effectively means a flux decline of 3% per minute (Schippers et al., 2014). This is far beyond than the rates observed in practice.

MFI

To overcome these disadvantages of the SDI, MFI was introduced by Schippers and Verdouw in 1980. Major phases that take place, when filtering an inlet containing colloidal and suspended matter, are blocking filtration followed by cake filtration and cake compressibility (Fig 1). MFI takes into account the filtration phases. Assuming that the cake filtration as the major filtration phase, modified fouling index can be obtained from the minimum tangent slope ($\text{tg}\alpha$) of the time/volume (t/V) versus volume (V) curve of this phase (Schippers and Verdouw, 1980).

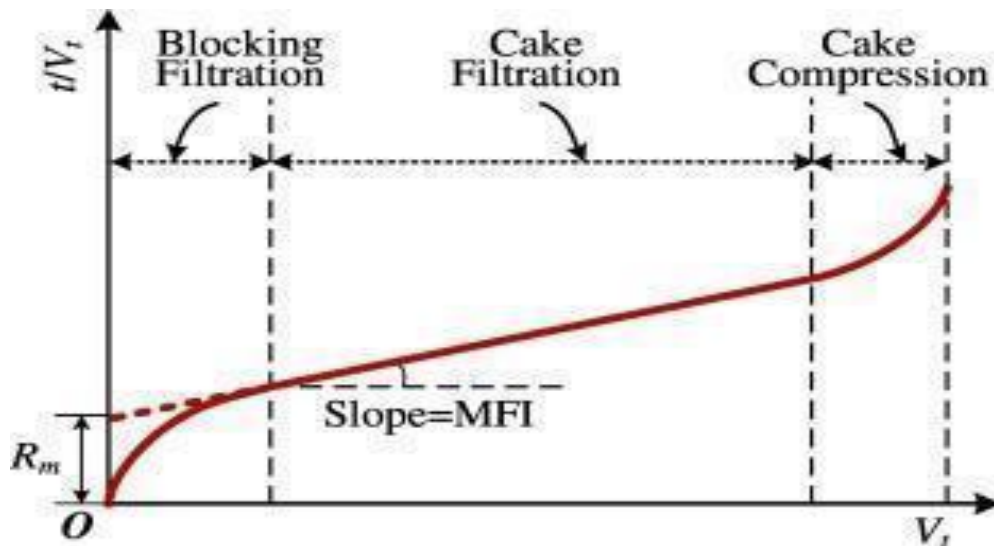


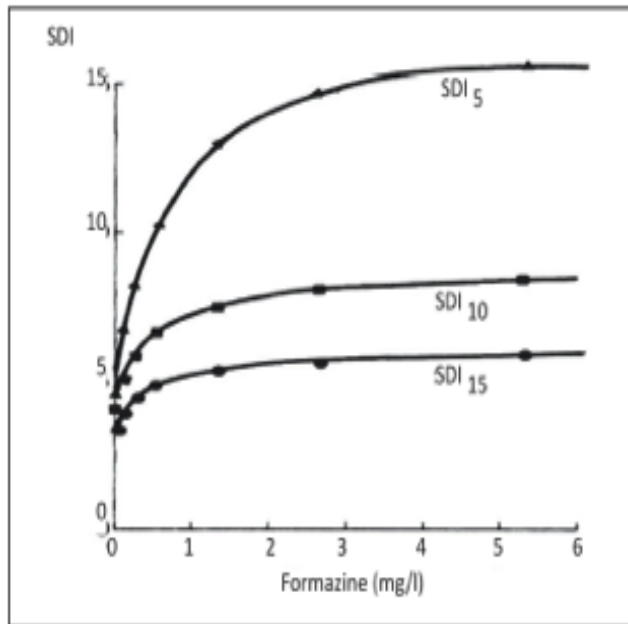
Figure 6. Filtration curve t/V versus V . (Li et al., 2017).

The calculation of MFI includes the temperature correction and it has a linear relationship with the colloidal particles.

SDI vs. MFI

The most important difference between SDI and MFI would be their relationship to the colloidal particle present in the feed. This difference was illustrated in the experiment with formazin (Fig. 7).

Non-Linear



Linear

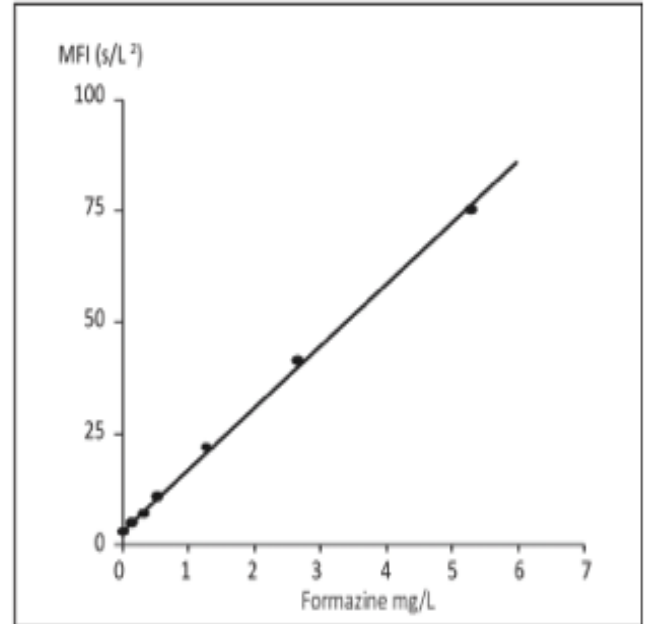


Figure 7. Formazine experiment on SDI and MFI. (Schippers & Salinaz-Rodriguez, 2014).

From Figure 2, it can be seen that the MFI values increase linearly when the formazine concentration in the feed was added while SDI values don't relate to the concentration.

In contrast to SDI, MFI has no value boundaries and limits (maximum and minimum). This makes it difficult to compare the broad range values in terms of the fouling potential and examine the actual fouling risk.

Summary of the differences between the two indexes expressed as disadvantages and advantages are provided in Table 2.

Table 2. Differences and common disadvantages of SDI and MFI (Rachman, 2011).

	Advantages	Disadvantages
SDI	Simple procedure	Has no correlation to the foulant concentration
	Standardized	Has no base of the filtration theory
	Easy comparison	No correction for the temperature
MFI	Based on the filtration theory	More complex and expensive

	Correction for the water parameters	Difficult to compare
	Broader range of values	Value solely depends on the method of the operator
	Linear relationship with foulant	Independent from the pressure
SDI and MFI		Doesn't reflect the reverse osmosis process
		Dead-end operation
		Inaccuracy, precision problem
		Not suitable for high concentrated samples

The inaccuracy and the precision of the values were constant issues of these indexes, thus throughout the history of its implementation, MFI, which is derivation of SDI, was continuously adjusted and improved (Fig. 8).

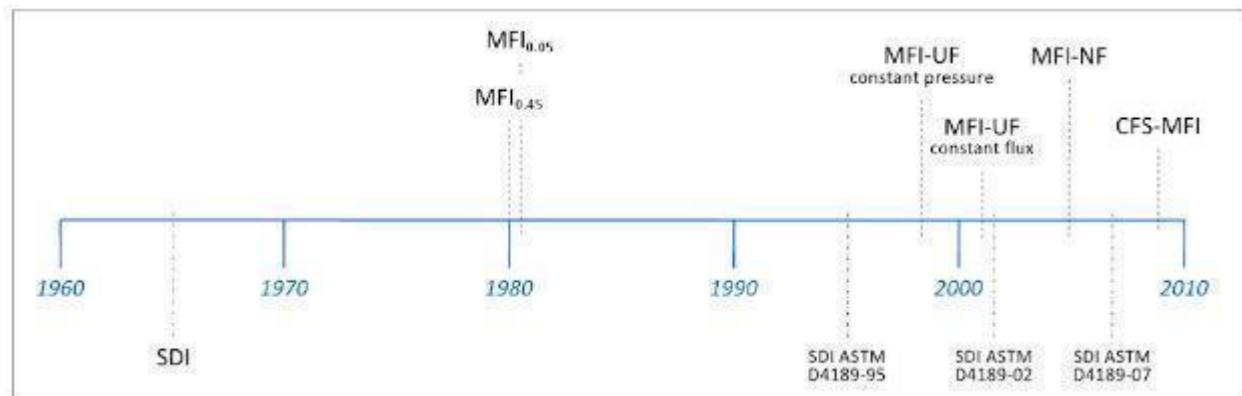


Figure 8. Chart of the history of fouling index developments (Salinaz-Rodriguez et al., 2010).

The methods of the measurements are constantly improved. The fouling indexes are following the trend to fully reflect the reverse osmosis membrane system. The detailed procedures of each index determination methodology will be further discussed.

3.3.2 Parameters affecting the MFI and SDI values

It is essential to fully understand the processes that take place during the dead-end mode filtration and the feed parameters that affect the filtration process, in order to scale the values generated as a fouling index. The following section provides information on the critical parameters that play the crucial role.

Membrane characteristics

The material, porosity, filter thickness, roughness, and membrane resistance

The standard pore size of the filter for the measurements of the MFI and SDI is 0.45 μm . However, it was proven that the particles smaller than 0.45 μm play a major role in the process of formation of foulant. MFI values derived with the filters with pore size of 10 kDa (unified atomic mass unit is unified kiloDaltons, as for reverse osmosis membrane pore sizes are too small) were 4 times higher than filters with 100 kDa (Salinaz-Rodriguez et al., 2015), thus for accurate measurement, it is suggested to use filters with lower pore sizes for the experiment.

Even though the latest version of ASTM state that the standard membrane/filter material to be used in SDI and MFI measurement would be cellulose acetate, researchers have introduced and proposed to utilize different membrane material available in the market such as polycarbonate, Polyvinylidene fluoride (PVDF), acrylic polymer etc. They all differ in many parameters like molecular weight cut off, pore distribution, form of the pore etc.

It was suggested, that the resistance of the membrane would be the core property affecting the derived index values. This can be supported by the experimental study of Alhadidi where several filters with the different materials were used for SDI measurement. SDI value was the highest when the Nylon 6,6 membrane was used and lowest when polycarbonate material was used. Nylon 6,6 expressed highest resistance (2.65) among other membranes, where membrane with polycarbonate material generated resistance of 0.39 (Alhadidi, 2009). This concludes that the higher filter resistance will result in higher fouling index.

Membrane resistance increases with the membrane thickness. With flux, pressure and viscosity data, the resistance can be easily calculated via Darcy's Law. In general, it is considered, higher resistance values will be obtained with high thickness and small pore sizes.

The roughness of the membrane has a linear relationship with the permeate flux, meaning the rougher the membrane the more water is filtered. This leads to a higher fouling rate (Hirose et al., 1996).

Filter charge can be expressed as zeta potential of the filter. The zeta potential is the potential at the plane of shear between the surface and solution where relative motion occurs between them. Because the interaction of colloidal particles with filter surfaces in aqueous media depends on the charge of the filter, determination of the filter surface zeta potential is critical to membrane fouling inspection (Elimelech et al., 1996). There are several methods for determining the zeta potential of the membrane, for example, the classic Fairbrother-Mastin and Helmholtz-Smoluchowski equations. Zeta potentials have an indirect correlation with the pH value, meaning the lower the pH the higher the zeta potential value will get.

Also, when the molecular weight cut off increases the zeta potential value decreases. In general, it is proven that the lower values of zeta potential results in bigger fouling resistibility, in other words, lower the zeta potential of the membrane the lower the SDI and MFI values will get.

Hydrophobicity of the membrane can be represented as a contact angle value. There are many ways to determine the contact angle, including the conventional telescope-goniometer method, Wilhelmy balance method, and the more recently developed drop-shape analysis methods (Yuan & Lee, 2013). The sample is considered to be hydrophobic if the value is below 90 degrees, 90 degrees is the upper limit of the hydrophilic membrane. The particles in the feed are mostly hydrophobic thus when SDI and MFI measurement is done with hydrophobic filter the interaction between the two same properties will result in higher values of MFI and SDI.

Parameters of filtration operation

The viscosity of the solution is largely dependent on its temperature. Increase in temperature will cause a drop in viscosity. The less viscous solutions have higher flux through the membrane thus higher foulant resulting in higher MFI and SDI values. However, experimental study of SDI under different temperatures was compared with theoretical results, and it was concluded that SDI value increase with temperature rise, in which sensitivity for error is higher at low temperature than high temperature (Alhadidi, 2010).

Several studies show MFI and SDI values have a high dependency on most of the feed flux variation. This can be explained by the theory of cake compressibility which results in higher resistibility. The reason flux is mentioned separately than pressure is that the resistibility also is a function of particle deposition velocity. Thus, it is recommended to examine MFI at the flux similar to reverse osmosis system which is 20 L/m²/h for the complete simulation.

Standard pressure for the SDI and MFI measurement is 207 kPa. SDI test at room temperature showed that SDI exhibit higher values when exposed to higher pressure. SDI under different pressures (50, 207 and 300 kPa) demonstrate clear dependency of the SDI on pressure. Theoretical results were in accordance with the experimental measurements under 207 and 300 kPa. However, this trend was not apparent during the experiment of 50 kPa (Alhadidi, 2010). Also, it is essential to take into account whether the applied pressure is deforming the filter that is used in the experiment. Deformation means, compaction of the pores, resulting in decline of the flux and higher resistibility.

Back in 1980, it was proven by Schippers that MFI has a linear relationship with particle concentration. Formazin solution of 1 mg/L correlated with MFI value of 1 s/L² (Fig.2) (Schippers, 1980). It is worth noting that it is essential to consider the size of the particle. No matter the concentration, if the particles lower than 0.45 µm make up most of the particles present in the feed, the standard experiment of MFI and SDI would not be sufficient for generating reliable results. It would not reflect the real fouling potential of the feed.

Study on the permeability of a negatively charged sulfonated polysulfone NF membrane with 1 kDa molecular weight cut-off (MWCO) showed that the permeability decreased when using ultra-pure water with NaCl (93–4380 mg/L) (Braghetta et al., 2011).

Ionic strengths present in the feed causes the pores on the filter matrix to tighten. This then will cause the results of MFI and SDI to be higher than it is since more foulants will develop on the membrane surface and the velocity of the deposition will be higher.

3.3.3 Alternative indexes that have derived from SDI and MFI

Normalized SDI (SDI₊) and SDI_v

Assuming the cake filtration is the main phase or the phase that takes up the most time compared to other two filtration phases, the normalized SDI takes into account the temperature correction, pressure difference, resistance and generates a line chart. Same author proposed volume-based SDI. This method (SDI_v) compares the initial flow rate with the flow rate after filtering the standard volume. It has a linear relationship to the particle concentration and is independent of testing conditions and membrane resistance (Alhadidi et al., 2011). It was concluded that SDI_v is by far the best SDI method available in the market.

MFI-UF and MFI-NF

To overcome the size exclusion disadvantage of the standard measurement, researchers suggest using ultrafiltration or nanofiltration membranes as a filter under the same filtration circumstances (Cai et al, 2018).

Even though the values derived from this experiment shows more accurate results than of traditional MFI, it still demonstrates several drawbacks (Boerlage, 2011). And it's mostly due the cake compressibility of the membrane during the filtration. Cake compressibility occurs when the porosity of the cake, formed in front of the filter, decreases, inducing increase in resistance. Higher pressure is demanded in order to overcome this resistance, meaning that the accuracy of the MFI and SDI indexes for the prediction of the RO/NF is not reliable.

Hence, researchers proposed constant flux MFI-UF (modified fouling index with ultrafiltration membrane) method, where the pressure is added to obtain a constant flux (cake filtration also take place under constant flux) over time and it is documented every second. It was concluded that the MFI-UF with constant flux can generate a reliable index for the particulate and colloidal fouling potentials, as follows: considering 1 bar of pressure increase over a 6-month period, and a deposition factor equal to 1 (worst case), the maximum MFI value is equal to 280 s/L^2 for flux equal to $20 \text{ L/m}^2/\text{h}$, or 1120 s/L^2 for flux $10 \text{ L/m}^2/\text{h}$ (Salinaz-Rodriguez et al., 2014).

But still, the results of MFI-UF and MFI-NF exhibit a fundamental limit, as they largely depend on the selection of the type of the membrane (permeability, material, pore size etc.), also the dead-end mode method for the MFI examination does not fully reflect the process in the cross-flow mode. Hence, the problem arises starting from the standardization of the method for the determination. Moreover, MFI and SDI methods neglect the fundamental process in the fouling process which is interfacial interaction. The fouling process takes place as a result of foulant-membrane and foulant-foulant interactions. These interactions can be described by Derjaguin Landau Verwey Overbeek theory (Kim, 2008). Also, it is worth noting that the results are not comparable between different papers because of the different objectives of the experimental assessments. For example, some use MFI for the determination of pretreatments for the reverse osmosis system while others use it in order to determine the suitable membrane for the filtration itself.

Combined fouling Index

MFI-UF on different test membranes showed inconsistent results in prefiltered and not filtered inlets. On the other hand, same authors present more efficient results when using combined fouling index (CFI), where MFI and SDI values were determined by hydrophilic

and hydrophobic membranes with 0.45 μm pore size, as well as ultrafiltration membrane with 100 kDa (Choi et al., 2014).

Results of SDI and MFI are incomparable, as the values depend on the character of the filters and pretreatment type. The MFI of hydrophobic (HP) membranes show higher results than of hydrophilic (HL) membrane. This can be explained by the fact that most of the foulants present in the feed have a hydrophobic character. MFI results of the ultrafiltration membrane showed the highest results (on average 10-fold), this is due to the fact that the particles and colloids smaller than 0.45 μm are the primary reason for the fouling. Values from the ultrafiltration and microfiltration pretreatment feed were not obtainable for MFI-HP and MFI-HL membranes, since the calculation of these values requires particles bigger than 0.45 μm .

In order to compare the values generated, the flux decline rate (FDR) was introduced. If the MFI values have a linear relationship with FDR, the result is considered reliable. SDI results were not linearly proportional to FDR as well as MFI-UF, MFI-HL, whereas MFI-HP shows the most accurate correlation.

The combined fouling index was calculated by summing the MFI values with the corresponding weighting factor. This then was plotted on the graph against FDR, which had a linear relationship to it ($R^2=0.9$). Allowing comparing the results derived from several different membranes it was concluded that the combined fouling index is a reliable index for the prediction of the fouling potential of the feed that at least was used in this experiment.

Cross-flow sampler MFI

In the cross-flow mode the mechanism that drives particles against the membrane surface is: convection by permeation drag and settling by gravity. However, the particles also transport away from the membrane and that is via inertial lift, shear-induced diffusion, and Brownian diffusion. The differentiation of the mechanisms is mostly based on the particle size distribution.

To take into account above-mentioned mechanisms, cross-flow sampler fouling index was introduced, where the feed goes through multiple pretreatments prior the cross-flow filtration system that simulate the reverse osmosis system, after which the SDI and MFI values are determined by the standard procedure of ASTM. The main difference of this measurement is that it involves selective removal of the particles that are most likely to develop a fouling (particles lower than 0.45 μm). Studies suggest that particles with size around 0.2 μm are most likely to develop most of the fouling (deposition velocity is the slowest for particles with sizes around 0.2 μm) (Adham and Fane, 2008).

Results showed that the SDI and MFI values generated after the CFS system, are significantly lower than of the standard measurement, whereas no significant difference was noticed when the pretreatment (ultrafiltration and microfiltration) systems were introduced. It was concluded that in the CFS system, separation of the particles does not depend on the size distribution of the particles but rather it relies on its hydrodynamics.

MPI-FFF

Novel method in determining the characteristics of membrane fouling was introduced by means of flow-field flow fractionation technique (fI-FFF). Membrane performance index

by means of flow fractionation technique (MPI-FFF) represents not only the capacity of the membrane to resist the fouling but also rejection rate of the foulants.

Field flow fractionation is a partitioning technique where the field is used in a perpendicular direction towards the solution which is flowing in the channel, resulting in a separation (particles ranging from 1 nm to 0.5 μm) of the particles depending on their diffusivity. This technique can be used in determination of the fouling indexes when membranes are applied at the entrance of the channel and the intensity of the separation can be inspected with detectors. This intensity is generated as a graph which is a function of channel flow rate, the concentration of the foulants and sample accumulation (Kim et al., 2008). High MPI-FFF values show low fouling.

Different membranes showed that the results derived from MPI-FFF experiment are in accordance with the salt rejection, foulant removal efficiency, and membrane resistance. Meaning, membranes with higher MPI-FFF values had better performance with above-mentioned parameters. It is also worth noting that the calculation of MPI-FFF takes account whether the particles deposited on the membrane or penetrated through it, which is neglected in SDI and MFI derivation calculations (Kim, 2009).

Multiple membrane array system (MMAS)

In recent studies specification of the fouling forming substances has been mentioned regularly. Organic foulants ranging from 30-300 kDa, from which the humic acids (3-7 mg/L in seawater) take up the major part, are prone to cause the most severe fouling in reverse osmosis system. Subsequently it was proposed if the fouling indexes could target the substances that are most likely to foul the membrane.

Multiple membrane array system utilizes several different types of membranes such as microfiltration, loose and tight nanofiltration. This then allows to target the fouling substances in a way that it can be categorized by size distribution. Large particles will be filtered by microfiltration membrane, followed by filtration by loose nanofiltration to capture the colloids. In the end the organic matters can be captured by tight nanofiltration membrane. The filtration runs under different pressure to membrane to membrane. These than allows obtaining MFI of different substances, as follows: particle MFI, colloid MFI and organic MFI. In order to show the brief description of the procedure of the experiment, Figure 9 is provided.

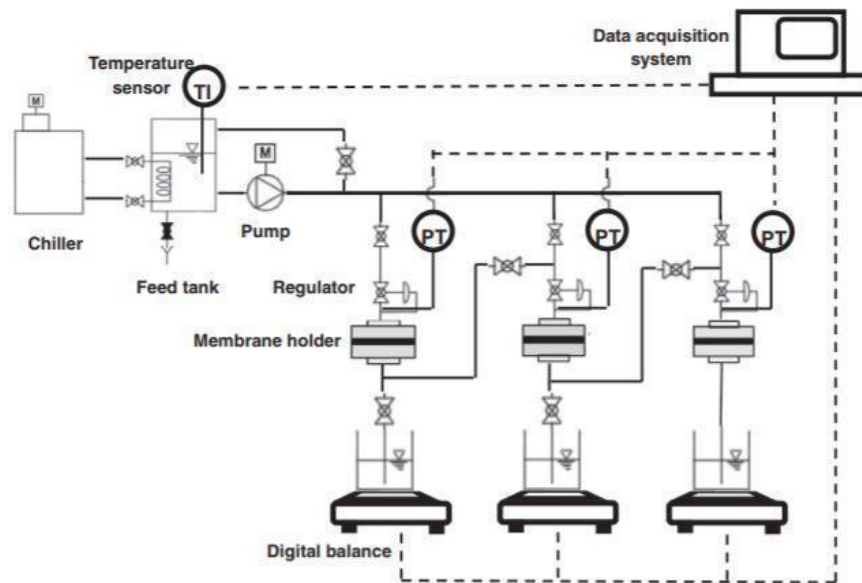


Figure 9. Description of the multiple membrane array system (Ju et al., 2015).

Moreover, the MFI values derived from MMAS can simulate the flux decline of the reverse osmosis system with same feed, concluding that MMAS as reliable method for predicting the fouling potential of the feed (Ju, 2015).

Dimensionless fouling index

Dimensionless fouling index was proposed. The equation of the cake compressibility model is simplified by the Ruth's equation, as a result new linear dimensionless equation is derived, which is dependent on the membrane compressibility, cake compressibility and the bulk concentration of the feed. The novel equation is promising but for now no experimental evidence is available (Messaudene & Naceur, 2014).

4. Materials and methods

This master thesis project consists of three separate phases. First phase is the SDI and MFI standard measurement. The derived values will be used to interpret the correlation to the water quality parameters. Moreover, these values will be compared with the values derived from the INSPECTOR apparatus.

Second part of this master thesis is trial with reverse osmosis pilot plant with the same samples used in the SDI and MFI trial. Lastly, examination of the separation efficiency of the reverse osmosis pilot plant in terms of nutrients heavy metals and pesticides was conducted as well.

This chapter will first of discuss about material and method RO trial, followed by SDI and MFI experiment trial.

4.1 Reverse osmosis pilot plant unit

Apart from the MFI and SDI measurement unit reverse osmosis pilot plant was built. Scheme of the reverse osmosis pilot plant unit is illustrated on the Figure 10. The membrane that is used in the experiment is reverse osmosis membrane with thin film composite TFC-3013-400 membrane which consists of three layers:

- Cross-linked fully aromatic polyamide (0.3 μm).
- Polysulfone (45 μm).
- Non-woven fabric polyester (100 μm).

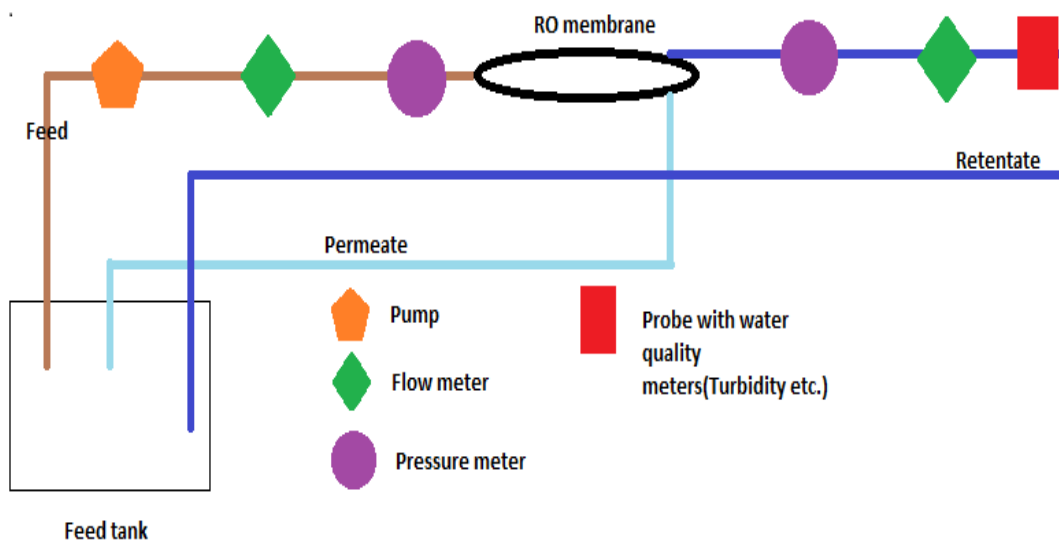


Figure 10. Reverse osmosis pilot plant sketch.

The feed flows from the feed tank through the pump in to the membrane where the retentate and permeate is separated and collected in to the feed tank again. Meaning the system run in a loop way. Pressure sensors are placed before and after the membrane, so does

the flow meters. On the first period of the experiment, pressure and flow rates of the retentate were collected, after which it was rearranged on the permeate side. The probe for the water quality measurement were connected on the retentate side at first and then it was switched to the permeate side as well. Water quality parameters that were measured: temperature in °C, turbidity in NTU, total dissolved salts in mg/L, pH and, conductivity in $\mu\text{S}/\text{cm}$. The technical information of the reverse osmosis pilot plant is provided in Table 3 and illustrated in Figure 11.

Table 3. Technical description of the water quality measuring devices.

Device	Description	Data	Capacity
Tank		75 L	
Pump	Membrane pump	Max. 9.0 bar. 130L/h	32 VDC
RO	Reverse osmosis membrane		
P1	Pressure sensor before membrane	0-16 bar/ 0-10 VDC	12-30VDC
P2	Pressure sensor after membrane	0-16 bar/ 0-10 VDC	12-30VDC
F1	Flowmeter before membrane	G1/8";0,015-1 L/min	5-24 VDC
F2	Flowmeter after membrane	G1/8";0,015-1 L/min	5-24 VDC
M	Multimeter		
Q1	Conductivity meter	0.01 $\mu\text{S}/\text{cm}$ - 1.999 S/cm	
Q2	pH meter	pH 0-14	
Q3	ORP meter	-2000 mV - 2000MV	

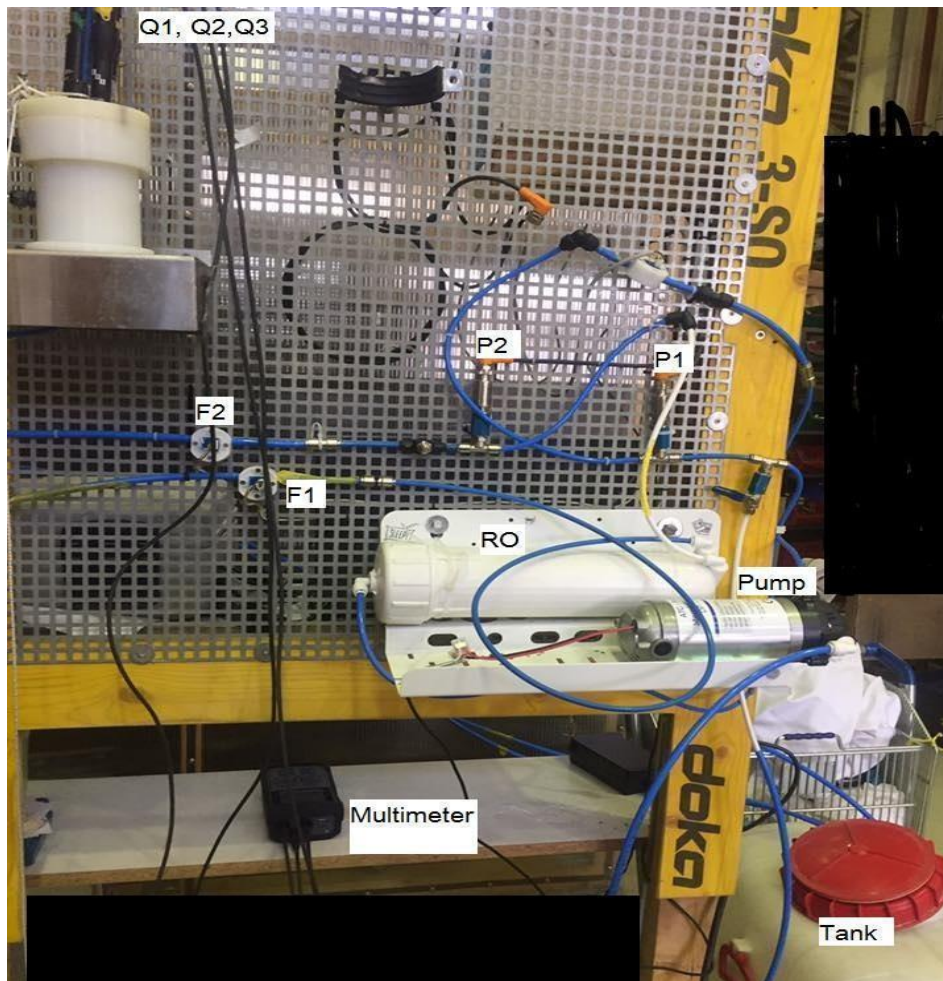


Figure 11. The reverse osmosis pilot plant.

Moreover, the pressure of the feed and the retentate side, as well as flow rate was measured every second throughout the filtration time. The filtration of each sample continued for 5 hours. The documentation is done with the help of arduino microprocessor.

4.2 Microcontroller Arduino

Arduino Uno is ATmega328P microcontroller with 14 digital pins, 6 analog inputs with USB connection (Fig. 13). Arduino was connected to the flow meter and pressure sensor which was placed on the feed and retentate side and before and after membrane, respectively. With the right coding, it can read the values every second and give them out to the computer as digital information, which can be converted into a text document with additional program CoolTerm, with the actual timestamp.

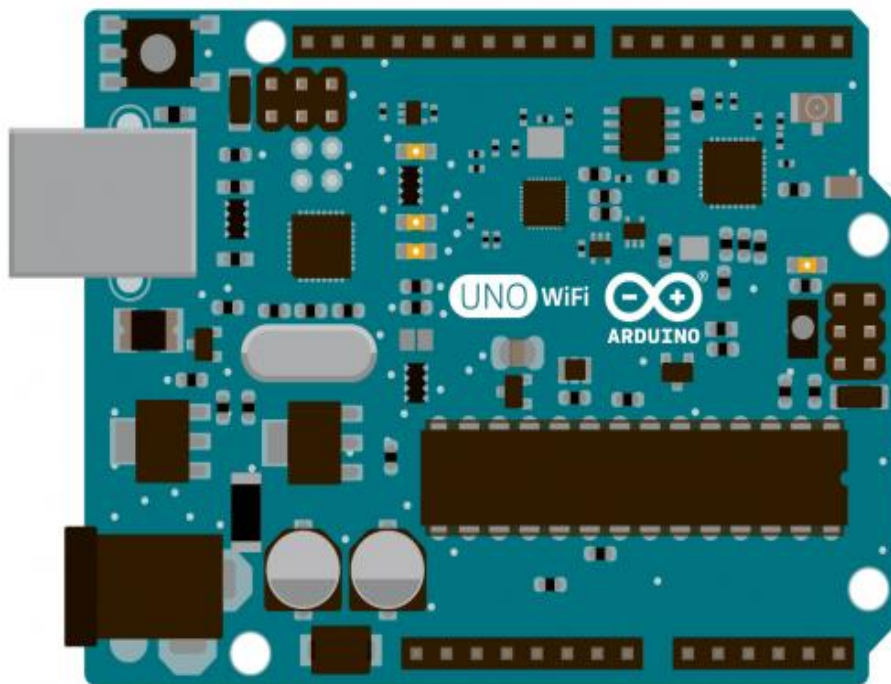


Figure 12. Arduino Uno board.
Technical information about the board is provided in the following Table 4.

Table 4. Technical information of the Arduino microprocessor board.

Microcontroller	ATmega328P	DC Current per I/O Pin	20 mA
Operating Voltage	5V	DC Current for 3.3V Pin	50 mA
Input Voltage (recommended)	7-12V	Flash Memory	32 KB (ATmega328P) of which 0.5 KB used by boot loader
Input Voltage (limit)	6-20V	SRAM	2 KB (ATmega328P)
Digital I/O Pins	14 (of which 6 provide PWM output)	EEPROM	1 KB (ATmega328P)
PWM Digital I/O Pins	6	Clock Speed	16 MHz
Analog Input Pins	6	LED_BUILTIN	13
Width	53.4 mm	Length	68.6 mm
		Weight	25 g

For our project, work of Arvind Sanjeev (<https://diyhacking.com/arduino-flow-rate-sensor/>) was used for coding the Microcontroller.

Flow rate was obtained thanks to the hall effect. Inside the flowmeter there are rotors placed, which moves by the force of the liquid that was introduced in the path. Spear of the rotor, which is connected to the Hall Effect, gives out voltage which transfers to the electric current. Arduino measures the number of pulses, from which we can derive the flow rate in liters per hour. B.I.O-Tech e.K. flow meter was used on our project.

The calibration of the Arduino microprocessor was done with reverse osmosis water. The cumulative volume of permeate was collected on the digital weight, whilst documenting the filtration time (noted as actual values on Table 5). Calibration factor was derived as follows (Table 5 and Fig. 14):

Table 5. Calibration of the flow rate measurement.

Arduino values [ml/min]	Actual values [ml/min]	St.dev
1830	1830	0
3630	3630	0
5340	5430	63.6
7130	7230	70.7
9000	9030	21.2
10800	10830	21.2
12470	12630	113.1
14220	14430	148.5
15950	16230	197.9
17820	17800	14.1

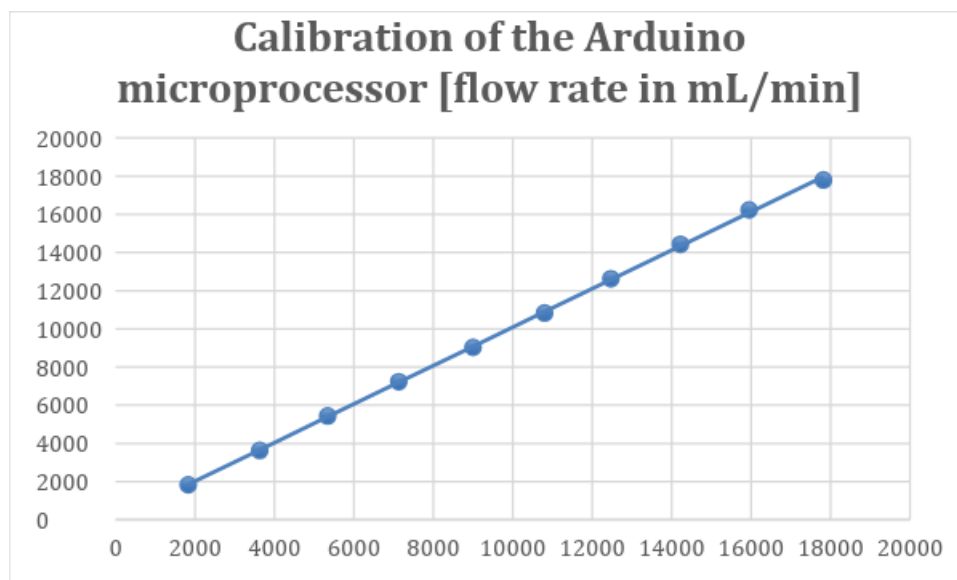


Figure 14. Calibration of the flow meter.

Pressure sensors were from IFM electronic GmbH, which can measure the pressure in a range of 0-16 bar. These values will give out Analog signal of 0-10 V, which Arduino Microcontroller can convert into millibars.

4.3 SDI and MFI measurement

SDI and MFI measurement setup were assembled in succession to the standard measurement of the ASTM and the sketch scheme is provided in Figure 9 (ASTM D4189-07(2014)).

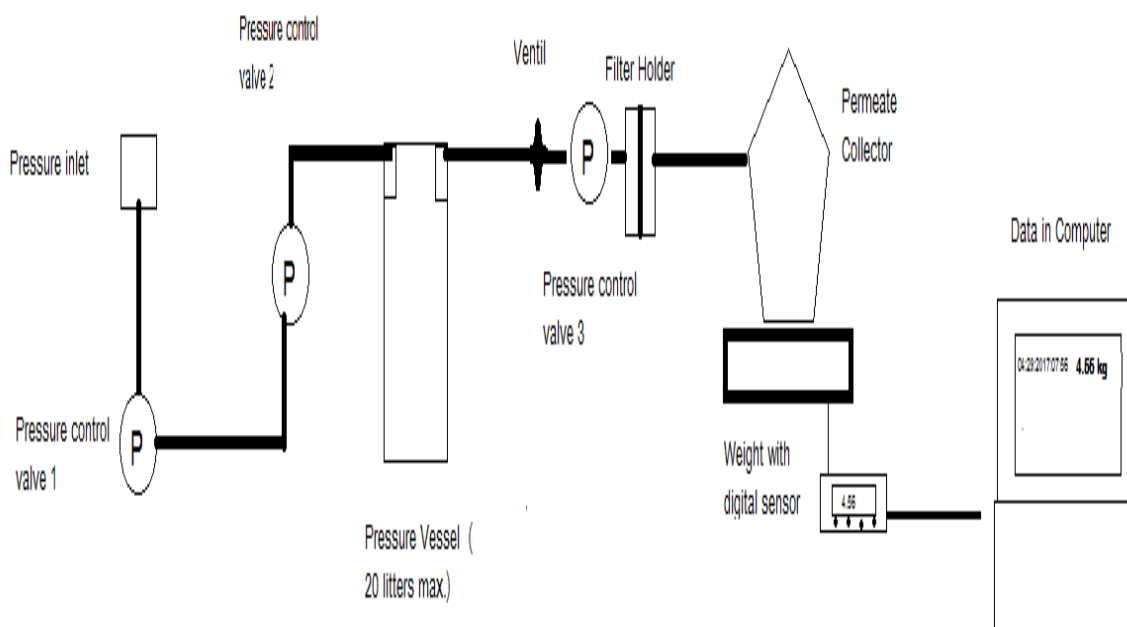


Figure 13. Sketch scheme of SDI and MFI measuring set up.

The pressure inlet with 2 pressure control valves, is connected to the vessel with a capacity of 20 liters. On the other side of the vessel is the filter holder where the filter is placed with a ventil, which allows the pressure to pass in. Filtrate is collected in a container from which the weight is measured on the digital weight. The weight of the filtrate is documented with timestamp in computer via USB. Technical information of the equipment is provided in Table 6.

Table 6. Technical information about the equipment of the SDI and MFI trial.

<u>SDI measuring device:</u>	
Manufacturer	Purification products Co.
Model	PPC-1000K
Serial number	398
<u>Filter</u>	
Manufacturer	Merk Millipore Ltd.
Type	0.45 µm HAWP; 0.8 µm AAWP, 0.22 µm GSWP
Material	Mixed cellulose ester

Calculation of SDI

Time that is required to filter the first 500 ml is noted following the notation of the second time that is required to filter the second 500 ml after 15 minutes of filtration.

The values are inserted in the following equation:

$$SDI = \frac{t_x - t_o}{T} * 100 \quad (22)$$

where,

- t₀ - is the initial time to collect 500 milliliters
- t_x - is the second time to collect 500 milliliters
- T - is the total filtration time

As a result, we can obtain SDI15, which is percentage decrease in flux per minute. If the part ($\frac{t_x - t_0}{t_x} \times 100$) of the equation is more than 75, than the second notation of the 500 milliliters should be done after 10, 5 or 2 minutes, from which SDI10, SDI5 and SDI2 values will be derived.

Calculation of MFI

MFI measurement is obtained from the same set up as SDI. The main difference is that the flux is documented every second throughout 15 minutes. Documented values can be generated in Eq. (23), which depicts the cake filtration phase of the filtration:

$$\frac{t}{v} = \frac{\mu * R_m}{dP * A} + \frac{\mu * I}{2 * \Delta P * A_M^2} * V \quad (23)$$

where,

- V - total filtrate volume (L or m³)
- T - time (s)
- A_M - area of the membrane (m²)
- dP - applied pressure (Pa)
- R_M - membrane resistance (m⁻¹)
- μ - water viscosity (Pa s)
- I - fouling potential index (m⁻²)

The graph t/V versus V is used to derive the MFI and it is given in equation (24).

$$MFI = \frac{\mu * I}{2 * dp * A_M^2} \quad (24)$$

where

- μ - Viscosity (N*s/m²)
- I - Fouling potential (m⁻²)
- dp - Net driving pressure (N/m²)
- A - Surface area of filter (m²)

By definition, MFI is equal to the minimum slope tgα of the graph t/V versus V under circumstances where the filtration was done with filters with area of 13.8 m² (47 mm diameter), where temperature of the water is held constant 20°C and the pressure equal to 30 psi (207 kPa). MFI is corrected for the pressure and temperature.

$$MFI = tg\alpha * \frac{\mu_{20}}{\mu} * \frac{dP}{dP_0} * \left(\frac{A_M}{A_{M0}} \right) * 2 \quad (25)$$

where:

- μ- viscosity of the feed (Pa*s)
- μ₂₀ - viscosity constant at 20°C, 0.001 (Pa*s)

Δp_0 - constant pressure, 207000 (Pa)

A_0 - 0.00138 (m²)

A- area of the filter (m²)

As the viscosity depends drastically on temperature, correction is applied by equation

$$\mu = 0.497 * (T + 42.5)^{-1.5} \quad (26)$$

where,

μ - viscosity of the feed (Pa*s)

T- temperature of the feed (°C)

Apart from the MFI and SDI measurement the water quality parameters were constantly checked before and after the filtration and those parameters include: temperature in °C, turbidity in NTU, total dissolved salt in mg/L, pH, and conductivity in $\mu\text{S}/\text{cm}$.

Membrane filters were dried in the oven with the temperature of 105°C for one hour, weighed afterwards and were used for the filtration. After the filtration, the filters were dried once more for another one hour and then weighed again. The values can be used to determine the suspended solids present in the feed in milligram per liter.

4.3.1 INSPECTOR apparatus from Convergence Ltd

Same samples used in MFI/SDI setup was used for INSPECTOR apparatus, in order to see whether there are differences in the values. Technical information of the INSPECTOR apparatus is provided in Table 7.

Table 7. Technical information of the INSPECTOR apparatus.

Power supply	LiPo battery powered Charged with adapter Sufficient for more than 50 tests
Main protection for consumers Power consumption	Via charging adapter
Protection class Conformity	I JP40
pH range	Normal 4-10 Cleaning 2-12
Ambient temperature	10-40 °C
Theoretical measuring range	SDI 0 – 6 MFI 0 -12 s/L2
Accuracy in nominal measuring range SDI: 0.5 – 5 MFI 0.1 – 8 s/L2	5%
Interface	HMI: color touchscreen Data :USB 2.0
Dimensions	300 x 200 x 200 mm
Weight	8 kg
Water inlet	6 mm hose via push-in connector
Water outlet	6 mm hose via push-in connector
Water temperature	10 - 40 °C
Pump capacity	15 – 300 mL/min PWM controlled at 207 kPa
Filter cartridge	ASTM 0,45 µm
Temperature sensor	± 0.1 °C in the range 5 – 45 °C

The INSPECTOR device not only can measure the SDI and MFI but also SDI+, SDIv. Measurement techniques are fully complying the ASTM standard D418907. It is fully automated with flow sensor, pump with pressure and temperature sensors. The INSPECTOR comes with its own costume designed filters. Technical characteristics of the filter which is inside the filter cartridge is provided in Table 8:

Table 8. Technical information about the filter of the INSPECTOR apparatus.

Mean pore size	0.45 micrometer
Diameter	25 mm, flat
Thickness	115-180 micrometer
Material	hydrophilic, mixed cellulose nitrate and cellulose acetate
Pure water flow	500 mL per 25 - 50 s
Pressure	91.4 - 94.7 kPa
Bubble point	179-248 kPa

Components of the device:



Figure 14. INSPECTOR apparatus

The components of the INSPECTOR are illustrated in Figure 14. The feed can be sucked in through 6mm hoses into the inlet (1), and the filtrate will be discharged from the outlet (2). On the color touchscreen (3) it can be seen the options, such as power on/off, archive with the data of the last measurement as well as settings are shown. The power button (4) allows to turn on and off the device. Membrane holder (6) is connected to the inlet (5) through 6mm hose.

Measurement procedure:

1. Pressing the power button will turn the device on.
2. The feed is connected via 6 mm hoses through an inlet, labeled as “in”.
3. Effluent will be discharged from the “out” outlet through 6mm hose.
4. The membrane will be held on the membrane holder with an O-ring.
5. The measurement procedure will start by pressing the start button

The measurement will continue around 20 minutes, after which the values will be shown on the screen. Moreover, the amount of water that is filtered is documented with the time series and pressure values each second. These than can be obtained from the INSPECTOR via USB. The values from the INSPECTOR were placed in the template of the calculation of the first part of the MFI and SDI measurement. This allows an opportunity to compare the MFI and SDI calculation methodology.

Same water quality parameters as the previous trial were measured before and after filtration.

4.4 Sample preparation

4.4.1 SDI and MFI measurement

For the SDI and MFI measurement reverse osmosis water, tap water, waste water from the technical hall of the university, surface water from Ukraine as well as commercial salt (NaCl) was used with variety of concentration factors.

The waste water sample was collected from the outlet of the waste water treatment plant in the technical hall of the university. For low diluted samples (high concentration of waste water sample) experiment could run with one-time filling. For high diluted samples, the refill of wastewater sample was taken from the outlet, as each experiment had three trials. The content of the waste water differs every day, thus there was an effort to have the refill on the same range as the previous refill in terms of water quality parameters such as turbidity and conductivity (standard deviation is also calculated in results and discussion chapter).

Samples from the Ukraine was firstly thoroughly mixed by homogenizer for 10 minutes, after which was diluted in the measurement vessel.

Commercial salt was mixed with RO in a separate flask, from which it was diluted for trial. All samples were diluted with reverse osmosis water.

Reverse osmosis water was used prior every experiment to have a reference value also to clean the system. The samples were prepared in the vessel for the measurement. In order to keep the samples homogenous for the trial, thorough steering was done before the filtration. However, there is a possibility of the particles depositing after the steering was done. The

samples with lower concentrations were measured first followed by more concentrated samples. This is in an effort to reduce the possible error.

The concentration factors were back-calculated from the added milliliters of the sample in 20 liters (the SDI and MFI measuring vessel has capacity of 20 liters) of reverse osmosis water to the milliliters in 1 liter. For example, 1.25:1 means 25 ml is diluted by reverse osmosis water until it reaches the vessel capacity of 20 liters and it is provided in Table 9. Concentration factor 1 means undiluted sample. Each sample had gone through 3 trials.

Table 9. Concentration factors of the samples for SDI and MFI.

Sample	Concentration factor	Sample	Concentration factor	Sample	Concentration factor
<i>Reverse osmosis</i>	1	<i>Ukrainian surface water</i>	2.5:1	<i>Waste water</i>	2.5:1
<i>Tap water</i>	1		5:1		5:1
<i>Commercial salt</i>	1.25:1		7.5:1		7.5:1
	2.5:1		12.5:1		10:1
	5:1		17.5:1		12.5:1
	7.5:1		22.5:1		17.5:1
					22.5:1
					25:1

INSPECTOR trial samples

Samples for the INSPECTOR apparatus were less concentrated than the previous trial as it was impossible to run full filtration due to fouling rate. It is due to the fact that the filters from INSPECTOR apparatus are smaller than the filters that were used for the BOKU instrument. The samples went through the same preparation procedure as BOKU instrument trial. Concentration factor was back-calculated from the added milliliters of the sample in 8 liters (INSPECTOR measurement is done with 8 liters of sample) of reverse osmosis water to the milliliters in 1 liter, for example, 2.5:1 means 20 milliliters in 8 liters. Each sample was filtered 3 times, as well (Table 10).

Table 10. Samples for the INSPECTOR trial.

Sample	Concentration factor	Sample	Concentration factor	Sample	Concentration factor
<i>Waste water</i>	2.5:1	<i>Reverse osmosis</i>	1	<i>Ukrainian surface water</i>	15:1
	3.7:1	<i>Tap water</i>	1		31:1
	4.4:1	<i>Commercial salt</i>	2.5:1		44:1
	5:1		6.25:1		56:1

	5.6:1		12.5:1
	6.9:1		18.7:1
	8.1:1		
	9.4:1		
	10.6:1		
	12:1		
	13:1		

4.4.2 Reverse osmosis trial samples

Samples for the calibration of the Arduino microprocessor

As it was necessary to calibrate Arduino microcontroller for the pressure and flow sensors, the membrane was filtered with variety of inlets before the actual experiment. From each experiment 75 liters feed was prepared in a tank which has a capacity of 100 liters. The list of these samples is shown in Table 11. Samples were run in the same order as it is provided in the Table 11. The waste water samples had a concentration factor ranging from 2.5:1 (3 trials) than after which sample 5:1 (3 trials), followed by 10:1 (3 trials), lastly sample 22.5:1 (3 trials). Whereas, the sample with the commercial salt had a concentration factor of 1.25:1. The retentate and permeate was connected back to the feed.

Table 11. Numbers of samples for the calibration of the flow rate and pressure values of the reverse osmosis plant trial.

Sample	Total number of the trials
Reverse osmosis	12
Tap water	12
Waste water	12
Commercial salt	6

After the calibration was done, the real experiment started with reverse osmosis water, after which the tap water, waste water, surface water from Ukraine, lastly the sample with commercial salt was prepared in the same tank (75 liters) as the calibration trial and was filtered for 5 hours each. Throughout the filtration time, the water quality parameters such as pH, temperature, conductivity, oxidation reduction potential was measured. The concentration factor is provided in the following Table 12. Concentration factor was back-calculated to ratio of 75 liters, for example, 5:1 means 375 milliliters of sample was diluted by reverse osmosis water until the whole feed reached to 75 liters (375 milliliters in 75 liters). Each sample was filtered 3 times, as well (Table 12).

Table 12. Concentration factor of the reverse osmosis trial.

	Concentration factor		Concentration factor		Concentration factor
Waste water	2.5:1	Ukrainian surface water	2.5:1	Salt water	1.25:1
	5:1		5:1		2.5:1
	7.5:1		7.5:1		5:1
	10:1		12.5:1		7.5:1
	12.5:1		17.5:1		
	17.5:1		22.5:1		
	22.5:1				
	25:1				

In order to have comparable data, the samples for the experiment were in order of and in accordance to the MFI and SDI experiment.

Moreover, there was an effort to deviate the pressure valve in order to examine its effect on the membrane performance. There was only one pressure valve, so it was possible to deviate permeate or retentate side flow rate at a time. Also, depending on the inlet the maximum and minimum allowable pressure was different.

RO removal efficiency trial sample preparation

The reverse osmosis membrane was used to examine its removal efficiency of the pesticides, fertilizers and heavy metals. Atrazine, diurone and simazine were selected as a representative for the pesticide, nitrate as a fertilizer (NO₃) and copper, zinc for the heavy metals.

Stock solution, with fertilizer, pesticide and heavy metal, was prepared in the flask of 10 liters and was thoroughly mixed throughout the trial. From the prepared 10 liters stock solution, 500 mL was withdrawn and added to the tank with the capacity of 100 liters.

First, stock solution samples were mixed with 75 liters reverse osmosis, then after with tap water. The retentate and permeate flows were connected back to the feed (filtration is in a circuit way as well). The concentration of the chemicals in the stock solution is shown in Table 13.

Table 13. Concentrations of the stock solution.

Chemical compound	Concentration per in mg/L
Simazine	1.5
Atrazine	1.5
Diurone	1.5
Zinc	60
Copper	60
Nitrate	20

Materials and methods

Each experiment had 2 trials. Description of the sampling for the chemical examination from the old and new membrane is listed in the Table 14 and Table 15.

Table 14. Sampling of the old reverse osmosis membrane trial with chemical substances.

Inlet	Sampling source
<i>Reverse osmosis + Stock solution</i>	Tank
	After 10 minutes of filtration, permeate
	After 5 hours of filtration, permeate
	Retentate
<i>Tap water + Stock solution</i>	Tank
	After 10 minutes of filtration, permeate
	After 5 hours of filtration, permeate
	Retentate

Table 15. Sampling of the new reverse osmosis membrane trial with chemical substances.

Inlet	Sampling source
<i>Reverse osmosis + Stock solution</i>	Tank
	After 10 minutes of filtration, retentate
	After 5 hours of filtration, retentate
	Permeate after 5 hours of filtration
<i>Tap water + Stock solution</i>	Tank
	After 10 minutes of filtration, retentate
	After 5 hours of filtration, retentate
	Permeate after 5 hours of filtration

The experiment was done on the old membrane first. After which the membrane was replaced by the virgin membrane.

Microbial investigation of the reverse osmosis membranes

Microbial investigation was examined in order to assess the removal efficiency of the biocide. Biocide for the experiment was prepared by the guidance of the technician from the WTG. The membrane is rinsed with reverse osmosis water for 30 minutes. Then after, 5 mL of biocide is added to 1 liter of reverse osmosis water and this feed is run through the system in circuit way for one hour, after which the tap water is pumped through for 20 minutes.

Materials and methods

Samples are taken from the permeate and retentate side of the membrane operation. The samples were examined on the flow cytometer which shows the live and dead microorganism cells present in the water.

5. Statistics and calculation

Calculation of MFI

The calculation of the modified fouling index was done on the excel template (Figure 15). The cumulative volume of the filtrate, that was collected on the digital weight, was sent to the computer with the time stamp to the computer and it was inserted in the excel template for the calculation.

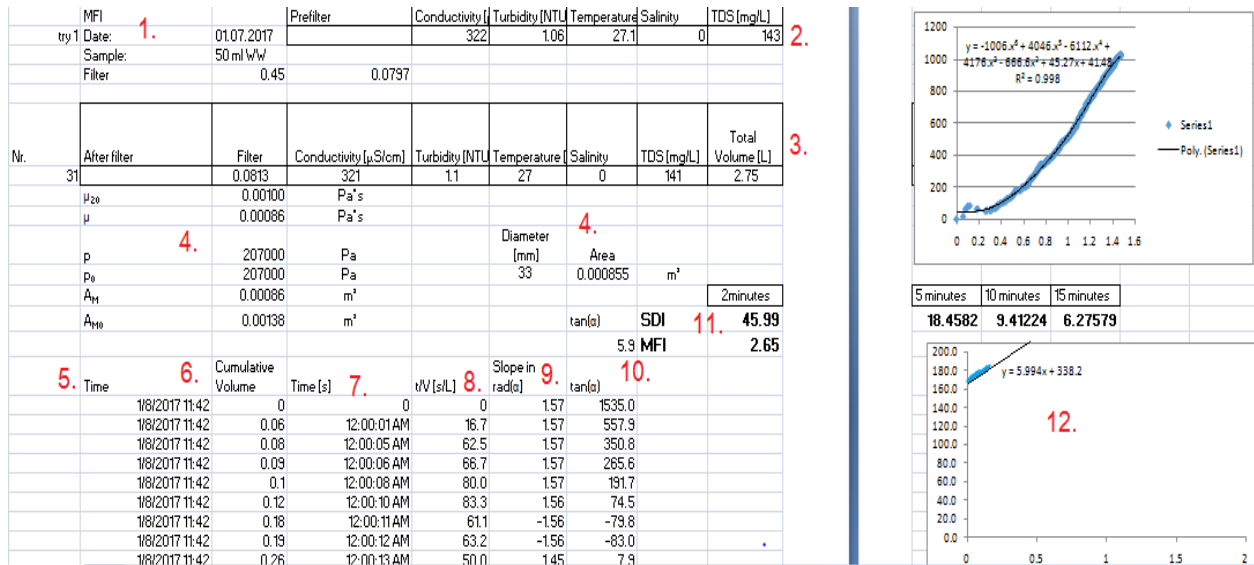


Figure 15. Calculation of the MFI.

The date, sample, filter pore size is noted on 1. The water quality parameters before the filtration (2) and after the filtration (3) with the weight values of the filters are placed. The pressure values, with filter area and diameter are inserted as constants. Time (5) with the date, cumulative volume in liters (6.) are firstly placed in separate columns. Then after the seconds are calculated by multiplying the time (5.) by 86400. From this t/V (8) is generated and shown as a graph. The fouling indexes are calculated (11).

For MFI value the increase rate in rad (α), as well as tan (α) needs to be calculated. Increase rate in rad(α) was calculated by ATAN function on excel, from which tan (α) value can be calculated. The tan (α) drops right at the beginning of the filtration and then it rises again. And at some point, the tan (α) decreases or stays constant for period of time, and it is shown on Figure as marked in blue. This is when the cake filtration is assumed to start. The t/V values corresponding to this phase is used for the MFI calculation (marked in green) (Fig.16).

1/8/2017 11:45	0.71	12:03:23 AM	285.9	1.57	710.2
1/8/2017 11:45	0.71	12:03:26 AM	290.1	1.57	710.2
1/8/2017 11:45	0.71	12:03:26 AM	290.1	1.57	710.2
1/8/2017 11:45	0.71	12:03:27 AM	291.5	1.57	710.2
1/8/2017 11:45	0.72	12:03:29 AM	290.3	1.57	709.3
1/8/2017 11:45	0.72	12:03:33 AM	295.8	1.57	709.3
1/8/2017 11:45	0.72	12:03:35 AM	298.6	1.57	709.3
1/8/2017 11:45	0.72	12:03:36 AM	300.0	1.57	709.3
1/8/2017 11:45	0.72	12:03:38 AM	302.8	1.57	709.3
1/8/2017 11:45	0.72	12:03:40 AM	305.6	1.57	709.3
1/8/2017 11:45	0.73	12:03:42 AM	304.1	1.57	708.6
1/8/2017 11:45	0.73	12:03:45 AM	308.2	1.57	708.6
1/8/2017 11:45	0.73	12:03:48 AM	312.3	1.57	708.6
1/8/2017 11:45	0.73	12:03:51 AM	315.4	1.57	708.6
1/8/2017 11:45	0.73	12:03:52 AM	317.8	1.57	708.6
1/8/2017 11:45	0.74	12:03:54 AM	318.2	1.57	708.3
1/8/2017 11:45	0.74	12:03:58 AM	321.5	1.57	708.3
1/8/2017 11:46	0.74	12:04:00 AM	324.3	1.57	708.3
1/8/2017 11:46	0.75	12:04:01 AM	321.3	1.57	708.3
1/8/2017 11:46	0.75	12:04:04 AM	325.3	1.57	708.3
Click to add footer					
Click to add header					
1/8/2017 11:46	0.75	12:04:06 AM	328.0	1.57	708.3
1/8/2017 11:46	0.75	12:04:07 AM	329.3	1.57	708.3
1/8/2017 11:46	0.75	12:04:13 AM	337.3	1.57	708.3

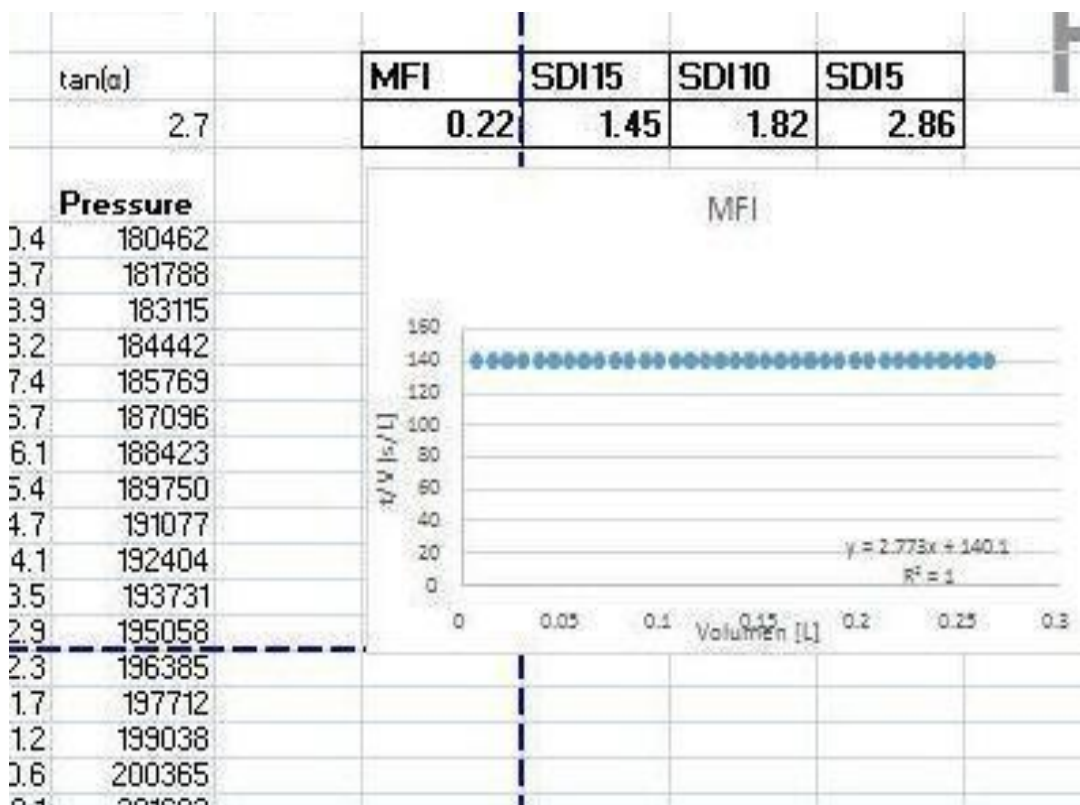


Figure 16. Generation of MFI.

Then the corresponding t/V vs. V values are highlighted into a separate graph from which the $\tan(\alpha)$ is used for the MFI calculation that is in accordance to the ASTM.

Detection of the outlier values of the INSPECTOR apparatus

As it was mentioned in result and discussion section, the values from the INSPECTOR apparatus requires an outlier detection and elimination. In order to highlight the outliers, the graph was plotted with the values from INSPECTOR. Z score, modified Z score and Interquartile range methods (IQR) methods were examined. IQR method was the most suitable as it was reflecting the plotted graph.

The data points are clustered at some central value. Interquartile method highlights the central value from the data, so that the outlier or the data point which divides the data in four equal sized groups. 1st and 3rd quartiles are equal to 25th and 75th percentile. Whichever inside this range is considered as median and whichever outside this range is an outlier. Turning this theory into equation:

$$\begin{aligned} &\text{first quartile} - 1.5 \cdot \text{IQR} \\ &\text{third quartile} + 1.5 \cdot \text{IQR} \end{aligned}$$

Values falling outside this range are outliers. The outlier detection was done to each triplet from each concentration factor. Example of the interquartile calculation is provided in Table 16. The SDI15 could not be generated (45 milliliters of waste water were added into 8 liters of reverse osmosis water) as the apparatus was giving out error sign. The upper and lower bounds are calculated from three values generated from three trials and the outlier is pointed out in blue color. This outlier is not included in further discussion.

Table 16. The outlier detection of the waste water sample (45:8) for the INSPECTOR apparatus via interquartile method.

Concentration factor	SDI5	SDI10	SDI15	MFI
45:8	15.9	9.3		5.3
45:8	16.2	9.4		0.005
45:8	16.1	9.4		5.8
Quartile	SDI5	SDI10	SDI15	MFI
Q1	16.00	9.35	#NUM!	2.65
Q3	16.15	9.40	#NUM!	5.55
IQR	0.15	0.05	#NUM!	2.90
upper bound	16.38	9.48	#NUM!	9.90
lower bound	15.78	9.28	#NUM!	-1.69

The comparison test on the mean values of the SDI and MFI values

The comparison of mean values was based on the statistical hypothesis testing, where the null hypothesis depicts that there is no variation exist between variables or that the single variable is no different than it’s mean. The alternative hypothesis is the one you would believe if the null hypothesis is concluded to be untrue. In order to determine, whether if the null hypothesis should be rejected or not, P value is generated. When a P value is less than or equal to the significance level (0.05), you reject the null hypothesis.

The means of the values have been generated and calculated via R software. T-test and Kruskal-Wallis test methods have been used in this master thesis work.

T-test is used to compare two groups of parametric values and Kruskal- Wallis test was used to compare multiple groups with non-parametric values.

6. Results and discussion

In this section, firstly the SDI and MFI results obtained from the BOKU equipment will be discussed, followed by the comparison of the values derived from the INSPECTOR apparatus. For this, multiple statistical analysis has been used.

Moreover, the reverse osmosis membrane experiment results will be reviewed.

6.1 Calculation of MFI

The MFI is extremely sensitive index. The values deviate from slight change in the content of the water matrices used for the experiment (for example calcium content), operating parameters such as pressure and air bubble removal technique. Most importantly, calculation methodology e.g., the identification of the cake filtration phase's exact starting point is quite difficult. As it is mentioned before, the MFI is the minimum tangent alpha of the slope of the t/V vs. V curve of the cake filtration phase. The cake filtration starting point changes when there is minimum delay in air bubble removal and slight change in the content of the water, even if it does not fully contribute to the fouling. As a result, the MFI from same trial can be valued as 2 to 200.

It is essential to configure the methodology for the identification. Time and the cumulative filtrate volume are 2 factors that help to indicate the cake filtration phase. These 2 factors vary depending on the sample and the filter pore size.

The starting point of the filtration phase lays (can be seen on the graph t/V vs V) sooner with the concentration increase and smaller pore size of the filters, meaning the more concentrated the sample and the smaller the pore size of the filter the earlier the cake filtration phase starts. The results of our experiment showed that for the filters with pore size $0.45\ \mu\text{m}$ the cake filtration phase starts no earlier than from 0.75 liters of cumulative filtrate. For the $0.2\ \mu\text{m}$ filters the cake filtration starts at least from 0.3 liters with 38 seconds. On the other hand, the filters $0.8\ \mu\text{m}$ need at least 1.7 liters and 65 seconds.

It was concluded that the measured amount of time (in seconds) to reach the cake filtration phase is more accurate indicator as it has more sensitive reaction to the concentration change (Fig.17).

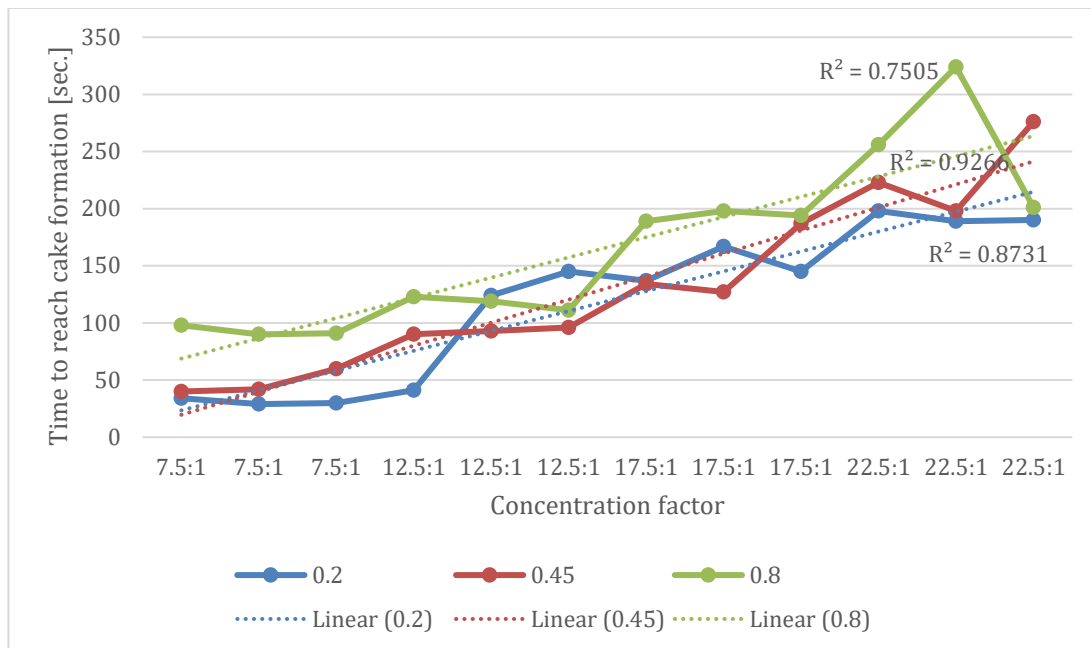


Figure 17. Correlation of the concentration factor and the duration of time that take up to reach cake filtration phase (Sample from the Ukrainian surface water).

It can be seen from the Figure 17 that for this specific sample, each increase in concentration factor prolongs the cake filtration phase starting point by around 50 seconds.

The experimental study by Krondorfer with the filter size of 0.45 μm concluded that cake filtration starts at least after 1 liter of the filtrate (Krondorfer, 2015). It is safe to say that the indicating factors (cumulative filtrate or duration of the time to take up to reach the cake filtration) may vary with other samples for further experiments. On the other hand, it is not impossible to have a precise methodology for the calculation.

Factors affecting duration of the filtration phases:

- Sample preparation. As it is already mentioned, there is a high risk of possible precipitating events of the particles right after the rinsing was done. It can cause the first trials to have longer pore blocking phase, allowing more cumulative filtrate to pass through the filter than the next trials. However, there was no apparent trend where the values increased with the number of trials.
- It is highly suggested to rinse the whole system with reverse osmosis water in between the trials. If this step is skipped than the sample to be filtered is more fouling with shorter pore blocking phase.
- Deformation of the filter due to the operator's mistake (e.g. hole in the filter).

The major reason for the varying filtration phase durations would be pressure inlet. BOKU instrument requires manually to open the cap on top of the filter holder to remove all the air bubbles inside it. This requires only 1-2 seconds (in some cases more) however the effect is tremendous as there is a high risk of water loss while opening the cap. Another question is whether the air is completely removed.

6.2 Dilution series

First, the examination of the concentration factor will be discussed. Turbidity and the suspended solids are the most feasible water quality parameters that reflect the concentration factor. Suspended solids were calculated from the weight of the filter before and after the filtration (Fig 18) and its relation to the concentration factor is shown in Figure 19.

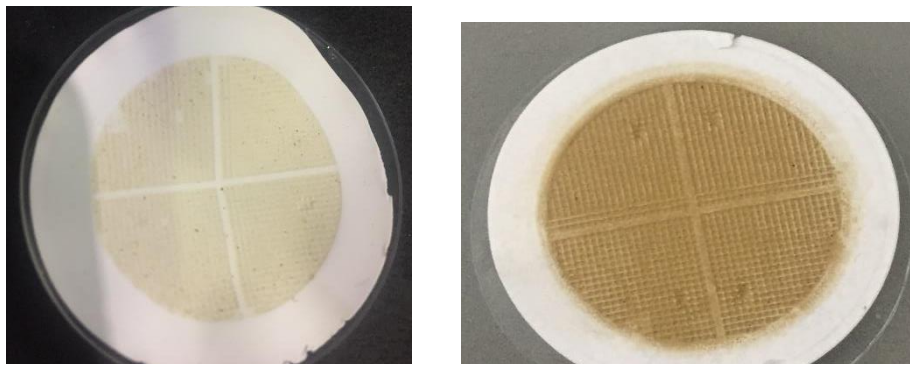


Figure 18. 0.45 filters after the filtration of surface water from Ukraine (left) and waste water (right) sample and drying in the oven for 1 hour.

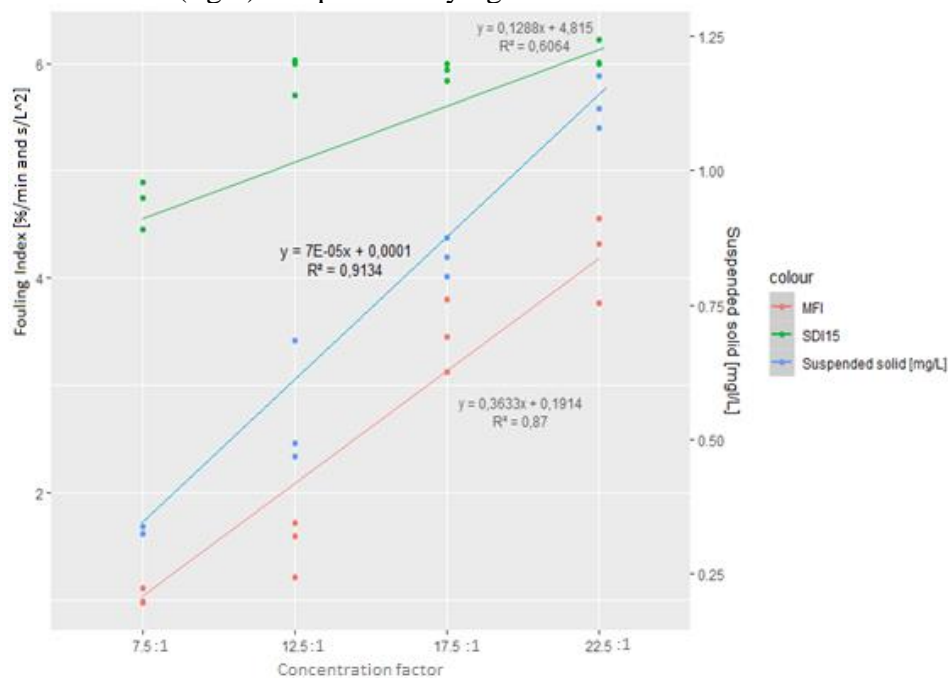


Figure 19. Correlation of the suspended solids and indexes to the concentration factor.

Even though the results for this particular sample (surface water from Ukraine) depict a high correlation between suspended solid and concentration factor ($R^2 = 0.9$), there is also a

high risk of particles settling down after the thorough stirring, resulting in non-homogenous mixture.

As observed in Figure 19, when the concentration factor is 7.5:1, the suspended solid is around 0.3 mg/L, where the SDI15 equal to 4.4 with MFI value equal to 1.1. Slight jump in the content of the suspended solids has been observed when the concentration factor is 17.5:1, at which MFI values have reacted more sensitive, following this trend, whereas SDI15 value have decreased instead. Once again, these errors might have originated from the rapid particle settlement. The correlation of turbidity values to the concentration factor is shown on Figure 20.

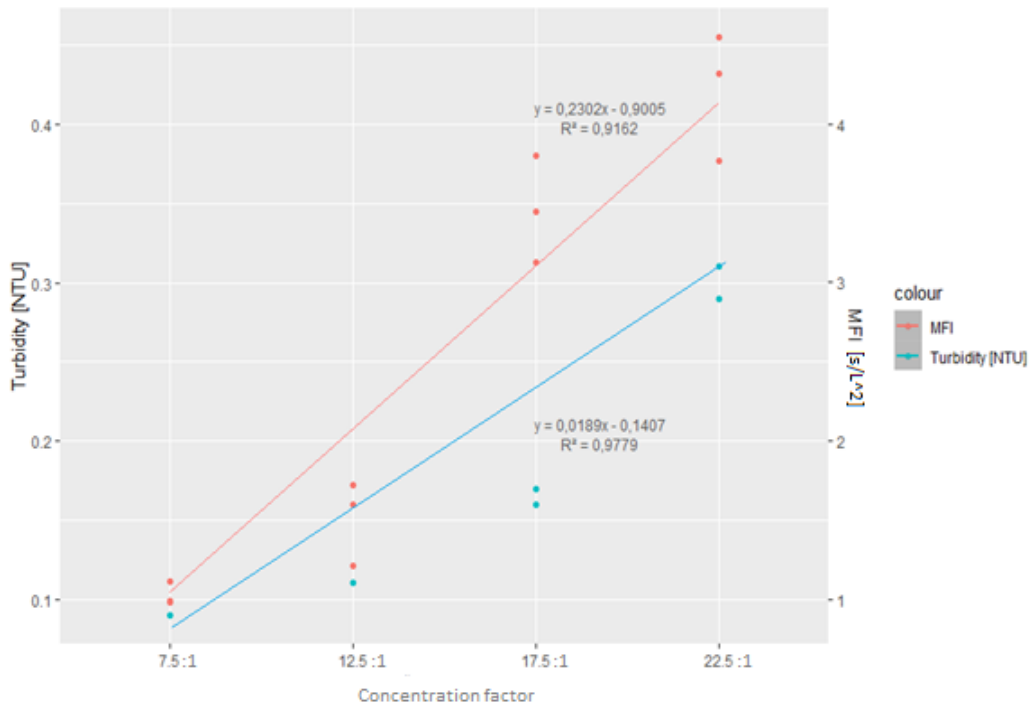


Figure 20. Concentration factor vs. Turbidity.

In Figure 20, the concentration factor of the waste water sample diluted with reverse osmosis water is shown. Both MFI and turbidity values have high correlation to the concentration factor. When the concentration factor increases by 5 units the turbidity increases by on average 0.15 NTU. On the other hand, the MFI increases per (on average) 1 unit. From this trial it can be concluded that for the sample of waste water, the increase in turbidity by 0.15 NTU causes the MFI to increase by 1 unit. This is extremely sensitive correlation, compared to other studies. For instance, experimental study by Johir with sea water concluded that decrease in MFI value by 10 s/L² caused the turbidity value to drop from 0.3 NTU to 0.2 NTU (Johir, 2009). On the other hand, the experimental study on the feed water remineralization by Skovby and Poffet imply that the feed with 0.3 and 0.2 NTU having MFI 0.1 s/L² and 0.3 s/L² values respectively, which is in the same range as our experiment (Skovby and Poffet, 2011).

6.3 SDI15 and MFI values

In succession to the ASTM the SDI15 and MFI values derived from filter with 0.45 μm pore size will be first discussed, followed by the further values with different filters.

6.3.1 The SDI15 and MFI results from the filters with pore sizes of 0.45 μm diameters.

As it was mentioned in the materials and methods chapter, samples were tested three times each. The standard deviations of each triplicates are provided in Table 17.

Table 17. Standard deviations of SDI15 and MFI values.

Sample	Concentration factor	SDI15 [%/min]	MFI[s/L ²]
Commercial salt trial	2.5:1	4.61	3.01
		4.56	3.12
		4.62	3.33
	Standard deviation [%]	3.09	16.23
Ukrainian surface water	17.5:1	6.00	3.13
		5.84	3.45
		5.94	3.80
	Standard deviation [%]	8.1	33.5
Waste water sample	5:1	6.43	3.59
		6.54	3.20

		6.50	3.22
	Standard deviation [%]	5.57	21.96

Standard deviation of MFI values is on average 4 times higher than SDI values. No apparent correlations of standard deviation and concentration factor were detected.

The experimental work from Rinaldi Rachman shows SDI of tap water ranging from 3.96-4.80, implying 8.1-8.8% in standard deviation (Rachman, 2011), which is in the same range as discussed results.

Reverse osmosis and tap water trials.

Reverse osmosis water and tap water are commonly used for the calibration for the newly developed fouling index instruments.

Interesting results have been obtained from the reverse osmosis water and tap water samples from the technical hall of the University (Table 18). Reverse osmosis sample should not have any particulate and colloidal matters; thus, the SDI and MFI values should be low.

Table 18. MFI and SDI 15 values of the reverse osmosis and tap water trials.

Sample	SDI15 [%/min]	MFI [s/L²]
Tap water	4.53	2.14
	4.63	2.15
	4.33	2.09
Reverse osmosis	1.17	0.42
	1.23	0.84
	1.11	0.77

These results imply that there is significant amount of particles present in these samples, especially for the tap water sample.

Reverse osmosis samples also show higher results than what was expected, as the suggested values for MFI should not exceed more than 0.22 [s/L²] (Convergence, 2015). The expected SDI15 value for tap water should also not exceed more than 3 [%/min] (Peck, 2017).

Two assumptions can be made for this experiment: the tap water and reverse osmosis water from the technical hall of the university does not comply with the standards of SDI15=3 [%/min], or the measuring equipment might be contaminated inside the system, hoses, pressure valve etc.

6.3.2 SDI2, SDI5, SDI10, SDI15 and MFI

According to the ASTM, it is relevant to report the SDI10, SDI5 and SDI2, when the plugging rate is more than 70% and it is provided in the Table 19.

Table 19. Comparison of SDI2, SDI5, SDI10, SDI15 and MFI values.

Sample	Concentration factor	SDI2 [%/min]	SDI5 [%/min]	SDI10 [%/min]	SDI15 [%/min]	MFI [s/L²]
Ukrainian surface water	7.5:1	10.2	8.78	6.70	4.75	1.11
	7.5:1	10.1	7.99	7.10	4.89	0.99
	7.5:1	10.8	7.23	7.30	4.45	0.98
	12.5:1	11.9	11.9	7.85	5.70	1.21
	12.5:1	14.5	14.5	8.35	6.03	1.72
	12.5:1	14.7	13.7	9.55	6.00	1.60
	17.5:1	31.2	16.1	8.75	6.00	3.13
	17.5:1	27.1	11.8	7.69	5.84	3.45
	17.5:1	25.0	15.4	8.57	5.94	3.80
	22.5:1	31.9	16.3	9.10	6.22	4.55
	22.5:1	27.8	15.8	7.96	6.01	4.32

Results and discussion

	22.5:1	25.9	15.6	7.77	6.00	3.77
--	--------	------	------	------	------	------

The data in the table would be values generated from the experiment with surface water from Ukraine. MFI values increase on average 4 times (from 1.11 to 4.55) when the concentration factor increase three times (from 7.5:1 to 22.5:1).

On the other hand, the SDI15 and SDI10 values have slightly increased relative to MFI values, whereas SDI5 and SDI2 values increased on average 2 times with the same increase rate in concentration factor. The results also support the fact that the MFI is far more sensitive to the particulate matters present in the medium than the SDI values.

From the Table 19 it can be concluded that starting from the sample 12.5: 1 the operator has to use an adequate pretreatment as the SDI15 values are over 5 (Kemperman, 2011). From this it can be concluded that the SDI15 values are on average 46% higher than the MFI value for surface water from Ukraine, and for all the samples the SDI15 is on average 40% higher than the MFI values.

Correlation of all indexes to the concentration factor is provided in the Figure 21.

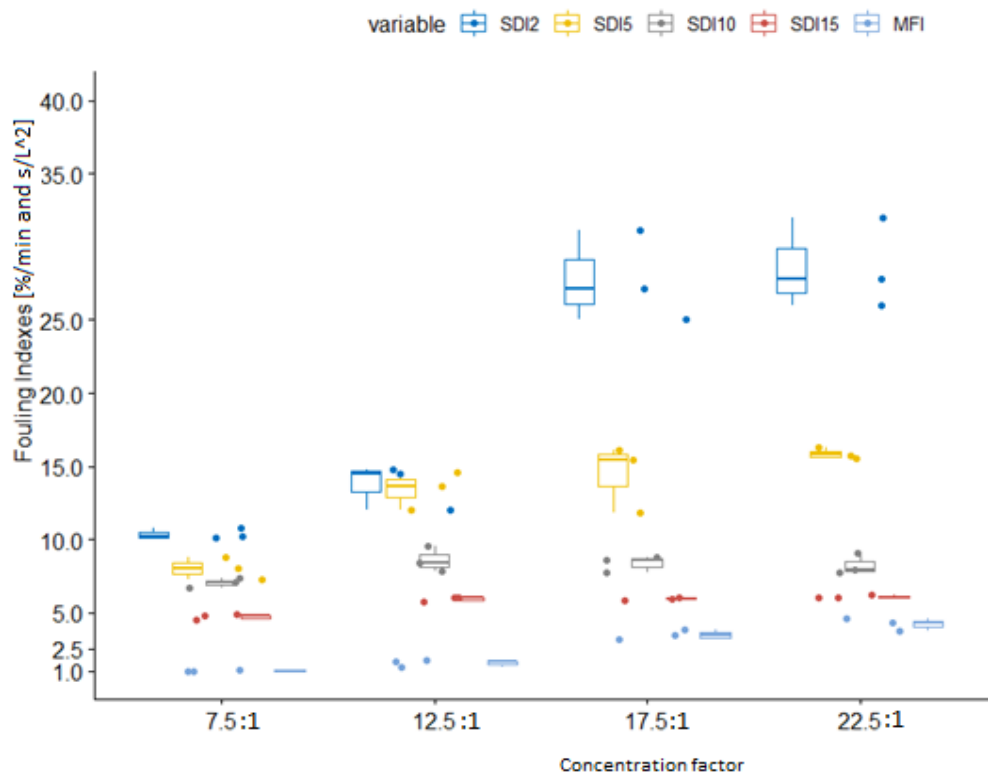


Figure 21. Comparison of the indexes relative to the concentration factor.

R- Squared values are generated in Table 20.

Table 20. R-squared values of the indexes.

Index	SDI2 [%/min]	SDI5 [%/min]	SDI10 [%/min]	SDI15 [%/min]	MFI [s/L ²]
R-squared	0.84	0.74	0.23	0.66	0.91

The highest correlation rate was recorded from the MFI value with $R^2 = 0.9$. From the SDI indexes, SDI2 has the highest correlation factor with $R^2 = 0.84$, followed by SDI5 with $R^2 = 0.74$ and SDI15 with $R^2 = 0.66$. The SDI2 and SDI5 values have bigger standard deviation than any other indexes and this distribution increases with the concentration addition.

Moreover, the most diluted sample of the surface water from Ukraine has lower value of MFI, and almost same value of SDI than tap water sample (surface water from Ukraine sample was diluted with reverse osmosis water).

Tap water samples have an electric conductivity of 230-280 $\mu\text{S}/\text{cm}$, and turbidity equal to 0.22 NTU, whereas the sample from the Ukraine with 7.5 concentration factors has a conductivity value equal to 66 $\mu\text{S}/\text{cm}$, and turbidity being equal to 0.09 NTU. This also supports the fact that the MFI reflects the water quality parameters better than the SDI.

6.3.3 Values obtained from the filters with different pore sizes

In order to examine the effect of the filter pore size on the index values, filters with pore size diameter of 0.2, and 0.8 μm were introduced to the experiment. The filters were all same material and manufacturer. MFI, SDI2, SDI5, SDI10 and SDI15 values were generated.

MFI values obtained from the waste water sample are provided on the Figure 22.

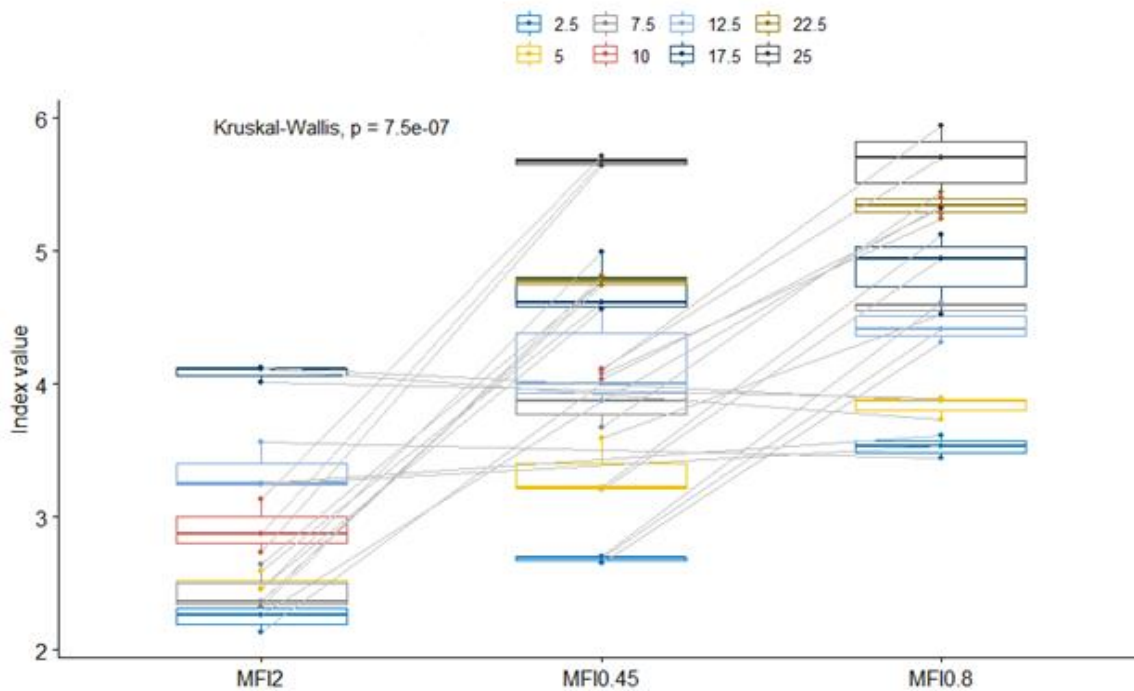


Figure 22. Correlation of MFI relative to the concentration factor.

Results and discussion

In order to compare the mean values of multiple groups on non-parametric data set, Kruskal-Wallis (pairwise analysis of variance) test was applied (this includes the confirmation of the Levene's test). The P value is significantly low ($p = 7e-10$, lower than when SDI15 and MFI were compared). Moreover, the MFI from filter 0.8 μm has almost as same result as MFI 0.45.

The calculation of the R-squared values is generated in Table 21.

Table 21. Calculation of the R-squared of MFI values derived from different filters.

Filter size	MFI0.2	MFI0.45	MFI0.8
R-squared	0.91	0.88	0.69

The MFI value obtained from the 0.2 μm filters have the highest correlation to the concentration factor ($R^2 = 0.91$), followed by the filter 0.45 μm ($R^2 = 0.88$), whereas the filter 0.8 μm has the lowest correlation rate ($R^2 = 0.69$). The trend has been observed in all samples and from SDI values too, from which the SDI2 expressed highest correlation rate to the concentration factor (Fig. 23).

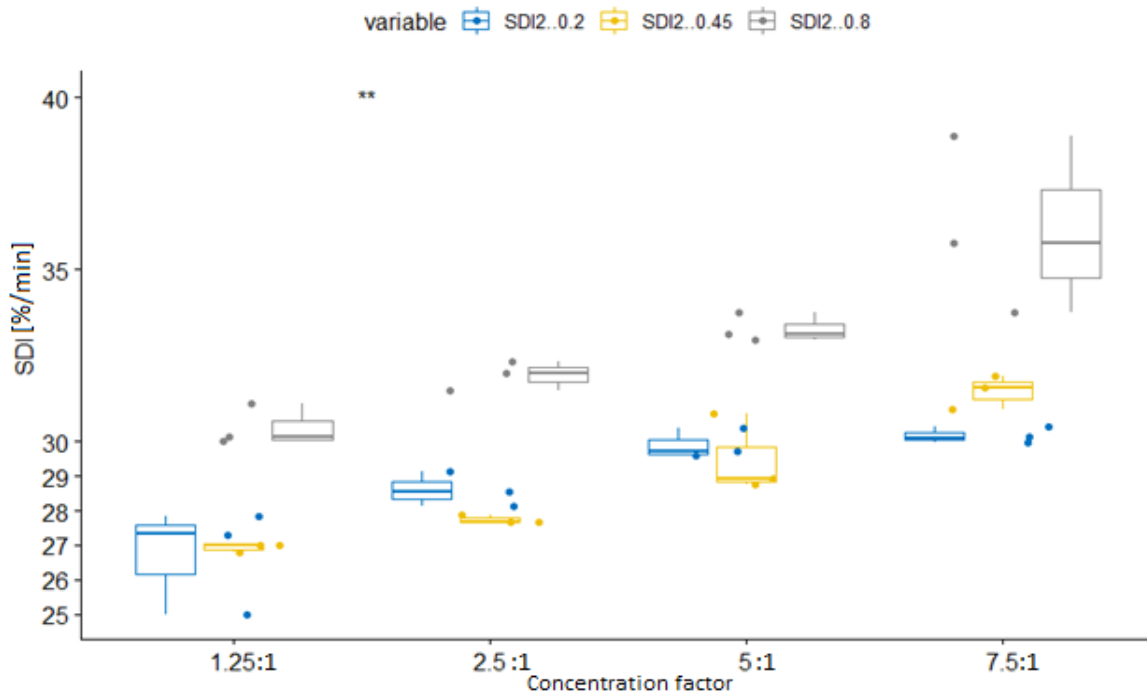


Figure 23 . Concentration factor vs. SDI2 values from different filters. Summary of the Figure 23 is shown in Table 22.

Table 22. Summary of the SDI2 values.

	SDI2.0.2	SDI2.0.45	SDI2.0.8
Min.	25	26.77	30.01
1st Qu.	28.05	27.5	31.41
Median	29.35	28.32	32.65
Mean	28.85	28.91	32.94
3rd Qu.	30.02	30.86	33.74
Max.	30.43	31.91	38.86

As it is seen, the filter 0.2 μm has a higher correlation despite the sample and index difference. As previously observed, this can be explained by the size exclusion mechanism of the filtration, as the fouling is majorly developed by the particles smaller than 0.45 μm . Therefore, bigger diameter of the filters, will not fully reflect the presence of the smaller particles in the feed which lead to a misleading information. Moreover, this experimental work also supports the current trend of fouling index research work. It is proposed by many researchers to use smaller pore sized membranes such as ultrafiltration membrane (MFI-UF) etc. (Boerlage, 2003).

6.3.4 Relations of the indexes with the water quality parameters

In order to describe the quality of the water, water quality parameters, such as conductivity, turbidity, pH, temperature and salinity were measured before and after each filtration. It is essential and of big importance to understand the relationship of the water quality parameters to each other.

Good correlations have been obtained from the water quality parameters and indexes (except from the temperature). For all the values, MFI values have higher correlation rates than the SDI values and in between the water quality parameters, turbidity and conductivity have shown highest correlation. Correlation of MFI to conductivity is shown on Figure 24.

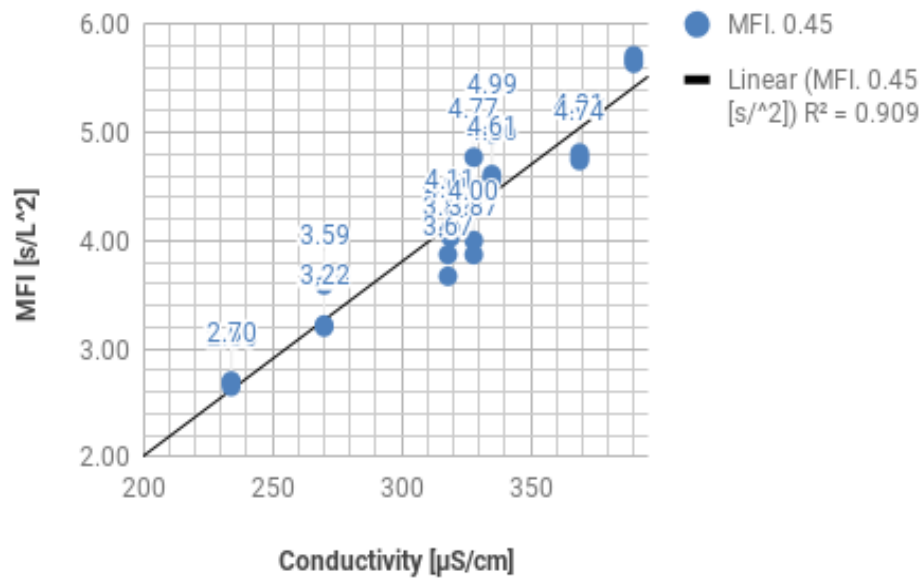


Figure 24. Conductivity vs. MFI 0.45 [s/L²] graph, from the waste water sample (R² = 0,91).

Figure 24 depicts that in the conductivity range between 250 and 400 µS/cm on average 100 µS/cm difference will cause the MFI value to change in about 1.5 unit. The correlation of MFI and conductivity values from the commercial water sample is given in Figure 25.

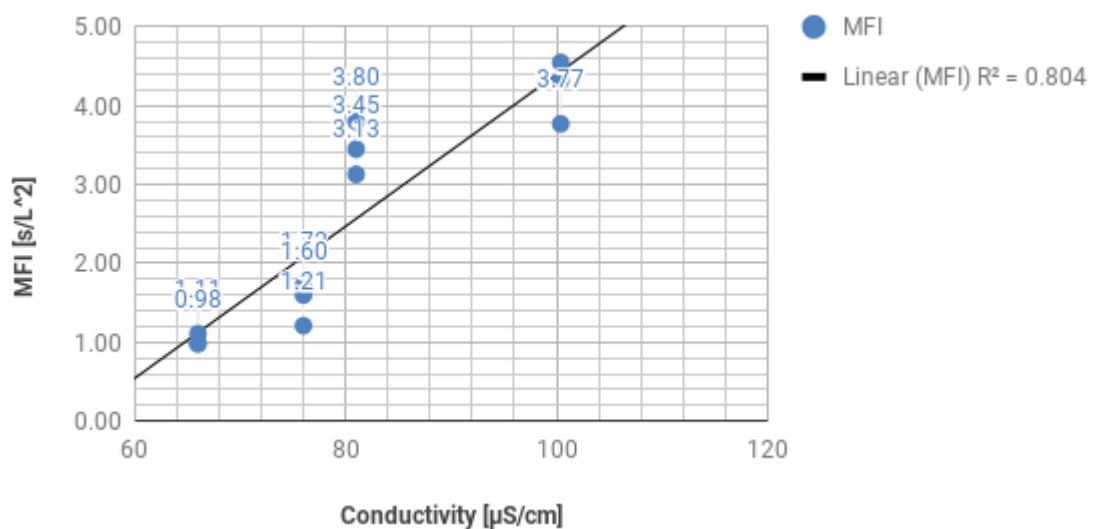


Figure 25. Conductivity vs. MFI 0.45 [s/L²] graph, from the sample from the surface water from Ukraine.

From the Figure 25 it can be concluded that in the range of conductivity of 60 to 120 $\mu\text{S}/\text{cm}$, MFI values increase by on average 1.5 s/L^2 when the conductivity increase by 17.2 $\mu\text{S}/\text{cm}$. This can be only concluded for the sample from Ukraine. On the other hand, correlation graph of MFI and conductivity of the commercial salt sample ($R^2 = 0,56$), shows that in the range of 5 to 19.79 mS/cm , the change in the MFI by 1 unit causes the conductivity values to increase by 7 mS/cm . Thus, the conductivity correlation to the MFI dependent on the sample type. The correlation of the turbidity values to the MFI from waste water trial is shown on Figure 25.

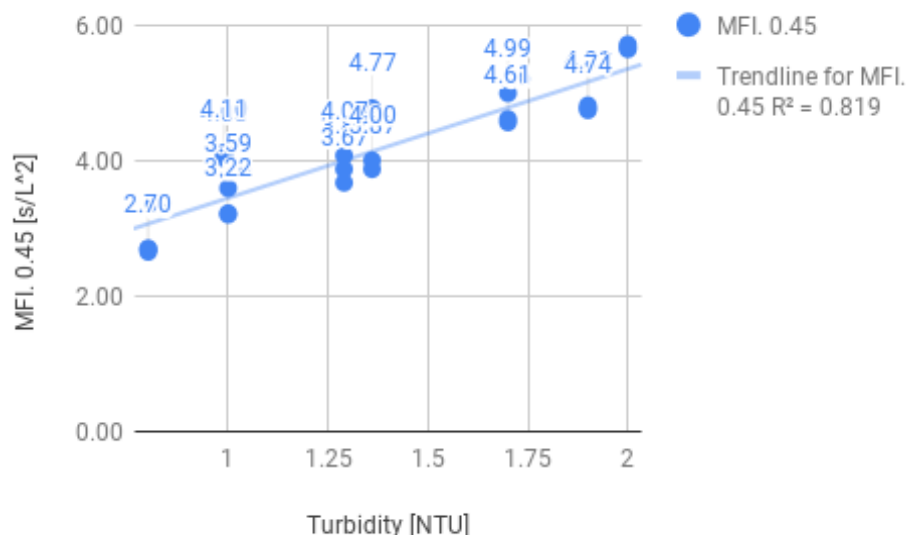


Figure 26. Turbidity NTU correlation to the MFI [s/L^2] ($R^2 = 0,82$), from waste water sample.

From the Figure 26 it can be concluded that 0.25 NTU causes the MFI values to increase by on average 0.6 units. Correlation of turbidity to MFI is shown on Figure 27.

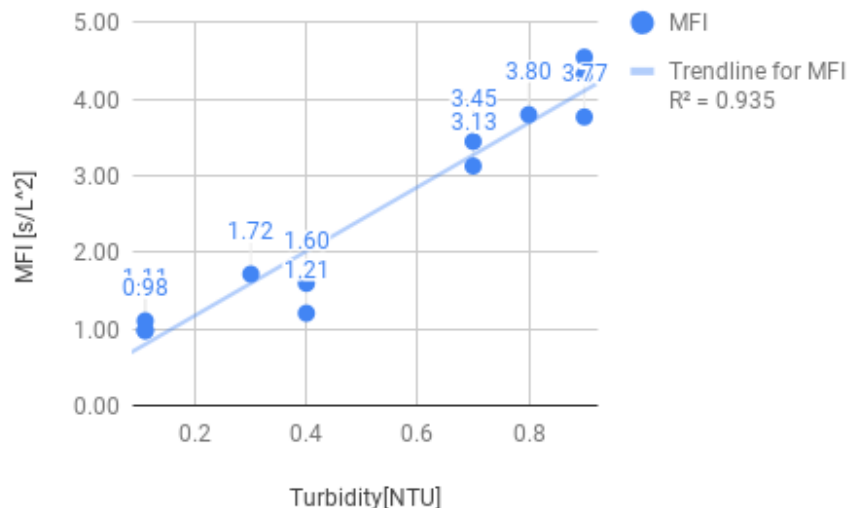


Figure 27. Turbidity NTU correlation to the MFI [s/L^2] ($R^2 = 0,82$), from Ukrainian surface water sample.

Each increase in turbidity by 0.2 NTU unit causes increase in MFI value on average by 0.84 s/L^2 . However, it was observed that, depending on the sample the exact water quality

parameter that would correlate with the index values vary. For instance, in the commercial salt trial the conductivity and salinity have higher correlation than other parameters (Fig. 28).

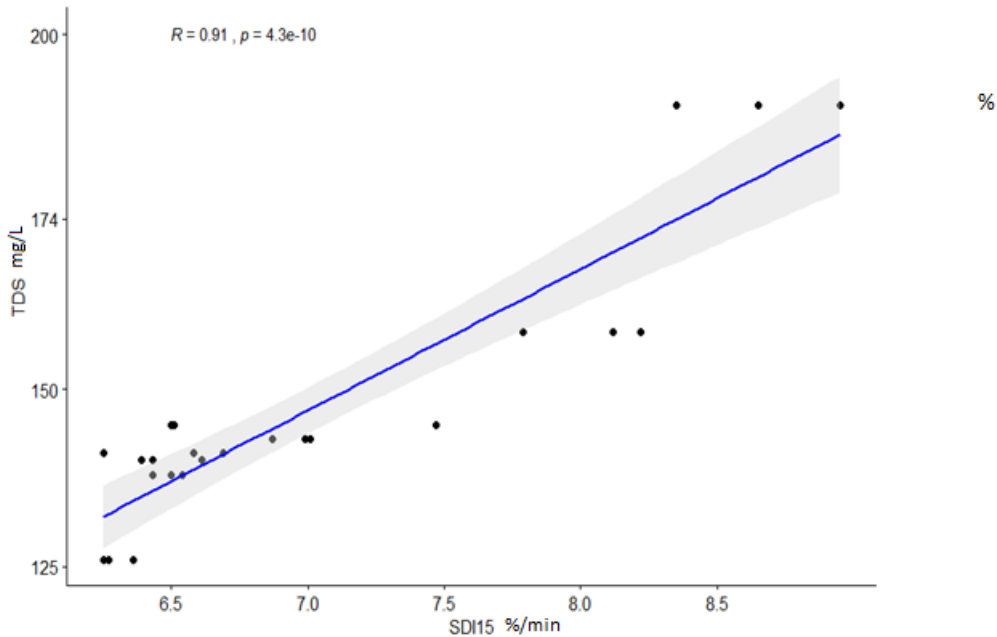


Figure 28. SDI15 and TDS correlation from the commercial salt trial.

From the Figure 28 it can be concluded that the sample from the commercial salt has a following trend: the increase in TDS by 25 mg/L causes the SDI15 value to increase on average 1.5 units. On the other hand, sample from the Ukraine showed a result where the SDI15 increased by 1.5 unit when the TDS was increased on average by 5 mg/L.

6.3.5 INSPECTOR apparatus results

As mentioned in materials and methods section, the INSPECTOR is a fully automated, innovative apparatus that will generate the results of the sample in 20 minutes maximum. In this section, results that have been obtained from the INSPECTOR apparatus will be discussed and compared with the results obtained from the BOKU instrument.

First of all, validation of the apparatus is done with the tap water and is compared with the results obtained from the instrument from BOKU. BOKU instrument results are noted as BOKU Inst. on Table 23.

Table 23. Standard deviation of the BOKU instrument and INSPECTOR apparatus values.

BOKU Ins.	SDI15 [%/min]	MFI [s/L²]	INSPECTOR	SDI15 [%/min]	MFI [s/L²]
	5.53	2.14		5.49	1.04
	5.63	2.15		5.00	0.63
	5.33	2.09		5.21	0.54
Stdev (%)	0.15	0.03	Stdev (%)	0.25	0.27

The standard deviation values for SDI15 and MFI is less for the BOKU instrument, with SDI15=0.15 and MFI=0.03. The MFI standard deviation from the INSPECTOR is on average 9 times higher than the BOKU instrument value, whereas the SDI values are 1.6 times higher for the INSPECTOR apparatus.

All generated results have been shown to and discussed by the representatives from the Convergence Ltd. It was informed that current model algorithm does give out false MFI when the MFI>20, thus it was necessary to remove the outliers.

The fouling index from the waste water trial with different concentration factors have been investigated and is shown on Figure 29. The concentration factors have been shown to the ratio of 8 liters (for example, 85:8 means 85 ml of waste water sample have been dilutes with 8 liters of reverse osmosis water).

Waste water trial

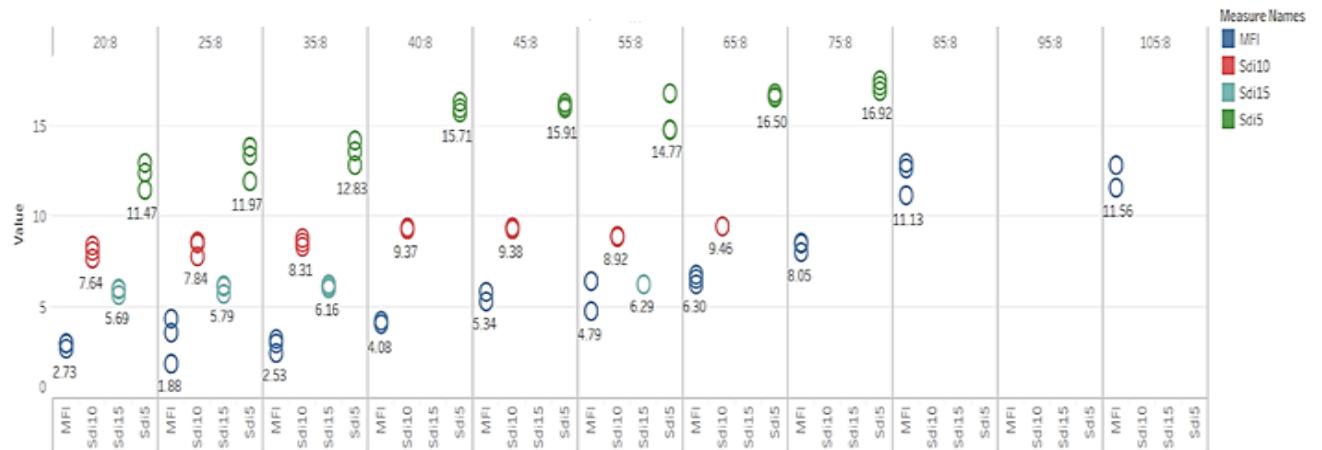


Figure 29 . Index results from the waste water trial.

The filters for the INSPECTOR are smaller (d=25 mm), and the calculation does correct filter size, however it plugs faster than 15 minutes when the sample is highly foulant. Therefore, there are no values generated for the SDI15 from 60:8 samples (It is written “Pressure is out of range” on the screen of the apparatus). The R-squared values are provided in Table 24.

Table 24. R-squared values of the trend lines of the index results.

Index	SDI5 [%/min]	SDI10 [%/min]	SDI15 [%/min]	MFI [s/L ²]
R-Squared:	0.79	0.59	0.40	0.74

As it was previously documented the SDI5 has also higher correlation than the SDI15. Standard deviations of above-mentioned values are provided on the Table 25:

Table 25. Standard deviation of the indexes derived from the INSPECTOR of the waste water sample.

Concentration factor	SDI [%/min]	MFI [s/L²]
20:1	5.99	3.00
	6.08	3.01
	5.69	2.73
Std. dev	3.43	5.45
25:1	6.18	4.37
	6.11	3.64
	5.79	1.88
Std. dev	3.50	6.71

Standard deviations fall in same line as the previous values, meaning the SDI values have higher standard deviation.

6.3.6 Comparison of INSPECTOR and BOKU Instrument values

Fouling indexes were generated by INSPECTOR and the instrument from the BOKU SIG department with the identical feed (refill was done from one source). There was a significant difference in the results and SDI and MFI values are illustrated on Figure 30.

Surface water from Ukraine

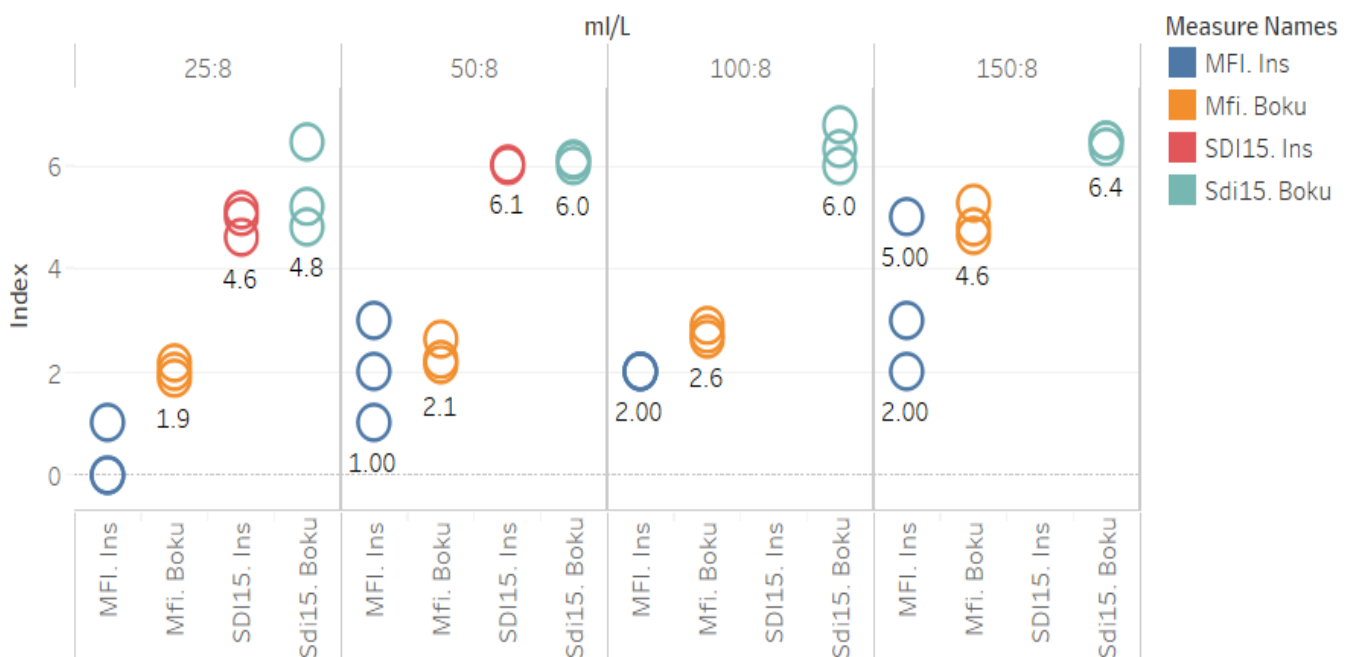


Figure 30. MFI and SDI values of the BOKU and INSPECTOR apparatus from the sample of the surface water from Ukraine.

Values from the INSPECTOR are noted as Ins. and values from the BOKU SIG department are noted as BOKU.

Values generated from the BOKU instrument are always higher. Moreover, it can be seen that the values from the INSPECTOR have a high standard deviation within the same sample. The difference of the results of the results of the trial with surface water from Ukraine (Fig.30) is shown in Table 26.

Table 26. Percentage difference between the MFI value from the INSPECTOR and the BOKU SIG instrument.

Concentration factor [mL/L]	MFI. Ins	MFI. BOKU	Percentage difference [%]
150:8	2.82	4.64	64.4
150:8	3.34	4.81	43.9
150:8	5.64	5.25	-6.8

The standard deviations of the MFI and SDI values of the samples with different concentration factors derived from waste water trial, have been pair-wise compared and is shown on Figure 31 and 32. The concentration factor indicated on the graph 25, 50, 100, 125 ml is ratio to 8 liters.

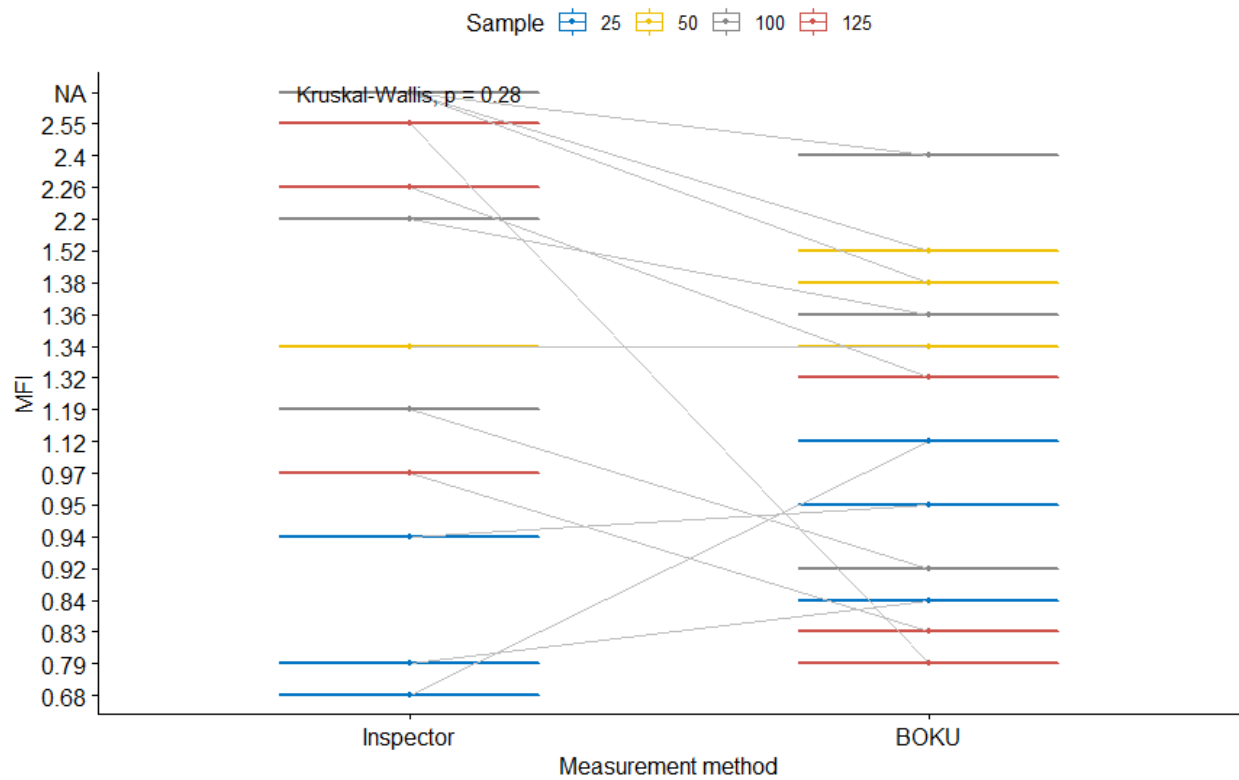


Figure 31. Comparison of MFI [s/L²] generated from INSPECTOR and BOKU instrument.

Kruskal-Wallis test generates p value equal to 0.28, meaning that there are statistically significant differences in the values ($\alpha= 0.05$).

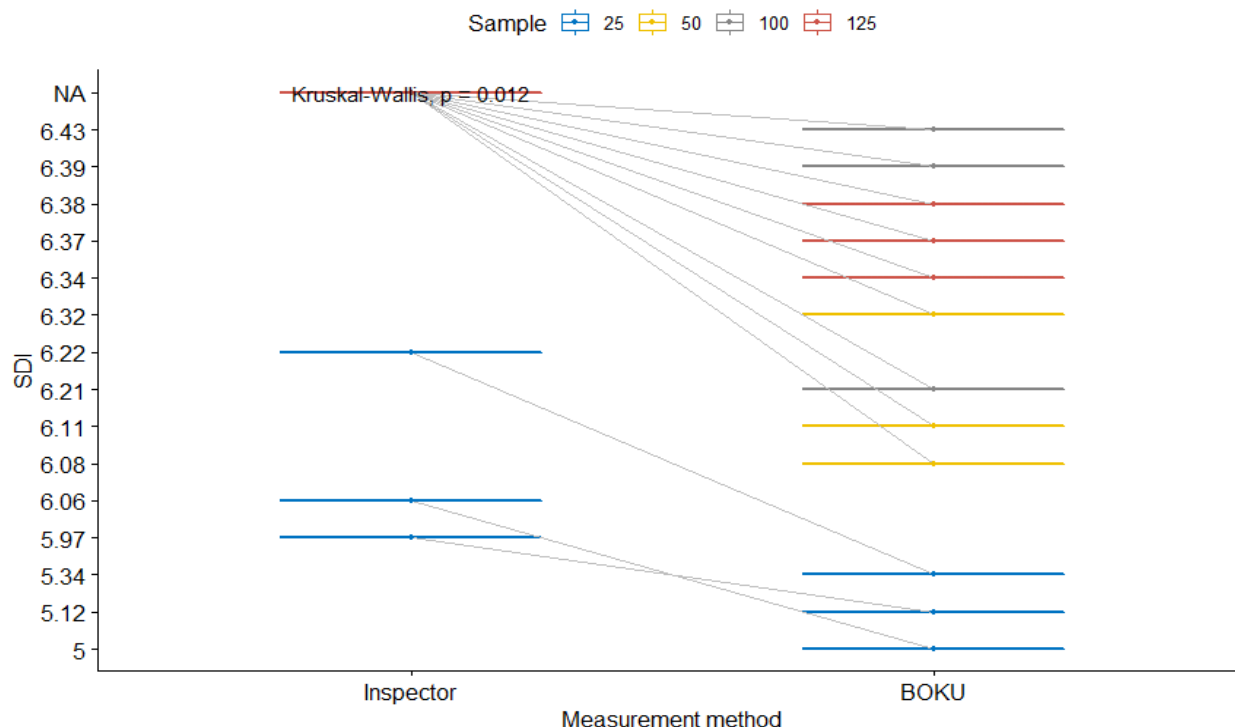


Figure 32. Comparison of SDI values generated from INSPECTOR and BOKU instrument.

The p value from the Kruskal-Wallis test run on the SDI show that null hypothesis can be rejected meaning that the differences in values are insignificant (Fig.32).

The INSPECTOR generates the data of the time series with the amount of the water filtered in liters and pressure values in Pascal unit. In order to examine the reason of the differences in the results, data from the INSPECTOR were recalculated according to the calculation of the BOKU instrument (indicated as calculation) was generated and is illustrated in Figure 33.

Waste water trial

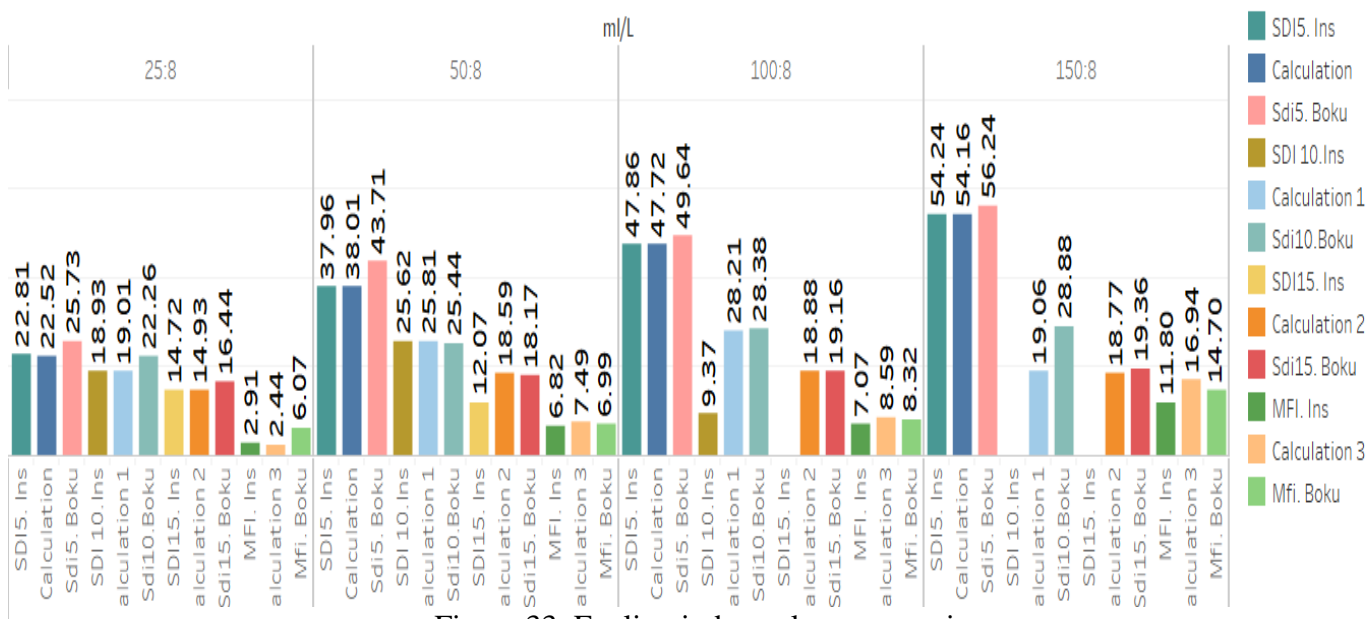


Figure 33. Fouling index values comparison.

Results and discussion

For each sample (e.g. 25:8), the SDI5, SDI10, SDI15, MFI values that have been obtained from the INSPECTOR is compared with the calculation results obtained from the calculation template, also with the results from the BOKU SIG instrument. When no values available for the reason of pressure was being out of range, there are no bars drawn. Values have been stacked up on the bar so that the values shown are the highest from the three trials.

There is slight difference in the calculation result and the INSPECTOR result, however fouling indexes derived from the BOKU instrument, are higher for almost all cases (inspector apparatus has a specific algorithm for the calculation of the indexes). The MFI and SDI15 derived from the BOKU instrument are also higher than the values generated from the INSPECTOR apparatus, on average 0.14 units. Standard deviations of the values from the same indexes are provided in the Table 27.

Table 27. Standard deviation of the fouling indexes illustrated on Figure 33.

Concentration factor	SDI5 [%/min]	SDI10 [%/min]	SDI15 [%/min]	MFI [s/L²]
25:8	0.95	1.27	0.56	0.59
50:8	1.09	0.27	0.11	0.50
100:8	0.56	0.06	0.27	0.33
150:8	0.40	0.09	0.12	1.08

For the SDI values the standard deviation decreases with the increase of concentration factor, however this trend does not apply for the MFI values. ASTM has noted that the difference in manufacturers of the filters is the cause of the incomparable results. Moreover, the ASTM suggests start taking the time measurement of the filtration as soon as the flow of filtration is stable or under a stable regulation. Stability is when the pressure is constant 207 kPa and there is no presence of air bubbles. This precision is difficult to achieve for BOKU instrument and the chances of having above mentioned errors with significant effect on the result is high, as it leads to inaccuracy in the time measurement of the SDI.

Also, the water quality parameters, especially temperature, turbidity and the filter resistance play crucial role. Changes of the temperature within the sample will cause the viscosity to alter, which leads to different resistance of the water flow against the filter. Normalization of these parameters is not mentioned in ASTM. Higher pH also causes higher scaling which leads to higher SDI results. Also, the difference in the measurement technique is a potential cause for the difference in the results.

As for the MFI values, there are normalization of the temperature, viscosity and pressure. However, the difference in measurement technique and the in the manufacturers of the filter size may cause the deviation in the values, which make it incomparable. To get more in-depth information of the causes of the difference, the graph of the t/V vs. V was plotted and compared from waste water trial 25:8 with the index values showed in Table 28.

Table 28. Index values from the different sources.

ml/ L	SDI5. Ins	Calculati on	SDI5 BOKU	SDI 10. Ins	Calculatio n	SDI10.BOK U
25:8	6.6	6.7	9.6	5.5	5.6	7
25:8	7.7	7.4	8.1	6.2	6.2	5.7
25:8	8.5	8.4	8	7.2	7.2	9.5
25:8	SDI15.Ins	Calculati on	SDI15 BOKU	MFI. Ins	Calculatio n	MFI. BOKU
25:8	4.6	4.6	5.2	0.8	0.8	2
25:8	5	5	4.8	0.9	0.7	2.2
25:8	5.1	5.3	6.5	1.2	0.9	1.9

The calculation gives almost the same as the INSPECTOR result; however, the generated values from two instruments are different, especially for the MFI values. The t/V vs. V curve was plotted in order to examine the reason for this difference.

Potential reasons for the differences in the index values:

1. The primary reason of the of BOKU instrument values being higher than the INSPECTOR values, is the area of the filtration. The system requires to have a zero resistance in order to reach a cake filtration phase. Smaller filters take relative short time to reduce its resistance to zero, whereas bigger area requires more time to reduce the resistance.

2. De-aeration method for the INSPECTOR is automatic whereas for the BOKU instrument, the valve had to be opened for seconds to run all the air bubbles, which means higher chances of the errors during the operation.

3. Even though the BOKU instrument was rinsed with reverse osmosis water in between the samples, there is high chance of foulant or debris present on the walls of the hoses and pipes as the instrument was used for a longer time than the INSPECTOR. This can lead to higher results.

4. Calculation method. As the rule depicts, the minimum slope of the cake filtration is the MFI. However, the identification of the pure cake filtration, whilst ignoring the two other mechanisms that take place is rather unclear. For example, the previous master student had identified the minimum slope at least after 1 liter of cumulative volume (Krondorfer, 2016). In this study, the cut was done after minimum 38 milliliters, not less and depending on the sample the cutting point was further. This problem was also mention in ASTM D8002-15 (Fig.34 and Fig.35).

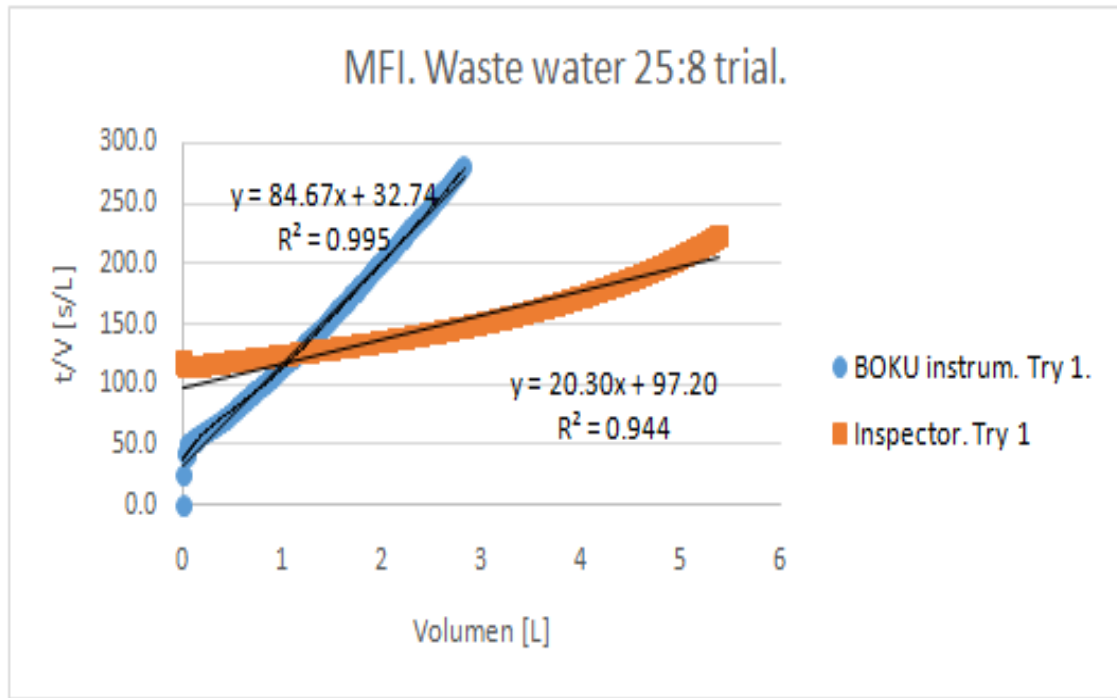


Figure 34. Wastewater trial 25:8, comparison of BOKU instrument graph with the INSPECTOR graph.

From the observed graph, there is a significant difference in the slope of the curves and especially the starting points. The primary reason for the difference would be the filter size, as it was mentioned before, the INSPECTOR uses a filter with the diameter of 25 mm.

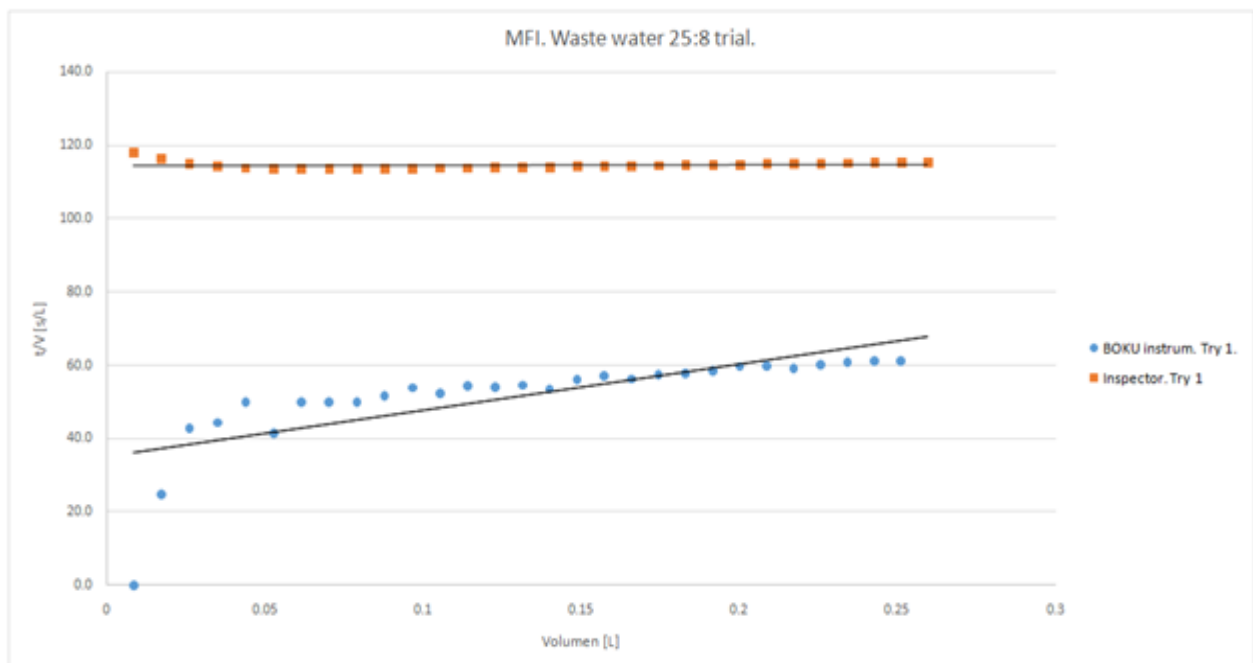


Figure 35. The graph of the filtration of the first 30 seconds of the BOKU instrument and INSPECTOR apparatus.

Interesting picture has been captured from the first 30 seconds of the graph. The linear increase in the graph is observed from the graph generated from the BOKU instrument. However, the INSPECTOR cuts the first 10 seconds of the filtration as the instrument goes through de-aeration. Meaning that the INSPECTOR assumes that after 10 seconds the resistance of the membrane filters is zero. From the BOKU instrument, it is hard to say at which time the resistance reaches to zero (as mentioned several times in this chapter). The resistance reaches to zero when there is no air bubble inside the filter holder. For BOKU instrument, the removal of the air bubble was done manually, and it is certain that there is difference in the duration of the de-aeration and delay for each trial, which influence the standard deviation of the generated MFI.

There was an effort the re-calculate the BOKU instrument values in accordance to the INSPECTOR apparatus calculation methodology (cutting the first 10 seconds of the filtration). The results showed no significant difference in the value of the fouling indexes when the first 10 second were cut.

6.4 Reverse osmosis membrane experiments

This section will provide the results of reverse osmosis membrane experiment with variety of feed with different concentrations. First, the results of the trials without pressure modification will be provided.

6.4.1 Reverse osmosis water trial without pressure modification.

As it was mentioned in the materials and methods section, the membrane was used several times, prior the real experiment, in order to calibrate the Arduino microprocessor. After the calibration was done, the reverse osmosis water was used again to finalize the Arduino microprocessor calibration with the pressure and flow sensor, as well as the sensors for the water quality parameters.

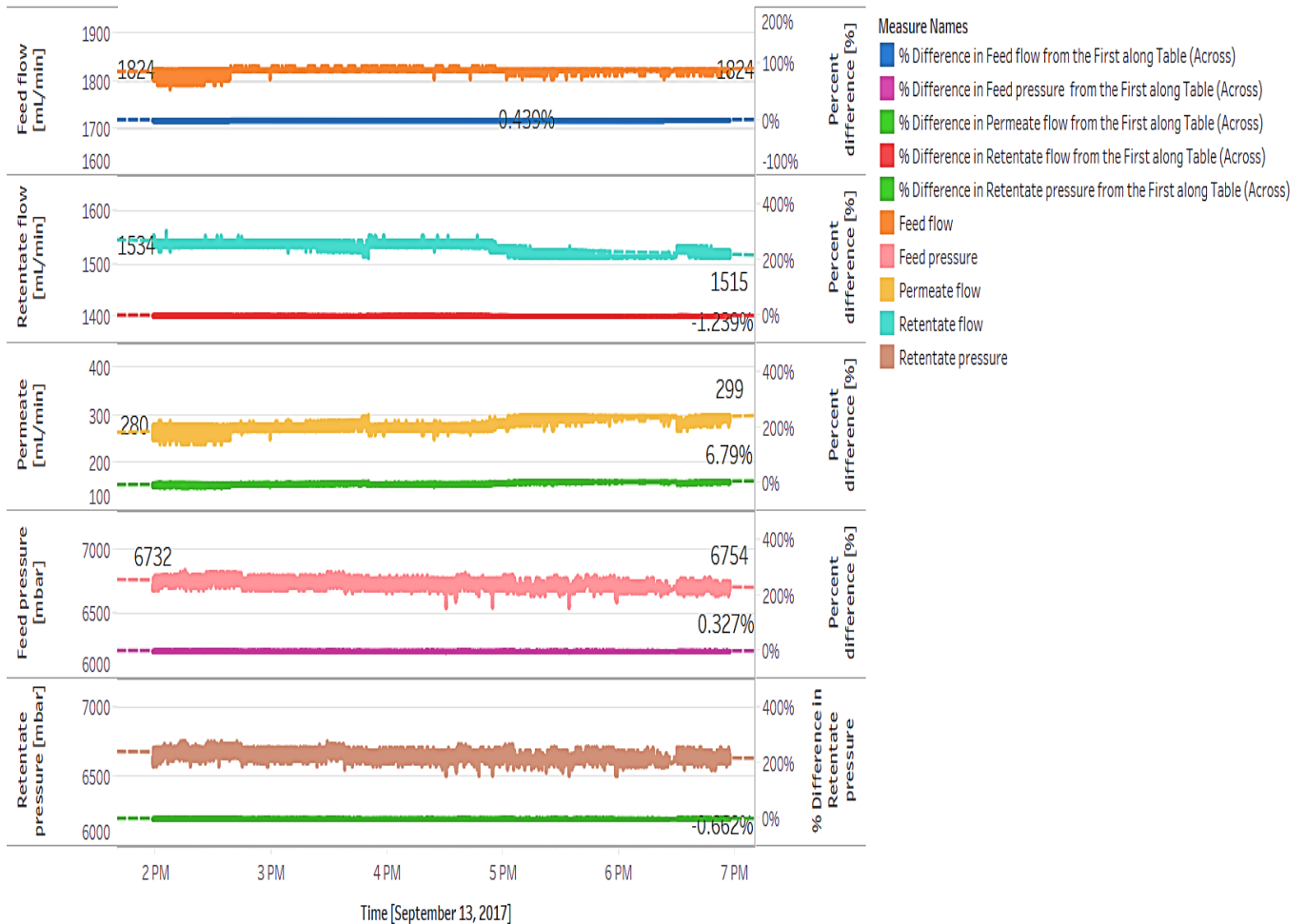
To define the characteristics of the membrane system and to test whether it complies the manufacturer's information, reverse osmosis water was filtered for 5 hours without pressure deviation. The pressure sensors and the probe for the water quality measuring equipment were first placed on the retentate side and the results are seen on the Figure 36. The reverse osmosis water sample had a conductivity of 7.4 $\mu\text{S}/\text{cm}$, 0.01 NTU, TDS 3 mg/L, 20 °C.

Results and discussion

Throughout the filtration and for all the samples, there was a constant interval in the flow rate. Meaning the pressure values changed in single measuring unit by on average 10 mbar and so does the flow rate (shown on Figure 36).

Figure 36. The filtration of the reverse osmosis sample without the pressure variation.

Reverse osmosis water trial from September



The indicated values on the generated graph were randomly chosen. The percentage increase/decrease are calculated by the mean value of the measuring parameter (this applies to every graph in this chapter). Throughout the filtration of 5 hours, the feed flow has increased by 0.4%, which correlates to the feed pressure increase which is 0.3%. Permeate increased with almost 7%. Summary of experiment is gathered in Table 29.

Table 29. Summary of the trial of reverse osmosis water.

Values	Feed flow, (mL/min)	Retentate (mL/min)	Permeate (mL/min)	Feed pressure (mbar)	Retentate pressure (mbar)
Average	1823	1531	282	6734	6654
Minimum	1784	1513	241	6556	6512
Maximum	1832	1563	301	6842	6754
Median	1824	1534	280	6732	6644

The flow rate is on average 0.11 m³/h from which the permeate flow takes up the 15.5% of the feed flow and is largely dependent on the retentate pressure. Maximum recovery rate reaches up to 16.4%, which is in line with the manufacturer’s information (10% of recovery). The average differential pressure for this sample is equal to 80 mbar.

The membrane with area of 1.7 m² has a permeability of 9.6 L/ (m²*h*bar) which also corresponds with the manufacturer’s information of net production of 1514 L/day. With this it is accepted to examine the further samples.

6.4.2 Deviation of the pressure valve.

There was an effort to deviate the pressure on both retentate and permeate side. Unfortunately, the valve was possible to be screwed and altered only to a certain extent (Fig. 37).

Reverse osmosis with pressure deviation

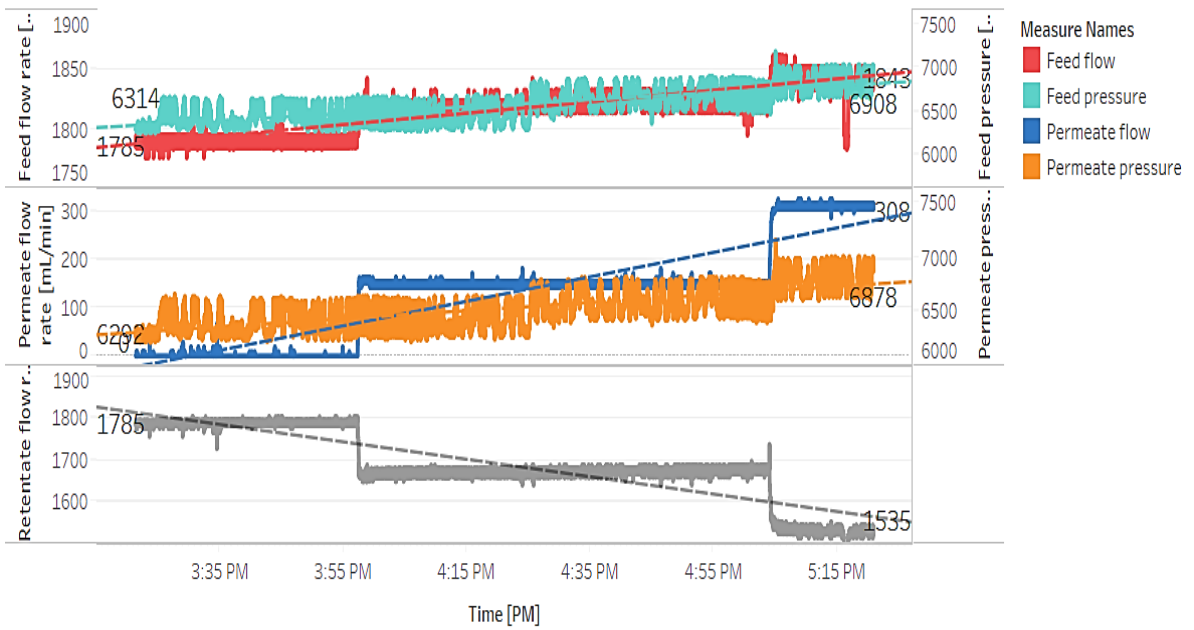


Figure 37. Reverse osmosis trial with the pressure deviation on the permeate side.

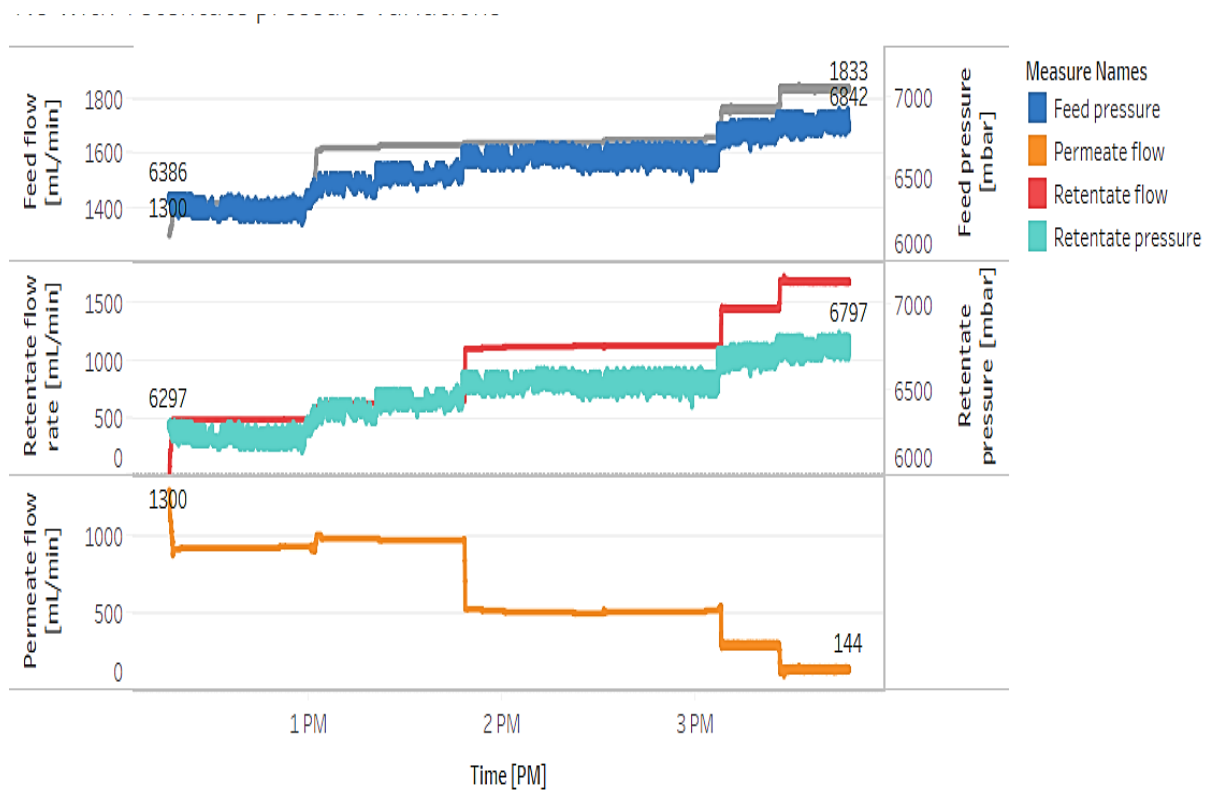


Figure 38. Reverse osmosis experiment with retentate pressure deviation.

Higher correlations ($R^2=0.9$) of the feed pressure and the retentate, permeate flux have been obtained from the trials where the pressure was deviated from the permeate side (Fig. 39).

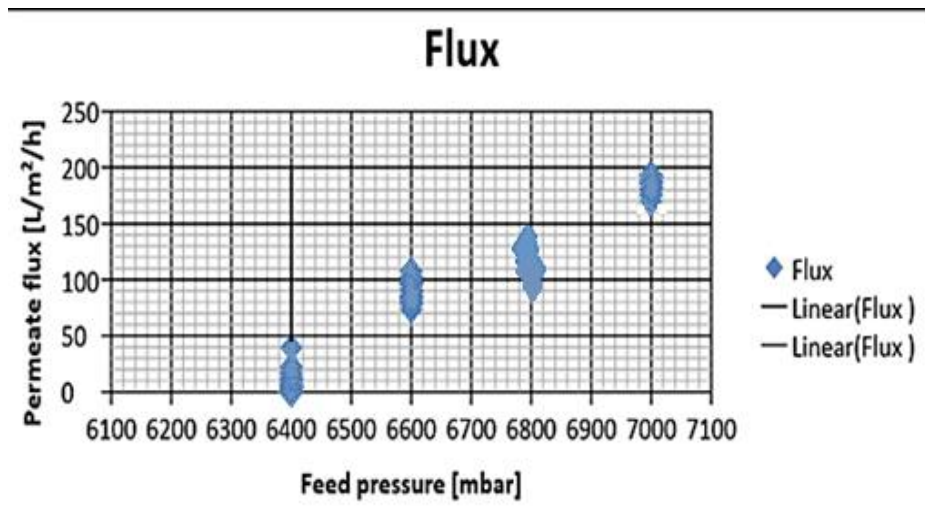


Figure 39. Correlation of the permeate flux and the feed pressure.

Reverse osmosis sample with conductivity of $7.4 \mu\text{S}/\text{cm}$, without the modification of the pressure showed the permeability of $9.6 \text{ L}/(\text{m}^2 \cdot \text{h} \cdot \text{bar})$. The pressure deviation on the permeate results in $38.65 \text{ L}/(\text{m}^2 \cdot \text{h} \cdot \text{bar})$ permeability with the maximum feed pressure of 7 bars. On the other hand, deviating the pressure on the retentate side resulted in only $9.4 \text{ L}/(\text{m}^2 \cdot \text{h} \cdot \text{bar})$ permeability with the maximum feed pressure.

Summary of these experiments are provided in Table 30.

Table 30. Summary of the reverse osmosis water trial with the pressure deviation on retentate and permeate side.

Permeate pressure deviation					
	Feed flow, (mL/min)	Retentate flow, (mL/min)	Permeate flow, (mL/min)	Feed pressure , (mbar)	Permeate pressure, (mbar)
Ave.:	1816	1688	128	6567	6527
Min.:	1776	1467	0	6248	6226
Max.:	1862	1804	328	7194	7164
Med.:	1824	1678	144	6556	6512
Retentate pressure deviation					
Ave.:	1622	972	650	6580	6491
Min.:	1300	0	96	6232	6143
Max.:	1853	1747	1300	6930	6841
Med.:	1640	1129	521	6608	6519

The feed flow rate is higher for the trial where the pressure was deviated on the permeate side. The valve allows to minimize the permeate flow rate to 0 but the maximum values are extent to a limited value. Permeate flow rate when the pressure reaches the maximum value of 328 mL/min which is around 19% of the feed flow. However, when the pressure valve was deviated on the retentate side it was possible to increase the permeate flow rate until 1300 mL/min which is 100% of the minimum flow rate of the feed flow.

6.4.3 Samples with different concentration

In order to determine the behavior of the membrane parameters towards the concentration change of the samples, waste water, surface water from Ukraine, commercial salt were diluted in different concentrations and filtered for 5 hours each. A general trend has been observed where the feed flow and the permeate flow decline throughout the filtration process. The rate of the decline differ within the samples. It was concluded that the conductivity and ORP values influence the permeate production the most.

Waste water and commercial salt water sample with high concentration showed a decline in permeate flow (Fig. 40).

Permeate flow rate of waste water trial, [mL/min].

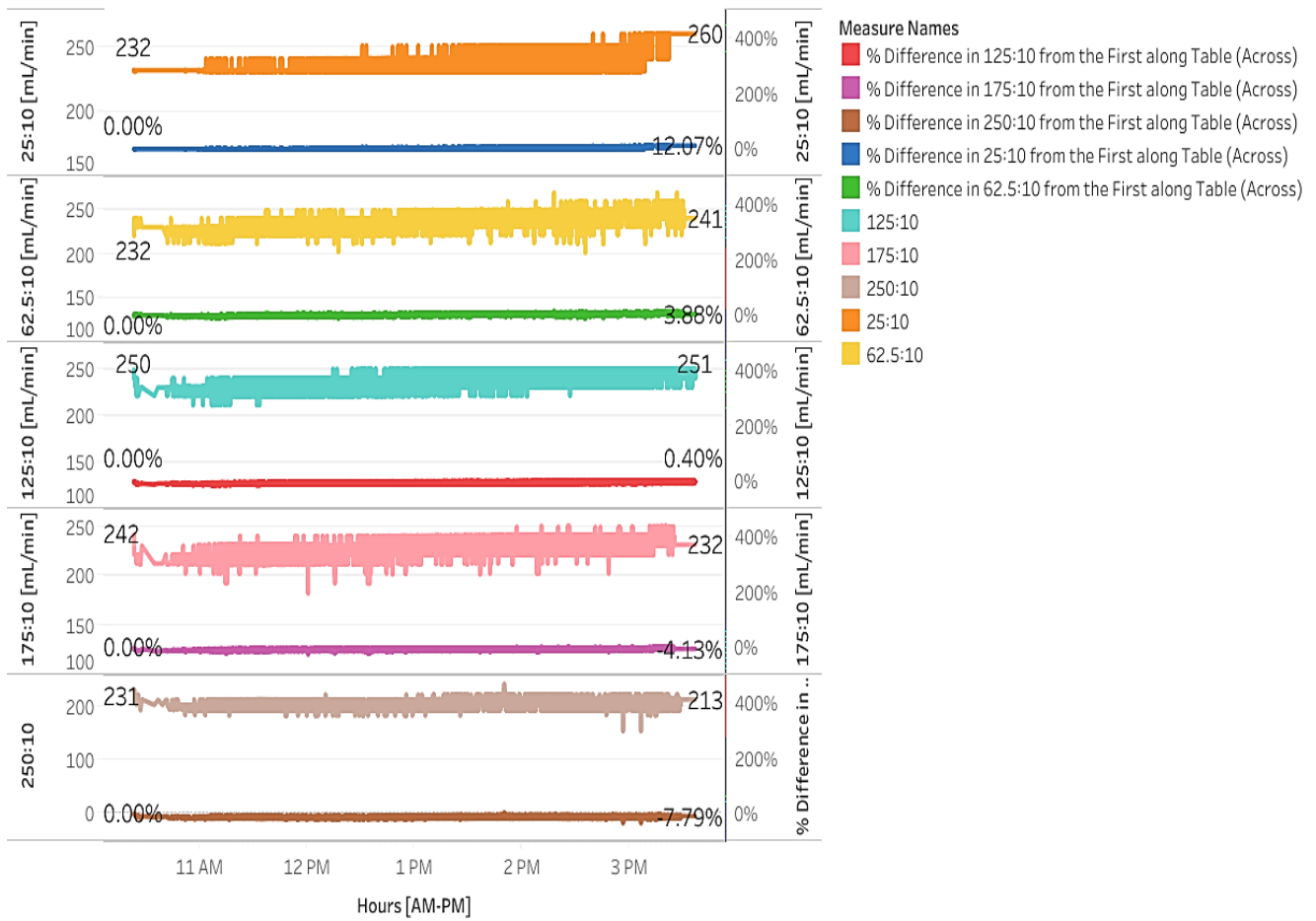


Figure 40. Permeate flow rate of the waste water sample with concentration variety.

Results and discussion

The samples 175:10, 250:10 showed that the permeate flow decrease by 4.13% and 7.79% respectively throughout the 5-hour filtration. This can be reflected in the values of the pressure of the feed, permeate and retentate. Permeate pressure gradually decreases in two high concentrated samples. The permeate flow rate decreases with the concentration increase. The permeate flow from the feed 62.5:10 has increased the most with 7.57%. The feed pressure follows the same trend, on the other hand retentate decrease (Fig. 41).

Retentate flow rate of waste water trial, [mL/min].

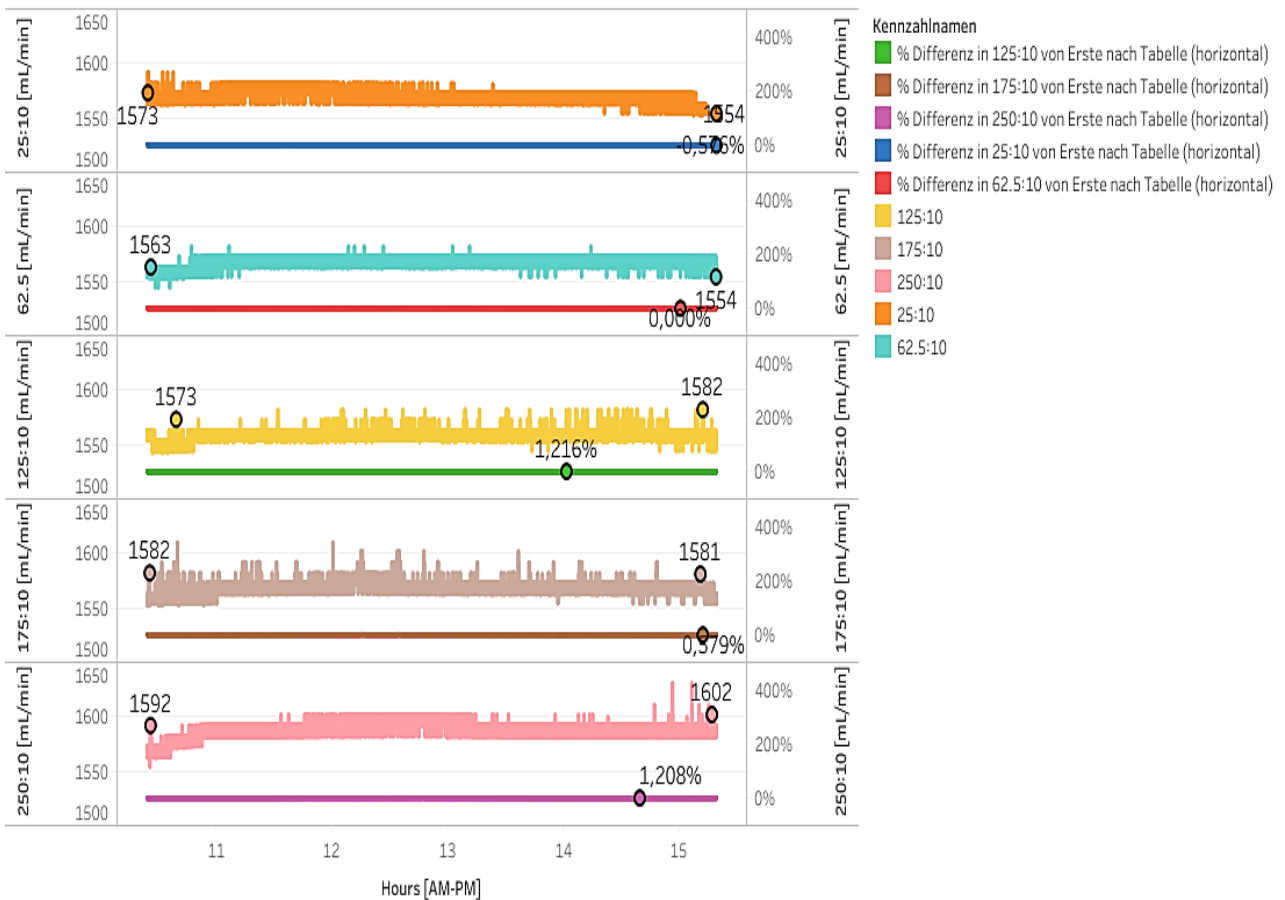


Figure 41. Retentate flow rate of the waste water trial.

The Figure 41 shows that the retentate flow rate increases for all the dilution series, except from 25:10. This can be reflected on the retentate pressure values and it is shown in Figure 42.

Retentate pressure values of waste water trial, [mbar].

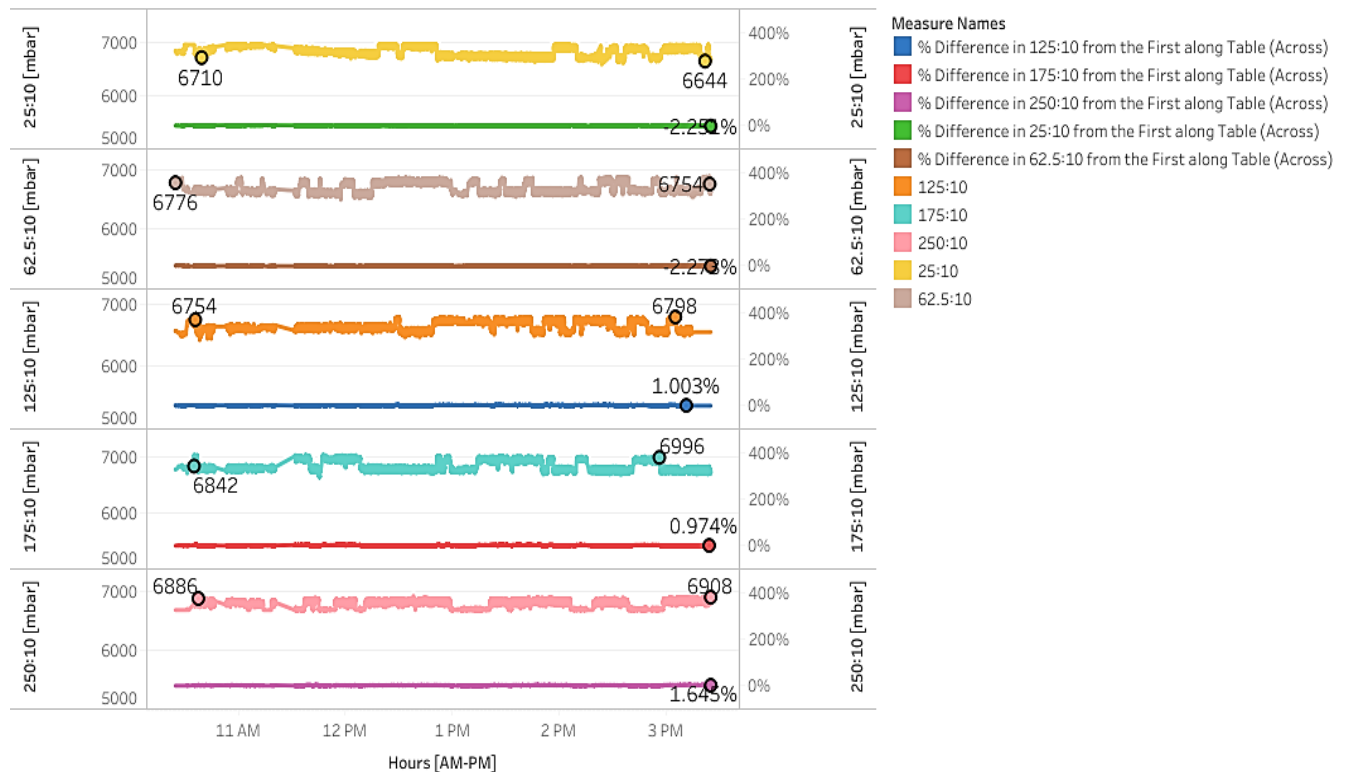


Figure 42. Retentate pressure values of the waste water trial.

The permeate flow rate started decreasing from the samples with the conductivity values of 173 $\mu\text{S}/\text{cm}$, ORP values -78.80 and pH 6.8. The measurement from the water quality parameters show that the conductivity values increase drastically on the retentate side. And it has been concluded that the higher the conductivity, lower the pH, and lower the ORP values the faster the permeate flow decreases. The conductivity values obtained from the filtration is shown in Figure 43. The intervals of the measurement of conductivity meter are different to sample to sample, that is why there are steps in the graph. The longer steps mean the conductivity did not change throughout the specific measuring interval.

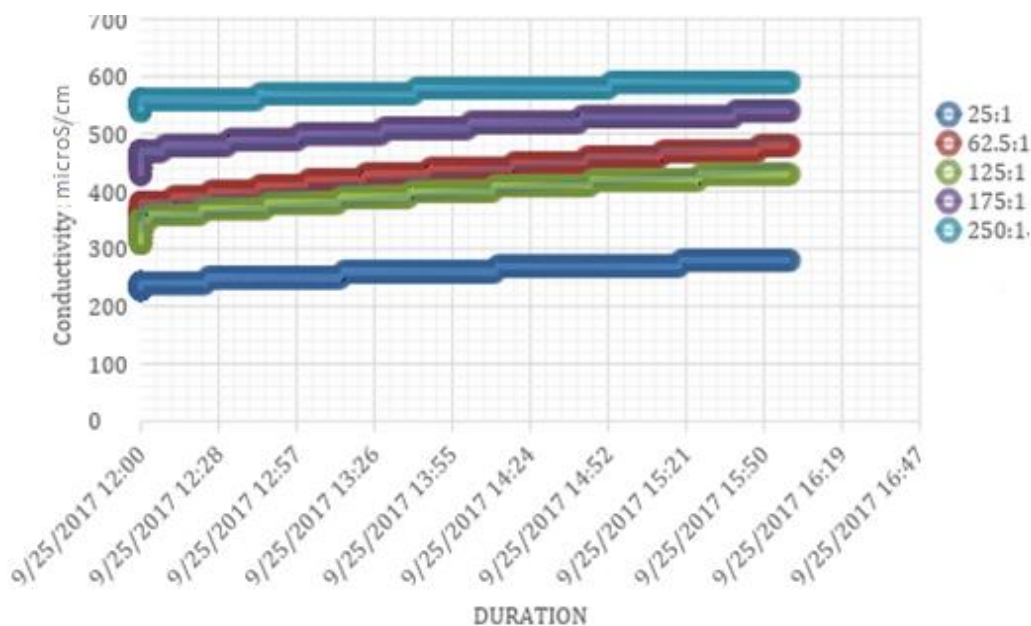


Figure 43. Conductivity values of the retentate of samples of the waste water trial.

Although, the concentration factor was increased 10 times, there was no big difference in the values of TDS and conductivity in the retentate, thus the osmotic pressure does not change drastically. Salt rejection of the waste water trial is given in Table 31 (TDS values from the permeate side).

Table 31. Salt rejection rate of the waste water trial.

Concentration factor	Salt rejection (%)	TDS (mg/L)
25:1	96.8	182
62.5 :1	94.6	205
125:1	94.8	223
175:1	93.7	247
250:1	92.6	271

The salt rejection rate decreases with the concentration addition. Experimental work by Makardij-Tossonian on regeneration of fouled spiral wound membrane showed (pressure around 13 bar), that the feed with TDS of 200 mg/L having a rejection rate of 98% at the end of 24-hour trial. The higher rejection rate might be due to the higher pressure presented to the system.

Trial with surface water from Ukraine.

As for the Ukrainian surface water trial, the permeate flow increase for all samples (Fig. 44).

Results and discussion

Permeate flow rate of surface water from Ukraine, [mL/min].

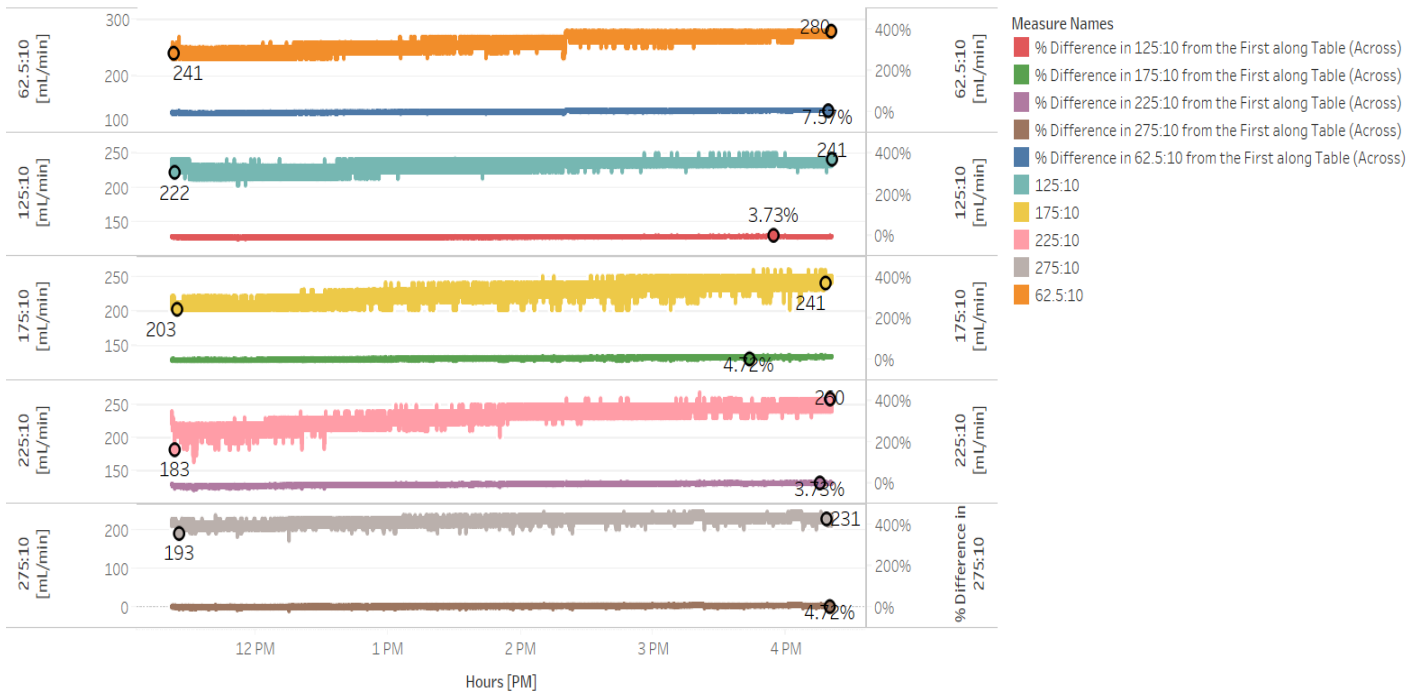
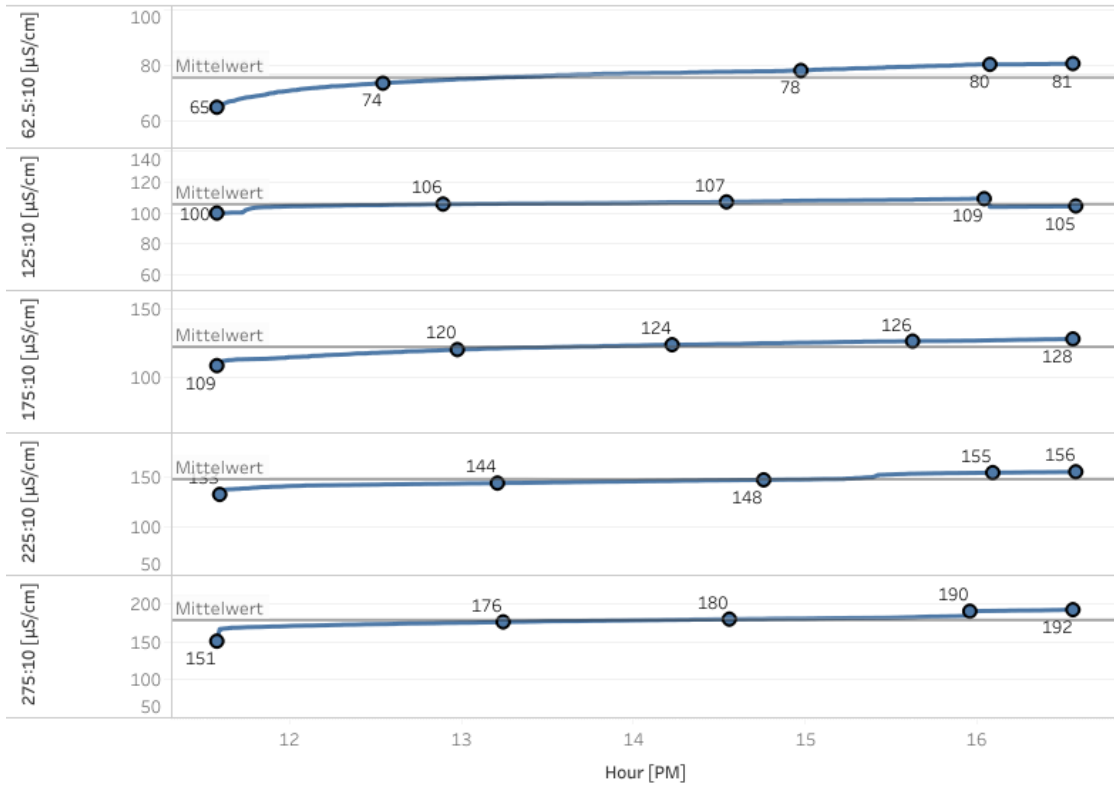


Figure 44. Permeate flow of the trials with surface water from Ukraine.

The permeate flow rate increase with the concentration decrease. The permeate flow from the feed 62.5:10 has increased the most with 7.57%. The feed pressure follows the same trend, on the other hand retentate decrease. If we compare the water quality parameter values from waste water trial and Ukrainian surface water trial, conductivity and ORP values differ drastically, e.g Ukrainian surface water trial has lower values of conductivity and higher values of ORP and are shown on Figure 45.

Conductivity Values of Surface Water from Ukraine, [$\mu\text{S}/\text{cm}$]



ORP values of surface water from Ukraine, [mV]

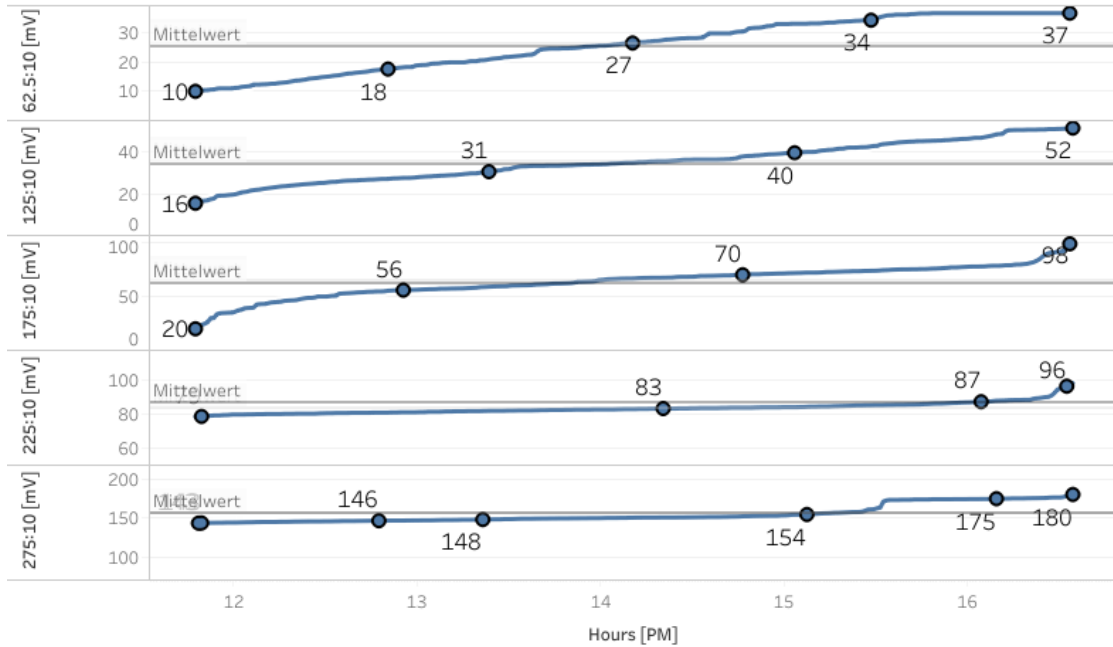


Figure 45. ORP and Conductivity values in the trial from Ukrainian surface water.

The increase rate of ORP is on average 65% and increase rate decrease with the increase of the concentration. On the other hand, conductivity values increase on average 20% for all the samples.

Trial with commercial salt.

The commercial salt was prepared to be in concentration of 1.5, 2, 4, 6, and 8 %. However, it was not possible to produce any permeate flow from the samples more than 4%. This sample with 4% had conductivity value in permeate of 1190 $\mu\text{S}/\text{cm}$, which has increased until 1397 $\mu\text{S}/\text{cm}$ at the end of a 2-hour filtration.

Relative to the other samples, the salt trial had an inconsistent behavior towards the addition of the concentration. Meaning, the increase rate in feed pressure was higher in the lower concentrated samples. This might be due to the differential pressure jump, as the system requires some time to get used to the introduction of higher salt content.

6.4.4 Rejection of pesticide, fertilizers and heavy metal

As it is mentioned in the materials and methods chapter, the sample was withdrawn from the tank once after the stock solution was added to the medium. These samples were taken to inspect whether the chemicals have an equal distribution for all the trials. Results show that the chemicals are relatively on the same range except for the zinc and copper (Table 32 and Table 33).

Table 32. Content of the zinc inside the tank before the filtration.

Old membrane	Try 1 [$\mu\text{g}/\text{L}$]	Try 2 [$\mu\text{g}/\text{L}$]
RO	418	431
Tap water	959	980
New membrane		
RO	443	439
Tap water	627	854

Table 33. Content of the copper inside the tank before the filtration.

Old membrane	Try 1 [$\mu\text{g}/\text{L}$]	Try 2 [$\mu\text{g}/\text{L}$]
RO	91.7	92.4
Tap water	97.7	96.8
New membrane		

RO	91.6	97.4
Tap water	91.5	97.3

The concentration in the reverse osmosis trial is always less than in tap water trial. Tap water sample has 959 $\mu\text{g/L}$ zinc where does reverse osmosis samples show 443 $\mu\text{g/L}$ zinc. This might be due to a sampling error or the heavy metal precipitated for the reverse osmosis samples as it has a higher pH. However, it is not the same for the cuprum. Flux of the trials have been calculated and it is illustrated in Figure 46.

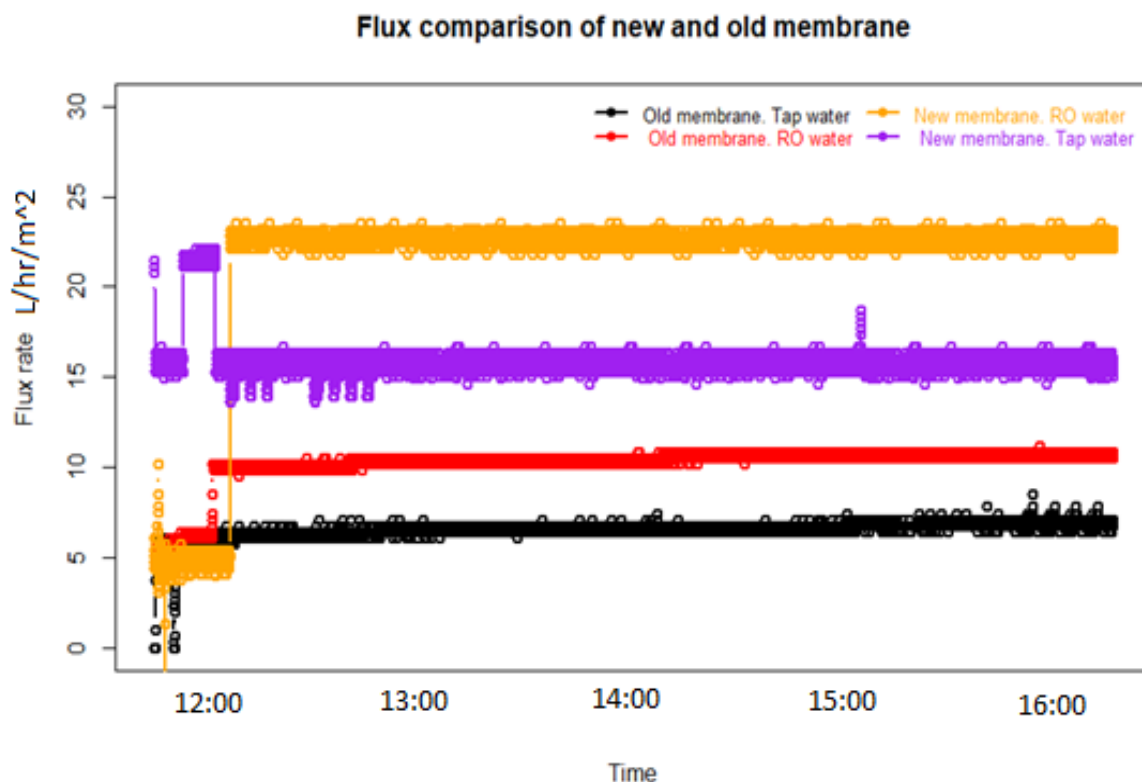


Figure 46. Flux of the sample with stock solution dilution.

The inlet for the first stock solution diluted with reverse osmosis water had following parameters: 283 mV, 105 $\mu\text{S/cm}$, 8.6 pH, 15.6 $^{\circ}\text{C}$. Whereas, the tap water and the stock solution has parameters: 117 mV, 7.9 pH, 413 $\mu\text{S/cm}$, 14 $^{\circ}\text{C}$.

Figure depicts that the highest flux is obtained for the new membrane when the stock solution was diluted with reverse osmosis water. However, it can be seen that it took some time for the new membrane to reach a stable filtration rate, as the flux was around 5 L/hr/m², it took around 16 minutes for the new membrane to reach the equilibrium of the flow rate of permeate with 15% and more. Summary of the filtration is provided in Table 34.

Table 34. Summary of the filtration parameters of the stock solution trial.

	Old membrane. Tap water	Old. membrane. RO water	New membrane. Tap water	New membrane. RO water
Flux [l/hr/m²]	6.6	10.2	29.2	41.5
Maximum feed pressure [mbar]	7326	7304	7204	7306
Minimum feed pressure [mbar]	6556	6666	6534	5214
Average feed pressure [mbar]	6934	7020	6978	6899
Maximum retentate pressure [mbar]	7216	7194	7172	6558
Minimum retentate pressure [mbar]	6446	6578	6446	5434
Average retentate pressure [mbar]	6809	6898	6866	6774
Recovery rate [%]	14.0	16.6	24.5	29.1

It can be seen from the summary that the new membrane has almost 1.5 times higher flux compared to the old membrane. Differential pressure on the feed side does not have big distinction, as the old membrane has 125 mbar and new membrane has 112 mbar.

Rejection rate of the chemicals present in the stock solution have been calculated both for old membrane and new membrane. For all the samples rejection rate was high for the samples with the reverse osmosis medium (except from atrazine). The rejection rate from different samples of the atrazine is shown in Figure 47 and Figure 48.

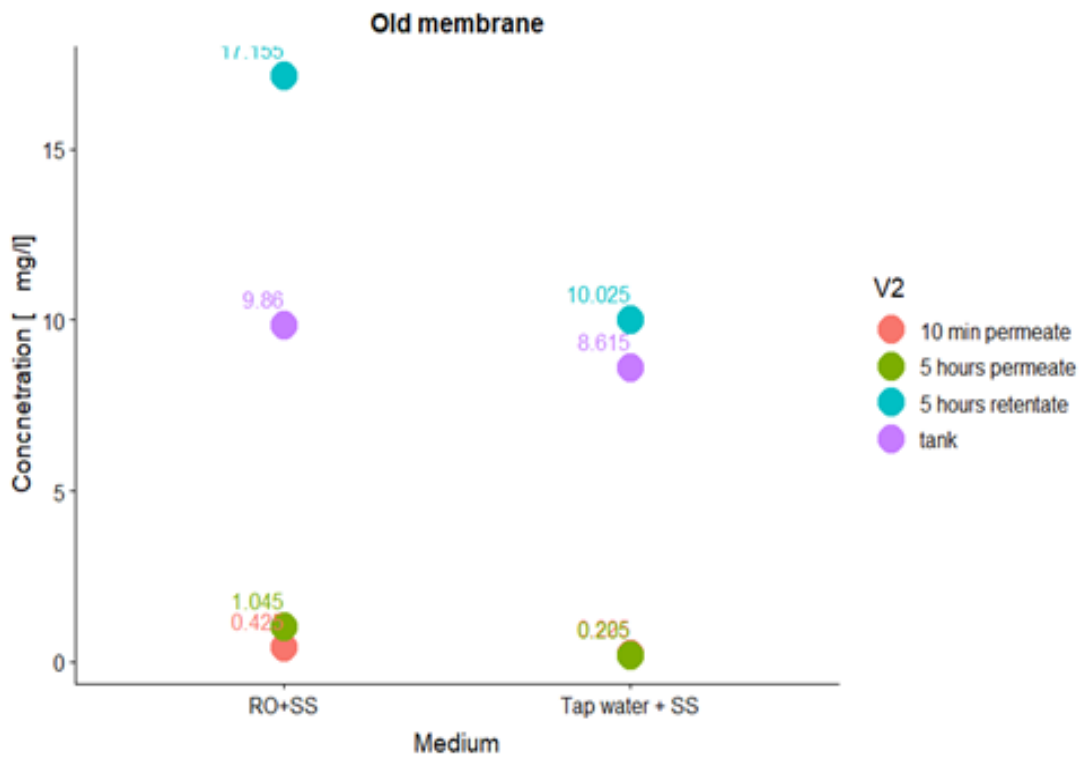


Figure 47. Concentration of atrazine in the experiment with the old membrane.

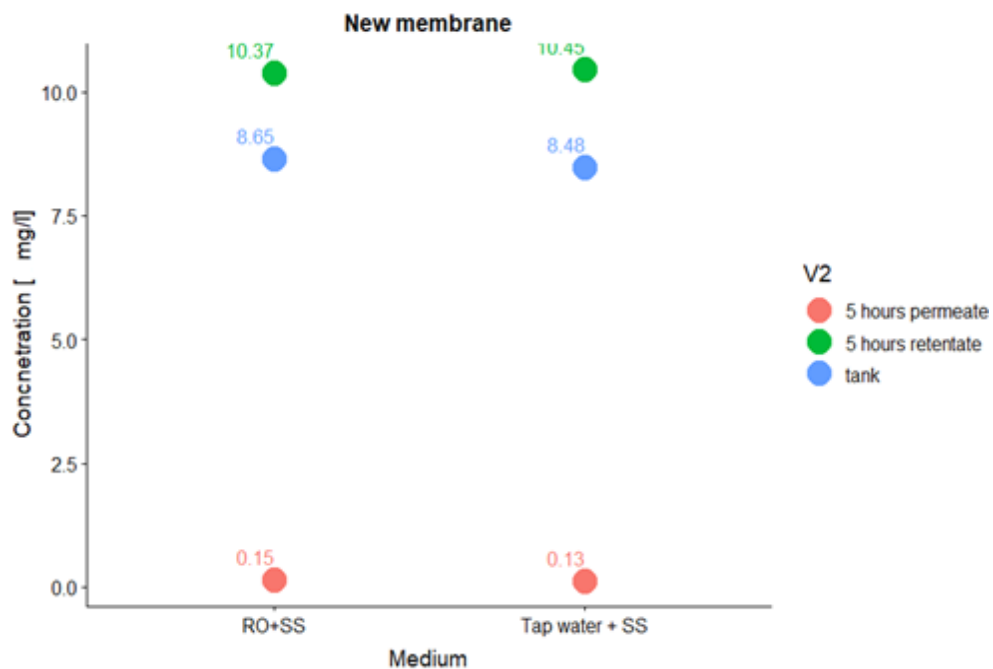


Figure 48. Concentration of atrazine in the experiment with the new membrane.

From these two figures (Fig.47 and 48) it can be concluded that the new membrane is almost 10 times as efficient in removal rate as the old membrane.

Results and discussion

The samples from the first 10 minutes and 5 hours of filtration show that the rejection rate decrease on average by 5% at the end of the filtration. Average removal rate of the old membrane with the reverse osmosis medium is 95.6%, whereas the tap water medium has 94.9% of removal rate. New membrane's removal rate with reverse osmosis water medium is equal to 98.3%, whereas the tap water medium removal rate is bit higher with 98.5%. The removal efficiency for the other chemicals are provided in Table 35.

Table 35. Rejection rate (%) of chemicals by the old and new membranes at the end of the filtration (5 hours).

	Diurone		Simazine		Copper	
Old membrane	Try 1	Try 2	Try 1	Try 2	Try 1	Try 2
<i>RO+SS</i>	91.7	92.5	87.6	88.5	>98.9	>98.9
<i>Tap water + SS</i>	92.5	92.8	92.3	91.7	>99.0	>98.9
New membrane						
<i>RO+SS</i>	90.1	89.2	80.7	80.5	>98.9	>99.0
<i>Tap water + SS</i>	91.8	86.6	87.6	88.3	98.6	97.8
	Zink		Nitrate		Atrazine	
Old membrane	Try 1	Try 2	Try 1	Try 2	Try 1	Try 2
<i>RO+SS</i>	98.6	98.1	94.6	95.6	87.7	91.5
<i>Tap water + SS</i>	98.4	98.4	89.8	90.3	96.5	98.7
New membrane						
<i>RO+SS</i>	>98.7	>98.9	94.2	97.6	98.1	98.4
<i>Tap water + SS</i>	98.7	98.2	86.2	88.9	98.8	98.1

The copper and zink samples showed undetectable results in the permeate after the filtration of 5 hours. However, copper removal rate (98.8%) is higher than the zinc removal rate (98.5%).

The $\log K_{ow}$ coefficient draws special attention. Hydrophobic attractions make up the first stage of rejection, the hydrophobic compounds would be rejected more. Nitrogen fertilizers have $\log K_{ow} = 0.67$, whereas urea $\log K_{ow} = -2.11$, meaning the fertilizer trial would be less rejected than the pesticide trial, as the pesticide has more hydrophobic characteristics.

The experiment results have shown that the atrazine has higher rejection rate (95.6%) than nitrate (92.6%) simazine (87%), and diurone (90.7%).

From the literature review it can be concluded that, no matter what membrane and what compound, the size exclusion mechanism is noted on almost every study, meaning that if this is the prevailing mechanism for our experiment and assuming the sizes of the chemicals can be described by their molecular weight, pesticides with the highest molecular weight will have the highest retention rate, following to fertilizers and lowest rejection occurring for heavy metals trial.

However, in our experiment the heavy metals were under detectable level followed by fertilizer and the pesticides have lowest rejection rate. This proves that the molecular mass of the chemicals is not a good parameter for the removal efficiency prediction.

The comparison experimental work on NF and RO membranes by Al-Alawy and Salih with electroplating waste water showed that the removal rate of the zinc by RO membrane was high as 99.49% whereas the removal rate of copper was 99.33% (Al-Alawy and Salih, 2017). This is higher rejection rate compared to our experiment.

The rejection rates of old and new membrane depended on the chemicals in the feed. For instance, the simazine and diurone are more rejected by the old membrane. This is also supported by the conclusion of the experimental study by Mehta. It is concluded in his work that the diurone rejection rate was increasing when fouling was increased by addition of polyacrylic acid (PAA) (Mehta et al., 2016).

6.4.5 Experiment with the biocide

The biocide was used in order to examine its microbiocidal efficiency. The biocide was prepared by the instruction of the technician from WTG (materials and methods chapter). The reverse osmosis water was filtered prior the biocide introduction, after which the sample was taken from the permeate side. After the biocide was filtered the sampling was done both from the permeate and the retentate side. The samples were measured using a flow cytometry technique and the results are shown in Table 36.

Table 36. The cell counts after the biocide introduction to the system.

Membrane type	Sample source	Live cells		All cells	
		Median for 50 µl	Cell count/mL	Median for 50 µl	Cell count/mL
New membrane	After RO water/ Retentate	12647	252940	23331	466620
New membrane	Permeate after biocide	38	760	144	2880
New membrane	Retentate after biocide	2599	51980	8281	165620

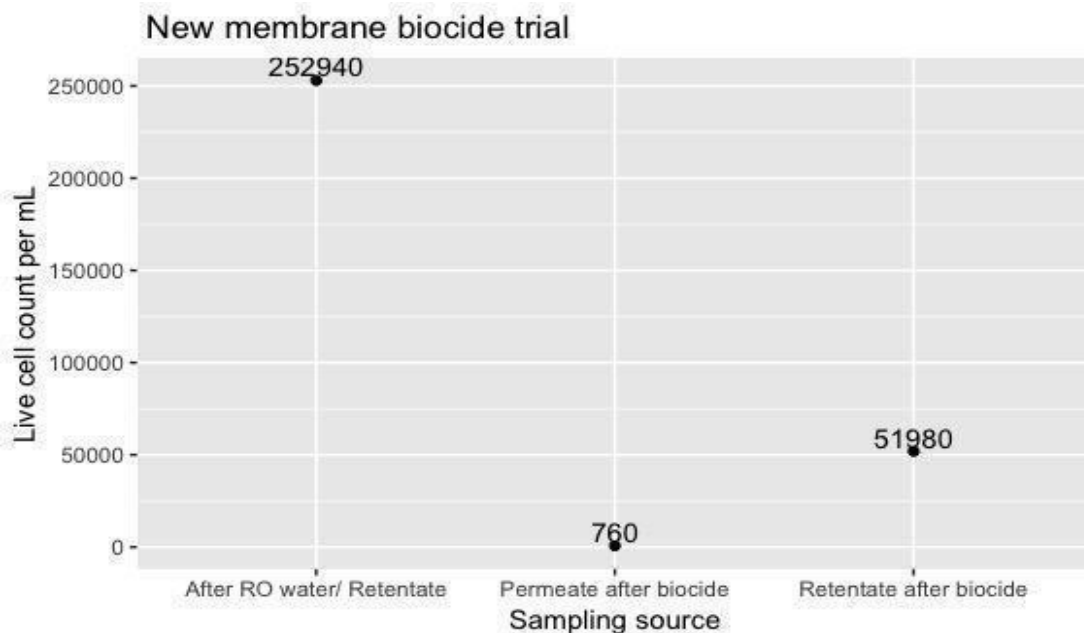
Results and discussion

Old membrane	After RO water/ Permeate	3427	68540	7043	140860
Old membrane	Permeate after biocide	368	7360	884	17680
Old membrane	Retentate after biocide	4565	91300	9996	199920

Table 36 depicts the cell counts of the total and the live cells per 1 milliliter and 50 microliters from different sources.

Results from the old membrane show that the biocide reduced the total cell count by almost 8 times on the permeate side. However, the sampling from the retentate resulted in around 50 000 more cells present. This shows the high fouling rate of the membrane due to the previous trials. It can be assumed that the biocide has been mostly used on the degradation of the foulant on the membrane. On the other hand, total cell count from the permeate of the new membrane showed that the biocide had reduce the cell number 162 times, than the retentate sample before introduction of biocide.

The live cell count of the old membrane shows that the permeate sampling is 12 times lower than the retentate sample. The new membrane has reduced its initial live cell count by almost 334 times. Live cell counts of the fresh membrane and old membrane are shown on Figure 49.



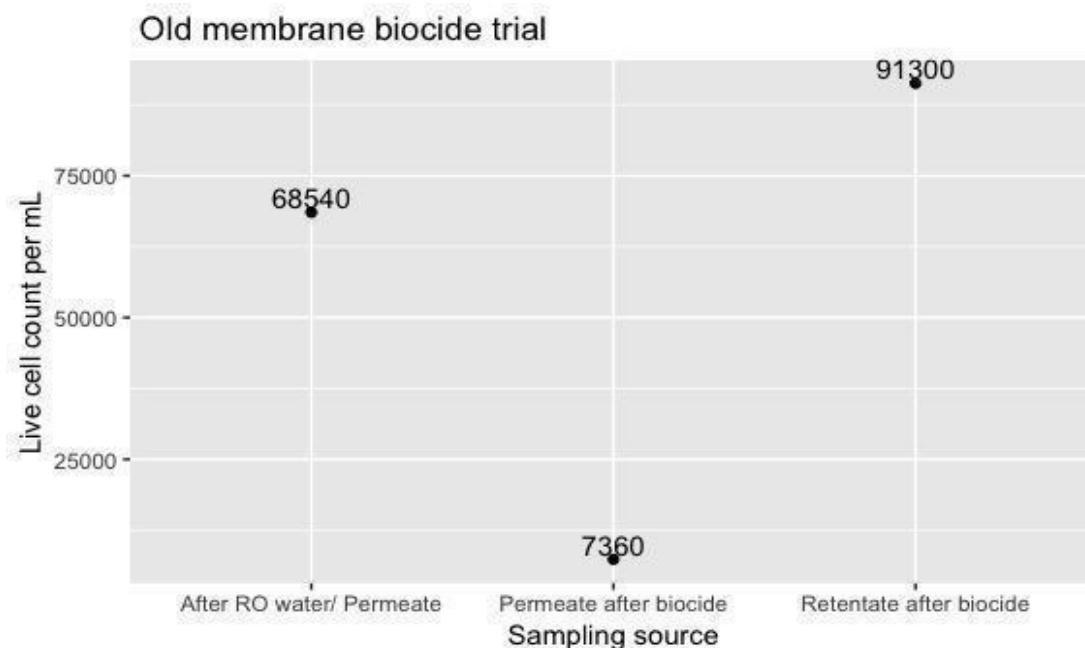


Figure 49. Live cell count after the biocide of the old and new membrane.

The biocide has removal efficiency on the old membrane as high as 89% whereas, the permeate from the new membrane has 68 times less live cell counts than the retentate. However, it is expected that RO membrane would remove all microbial cell as the microorganisms have bigger cell than the RO membrane pore size. This might be due to the conservation of the fresh membrane or due to the non-sterile system. The hoses after the pressure valve were never changed. So, when the experiment for the assessment of the effect of the pressure valve on the flow rate (the pressure valve was relocated on the permeate side) the hoses of the previous retentate side was used on the permeate side. Thus, there is a high risk of the potential growth of microorganisms inside the hoses both on retentate and permeate side.

7. Conclusion and outlook

In this chapter, the conclusion of the experimental work on indexes and its relationship with water quality parameters as well as results of the reverse osmosis membrane pilot plant investigation will be presented.

7.1 MFI and SDI

The very first step for the experiment was to determine the starting point of the cake filtration phase, in order to generate MFI value. For all the samples, the cake filtration phase did not start before 0.3 liters of cumulative filtrate. The duration of the minimum tangent was never less than 5 seconds. It is concluded that duration of the filtration/time as a better indicator of the cake filtration phase. Our system requires at least 45 seconds to reach to the cake filtration phase

The standard deviation values obtained from the three trials of each sample filtration, shows that the MFI values have on average 4 times higher standard deviation, than of the SDI15 values. At the same time SDI15 values almost always higher than the MFI values. This difference decreases with concentration increase. It is concluded that SDI15 is on average 1.7 times higher than the MFI value.

Correlation of the SDI15 and MFI to the water quality parameters was examined. The correlation rates differ within the sample and the fouling index. The MFI has higher correlation to the conductivity and turbidity, and SDI15 has higher correlation to the TDS relative to other water quality parameters. Exact correlations differ depending on sample type. The experiment on the waste water sample showed that the increase in conductivity value by 100 $\mu\text{S}/\text{cm}$ causes MFI to increase by 1.5 s/L^2 . However, the experiment with the commercial salt shows that 7 mS/cm change in conductivity value causes MFI change by 1 s/L^2 . In the experiment with surface water from Ukraine, the SDI15 increases by 1.5 $\%/ \text{min}$ when the TDS increase by 5 mg/L , whereas in trials with the commercial salt shows that on average 25 mg/L change causes SDI15 to deviate by 1.5 unit.

Comparison of the SDI2, SDI5, SDI10, SDI15 and MFI values relating to the concentration factor was done. MFI values and the SDI2 values showed the highest correlation factor ($R^2=0.9$ and $R^2=0.8$ accordingly).

Index values derived from the different filters with different pore sizes were compared. For all the experiments, fouling indexes derived from the filter with pore size 0.2 have higher correlation to the concentration factor. This is due to the prevailing size exclusion mechanism of the filtration system.

The fouling indexes derived from different measuring sources have been compared. The standard deviation of the index values generated from the INSPECTOR apparatus were on average 5.4 times higher than the values generated from the BOKU instrument. For almost all cases, the BOKU values were higher than the INSPECTOR values. Statistical comparison of MFI values generated from BOKU and INSPECTOR apparatus showed, that there is significant difference in the values ($p=0.28$). Statistical comparison of SDI15 values generated from BOKU and INSPECTOR apparatus showed that the null hypothesis can be rejected, meaning that there is no significant difference between values ($p=0.012$).

The indexes from the BOKU instrument were recalculated by the methodology of INSPECTOR apparatus. However, there were no significant difference between these values (were almost the same), meaning the reason for the difference in the values is not due to the calculation methodology, but rather the measuring technique.

7.2 Reverse osmosis membrane system experiment

There was an effort to assess the correlation of the fouling indexes to the flux decline rate of the reverse osmosis membrane filtration. However, for almost all cases the flux rate was increasing with the feed pressure increase throughout the experimental period of 5 hours.

Without modifying the pressure, membrane showed a higher performance than the manufacturer's sheet, with an average permeate reaching up to 16, 4%.

The set-up of the pilot plant influences the performance drastically. There was a difference in the flux when the pressure valve was replaced from the retentate side to permeate side (it was possible to connect on only one side). When the valve placed on the retentate side, it is possible to reduce the retentate to 0%, whereas 100% permeate was not possible to reach with the valve being on the permeate side. Thus, the overall flux was higher when the valve was on the retentate side with less pressure input. However, the flux, retentate flow have a higher correlation to the pressure values when it was placed on the permeate side, meaning that in this case the system has more control over the performance.

Permeability values show that the permeate side valve has 9.4 L/ (m²*h*bar) whereas the permeability reach up to 38.65 L/ (m²*h*bar) when the valve is placed on the retentate side.

The old membrane was compared with virgin membrane in terms of chemical removal rate. The recovery rate of the permeate flow of the new membrane is on average 1.7 times higher than the old membrane.

The difference in the medium (RO water or tap water) does not have a crucial effect on the removal rate. However, removal rate was slightly higher when the filtration was done with an old membrane with tap water medium and when the filtration was done with new membrane with reverse osmosis water medium. The removal rate of the new membrane and old membrane dependent on the chemicals in the feed and the fouling degree of the membranes. The higher the fouling the higher the rejection of the pesticides and fertilizers. The heavy metals were removed better with the new membrane. This is also supported by the literature study.

The experiment results have shown that the atrazine has higher rejection rate (95.6%) than nitrate (92.2%), simazine (87%) and diuron (90.7%). The highest removal rate was obtained from the trials of zinc and copper with the reverse osmosis medium both for new and old membrane.

The biocide has removal efficiency of live cells on the old membrane as high as 89% whereas, the permeate from the new membrane has 68 times less live cell counts than the retentate. The permeate from the old membrane has 12 times less live cell numbers than the retentate. On the other hand, the biocide removal efficiency is 55 times higher for the new membrane.

8. Summary

Reverse osmosis membrane system is used extensively not only in the water desalination sector, but also it is widely used for industrial purposes. The membrane system is constantly improved and developed in terms of technology and performance, however the biggest limitation for the efficiency of the system is still the fouling phenomena. Estimation of the fouling potential of the feed is very important, as it will help to determine the pretreatment options and the maximum allowable concentration of the feed. In order to do so, silt density index (SDI) and modified fouling index (MFI) were proposed. The standard methodology for the determination of the indexes is straightforward and cheap. However, there are several uncertainties present. Such as, relationship of the SDI and MFI, relationship of the fouling indexes to the water quality parameters, the incomparable values when different measuring techniques took place etc.

The objective of this master thesis is to compare the water quality by means of the fouling indexes, with determination of its correlation to the water quality parameters such as turbidity and evaluate whether the fouling indexes reflect the flux decline rate of the reverse osmosis membrane. The identification of the reasons for the differences in values from different measurement sources and samples is also on the goal list.

One of the main questions, is whether the fouling indexes predict the reverse osmosis membrane filtration flux decline rate. Thus, it is also one of the objectives of this master thesis. Moreover, the chemical removal and the biocide efficiency is also on the goal list.

In order to complete our objectives, the reverse osmosis pilot plant was constructed apart from the SDI and MFI measuring unit. SDI and MFI were measured with standard filters, after which filters with different pore sizes introduced. During all experiment, water quality parameters were measured before and after the filtration. INSPECTOR apparatus was introduced in order to compare the index values from different sources, and to determine the reason for the difference.

In order to compare the fouling indexes and reverse osmosis filtration, same samples for the SDI and MFI measuring unit were prepared and filtered with reverse osmosis membrane, however the results were incomparable (during the filtration the flux rate was increasing in almost all cases). In order to investigate the rejection rate of the new and old membrane in terms of chemicals, nitrate, copper, zinc, diurone and simazine, were prepared and filtered for 5 hours. Investigation of the efficiency of the biocide was also done.

First step for the experiment, was to determine the exact calculation methodology for MFI. For all the samples it is required to filter 0.75 liters and least 45 seconds to reach the cake filtration phase.

According to ASTM the SDI₂, SDI₅ and SDI₁₀ values were also measured and reported (as the fouling was more than 70%). The R-squared values depict that the SDI₂ and MFI has the highest correlation to the concentration factor.

MFI values increase on average 4 times (from 1.11 to 4.55 s/L²) when the concentration factor increase three times (from 7.5:1 to 22.5:1). The standard deviation of the SDI is on average 4 times higher than the MFI.

The fouling indexes were generated by membranes with different pore sizes. The correlation values show that the MFI values derived from the filters with smaller pore size have higher correspondence to the concentration change. This also, support the fact that the fouling phenomena is mainly formed by the particles smaller than 0.45 μm.

Summary

The fouling indexes SDI15 have higher correlation to TDS and MFI have higher correlation to the turbidity and conductivity. It was concluded from the sample waste water, that on average, each increase in turbidity value by 0.15 NTU causes the MFI value to increase by 1 unit. On the other hand, each 100 $\mu\text{S}/\text{cm}$ unit difference of conductivity causes to MFI values to increase by 1.5 unit. Whereas, SDI15 was increasing by 1.5 units when the TDS was increasing by 25 mg/L in the trial of the commercial salt. The exact correlation is dependent on the sample type.

The fouling indexes were generated with a different filtration equipments: BOKU instrument and INSPECTOR apparatus. The standard deviation of the values from the INSPECTOR is on average 5.4 times higher than the values generated from the BOKU instrument. From the same samples with same concentration, values generated from the BOKU instrument were almost always higher than the values generated from the INSPECTOR. The MFI values showed statistically significant difference in mean values, whereas the SDI15 values have no statistically significant difference in mean values. By doing the recalculation on the values generated from BOKU instrument (by methodology of the INSPECTOR apparatus) it was concluded that the main reason for the difference in the values is not the calculation methodology but rather measurement technique.

The performance of the reverse osmosis membrane solely depends on the set up, e.g. the position of the pressure valve. The permeate flow rate was higher and could reach up to 100% when the pressure valve was placed on the retentate side.

The samples were prepared in different concentrations and filtered for 5 hours each. It was concluded that, the permeate flow rate deviation at the end of the filtration depend on the feed conductivity and ORP. The results show that the trial will have a decreasing permeate, starting from the feed with conductivity value equal to 173 $\mu\text{S}/\text{cm}$ and ORP values -78 mV. The lower the ORP and higher the conductivity the faster the permeate flow rate decrease.

Throughout the filtration process the water quality parameters, such as turbidity, conductivity etc., were measured every 1- 5 minutes. The values of the retentate side have been calculated and the results show that the increase rate differ between water quality parameters.

The rejection rate of the membrane in terms of pollutants was tested with fertilizer (nitrate), pesticide (diurone, simazine, atrazine) and heavy metals (copper, zinc). In general, the rejection rate is higher than 87% for all pollutants. Within the chemicals copper was removed most efficiently (98.8%), followed by zinc (98.5%), atrazine (95.6%) and nitrate (92.2%). Simazine was rejected the least (87.2%).

The rejection rate depends on the membrane fouling and on the type of pollutant. For instance, a new membrane with reverse osmosis medium, has higher rejection rate of the heavy metals (around 3 times) than the old membrane. On the other hand, old membrane has higher rejection rate of the pesticides.

Within the trials with the same membrane, the rejection rate was also differing depending on the medium. Rejection rate of the new membrane with reverse osmosis medium expressed higher performance against heavy metal and fertilizer. However, the diurone and simazine were rejected better in the tap water medium.

The biocide performance is also dependent on the membrane type. The new membrane has on average 99,5% removal efficiency of live cells, whereas the old membrane has 88% of efficiency. The new membrane has 98.4% less live cell counts on the permeate than on the retentate side. On the other hand, old membrane permeate side has 92.4% less cell counts than the retentate.

9. List of Figures.

- Figure 1. Reverse osmosis membrane separation system diagram. (www.puretecwater.com)
- Figure 2. Concentration polarization (Wang, Z. et al., 2016)
- Figure 3. Molecular structure of Diurone
- Figure 4. Molecular structure of Atrazine
- Figure 5. Molecular structure of Simazine
- Figure 6. Filtration curve t/V versus V . (Li et al., 2017)
- Figure 7. Formazine experiment on SDI and MFI. (Schippers & Salinaz-Rodriguez, 2014)
- Figure 8. Chart of the history of fouling index developments (Salinaz-Rodriguez et al., 2010)
- Figure 9. Description of the multiple membrane array system (Ju et al., 2015)
- Figure 10. Reverse osmosis pilot plant sketch
- Figure 11. The reverse osmosis pilot plant
- Figure 12. Arduino Uno board
- Figure 13. Sketch scheme of SDI and MFI measuring set up
- Figure 14. INSPECTOR apparatus
- Figure 15. Calculation of the MFI
- Figure 16. Generation of MFI
- Figure 17. Correlation of the concentration factor and the duration of time that take up to reach cake filtration phase (Sample from the Ukrainian surface water).
- Figure 18. 0.45 filters after the filtration of surface water from Ukraine (left) and waste water (right) sample and drying in the oven for 1 hour
- Figure 19. Correlation of the suspended solids and indexes to the concentration factor.
- Figure 20. Concentration factor vs. Turbidity
- Figure 21. Comparison of the indexes relative to the concentration factor.
- Figure 22. Correlation of MFI relative to the concentration factor
- Figure 23 . Concentration factor vs. SDI2 values from different filters.
- Figure 24. Conductivity vs. MFI 0.45 [s/L^2] graph, from the waste water sample ($R^2 = 0,91$)
- Figure 25. Conductivity vs. MFI 0.45 [s/L^2] graph, from the sample from the surface water from Ukraine
- Figure 26. Turbidity NTU correlation to the MFI [s/L^2] ($R^2 = 0,82$), from waste water sample
- Figure 27. Turbidity NTU correlation to the MFI [s/L^2] ($R^2 = 0,82$), from Ukrainian surface water sample.
- Figure 28. SDI15 and TDS correlation from the commercial salt trial
- Figure 29. Comparison of SDI values generated from INSPECTOR and BOKU instrument.
- Figure 30. Fouling index values comparison.
- Figure 31. Wastewater trial 25:8, comparison of BOKU instrument graph with the INSPECTOR graph.

List of Figures

Figure 32. The graph of the filtration of the first 30 seconds of the BOKU instrument and INSPECTOR apparatus.

Figure 33. The filtration of the reverse osmosis sample without the pressure variation.

Figure 34. Reverse osmosis trial with the pressure deviation on the permeate side.

Figure 35. Reverse osmosis experiment with retentate pressure deviation.

Figure 36. Correlation of the permeate flux and the feed pressure.

Figure 38. Retentate flow rate of the waste water trial.

Figure 39. Retentate pressure values of the waste water trial.

Figure 40. Conductivity values of the retentate of samples of the waste water trial.

Figure 41. Permeate flow of the trials with surface water from Ukraine.

Figure 42. ORP and Conductivity values of the trial from Ukrainian surface water.

Figure 43. Flux rates of the stock solution experiment.

Figure 44. Rejection rate of the atrazine by an old membrane.

Figure 45. Rejection rate of the atrazine by new membrane.

Figure 46. Live cell count after the biocide of the old and new membrane.

10. List of Tables.

- Table 1. Pretreatment methods for specific SDI and Nephelometric Turbidity Unit (NTU). (Yiantios, 2003).
- Table 2. Differences and common disadvantages of SDI and MFI (Rachman, 2011).
- Table 3. Technical description of the water quality measuring devices.
- Table 4. Technical information of the Arduino microprocessor board.
- Table 5. Calibration of the flow rate measurement.
- Table 6. Technical information about the equipment of the SDI and MFI trial.
- Table 7. Technical information of the INSPECTOR apparatus.
- Table 8. Technical information about the filter of the INSPECTOR apparatus.
- Table 9. Concentration factors of the samples for SDI and MFI.
- Table 10. Samples for the INSPECTOR trial.
- Table 11. Samples for the calibration of the reverse osmosis plant trial.
- Table 12. Dilution factor of the reverse osmosis trial.
- Table 13. Concentrations of the stock solution.
- Table 14. Sampling of the reverse osmosis membrane trial with chemical substances.
- Table 15. Standard deviations of SDI15 and MFI values.
- Table 16. MFI and SDI 15 values of the reverse osmosis and tap water trials.
- Table 17. Comparison of SDI2, SDI5, SDI10, SDI15 and MFI values.
- Table 18. R-squared values of the indexes.
- Table 19. Calculation of the R-squared of MFI values derived from different filters.
- Table 20. Summary of the SDI2 values.
- Table 21. Standard deviation of the BOKU instrument and INSPECTOR apparatus values.
- Table 22. R- squared values of the trend lines of the index results.
- Table 23. Standard deviation of the indexes derived from the INSPECTOR of the waste water sample.
- Table 24. Percentage difference between the MFI value from the INSPECTOR and the BOKU SIG instrument.
- Table 25. Standard deviation of the fouling indexes derived from the different sources.
- Table 26. Index values from the different sources.
- Table 27. Summary of the trial of reverse osmosis water.
- Table 28. Summary of the reverse osmosis water trial with the pressure deviation on retentate and permeate side.
- Table 29. Salt rejection rate of the waste water trial.
- Table 30. Concentration of the zink inside the tank
- Table 31. Concentration of copper inside the tank
- Table 32. Summary of the filtration parameters of the stock solution trial.

11. Abbreviations.

Δ		Difference
Δp		Transmembrane pressure
A	[m ²]	Area
C	[mol/m ³]	Concentration
D	[m ² /S]	Diffusion coefficient
D	[m ² /s]	Diffusion coefficient
ε	[-]	Porosity
I	[1/m ²]	Filter cake index
J	[mol/(m ² *s)], [m ³ /(m ² *s)]	Convective passage of salt
K _w		Permeability constant
M _i	[kg/mol]	Molar mass
η	[Pa*s]	Dynamic viscosity
p	[bar]	Pressure
P	[mol/(m ² *s*bar)], [m ³ /(m ² *s*bar)]	Permeability
Q	[m ³ /s]	Flow rate
R	[-]	Recovery
T	[°C]	Temperature
T	[s]	Time
V	[m ³]	Volume
δ	[m]	Thickness of boundary layer
E	[-]	Porosity
Π	[bar]	Osmotic pressure

12.Literature.

1. Belessiotis, V., Kalogirou, S., & Delyannis, E. (2016). Desalination Methods and Technologies—Water and Energy. In *Thermal Solar Desalination*. <https://doi.org/10.1016/B978-0-12-809656-7.00001-5>
2. Tchounwou, P. B., & Zhou, J. (2015). International Journal of Environmental Research and Public Health Best Paper Award 2015. *International Journal of Environmental Research and Public Health*. <https://doi.org/10.3390/ijerph120101050>
3. Wilhelm, M., Bergmann, S., & Dieter, H. H. (2010). Occurrence of perfluorinated compounds (PFCs) in drinking water of North Rhine-Westphalia, Germany and new approach to assess drinking water contamination by shorter-chained C4-C7 PFCs. *International Journal of Hygiene and Environmental Health*. <https://doi.org/10.1016/j.ijheh.2010.05.004>
4. Von Gunten, U. (2003). Ozonation of drinking water: Part II. Disinfection and by-product formation in presence of bromide, iodide or chlorine. *Water Research*. [https://doi.org/10.1016/S0043-1354\(02\)00458-X](https://doi.org/10.1016/S0043-1354(02)00458-X)
5. Nguyen, T., Roddick, F. A., & Fan, L. (2012). Biofouling of water treatment membranes: A review of the underlying causes, monitoring techniques and control measures. *Membranes*. <https://doi.org/10.3390/membranes2040804>
6. Cai, B. J., Glucina, K., Baudin, I., Fabre, A., Arcangeli, J. P., & Ng, H. Y. (2011). Establishment of Membrane Fouling Propensity Approach to Evaluate Ultrafiltration Process Applied On Secondary Effluents. In *6th IWA Specialist Conference on Membrane Technology for Water and Wastewater Treatment, Aachen, Germany*.
7. Krishna Reddy, Y. V., Adamala, S., Levlin, E. K., & Reddy, K. S. (2017). Enhancing nitrogen removal efficiency of domestic wastewater through increased total efficiency in sewage treatment (ITEST) pilot plant in cold climatic regions of Baltic Sea. *International Journal of Sustainable Built Environment*. <https://doi.org/10.1016/j.ijse.2017.05.002>
8. Huang, H.-C., & Xie, R. (2012). New Osmosis Law and Theory: the New Formula that Replaces van't Hoff Osmotic Pressure Equation. *ArXiv Preprint ArXiv:1201.0912*. <https://doi.org/10.1007/s12403-013-0093-3>
9. Długolecki, P., Ogonowski, P., Metz, S. J., Saakes, M., Nijmeijer, K., & Wessling, M. (2010). On the resistances of membrane, diffusion boundary layer and double layer in ion exchange membrane transport. *Journal of Membrane Science*. <https://doi.org/10.1016/j.memsci.2009.11.069>
10. Prihasto, N., & Kim, S.-H. (2012). The sensitivity of SDI and MFI to a change in particle concentration and properties under saline conditions. *Journal of Water Reuse and Desalination*. <https://doi.org/10.2166/wrd.2012.064>
11. Wang, Z., Zheng, J., Tang, J., Wang, X., & Wu, Z. (2016). A pilot-scale forward osmosis membrane system for concentrating low-strength municipal wastewater: Performance and implications. *Scientific Reports*. <https://doi.org/10.1038/srep21653>
12. Loos, R., Locoro, G., Comero, S., Contini, S., Schwesig, D., Werres, F., ... Gawlik, B. M. (2010). Pan-European survey on the occurrence of selected polar organic persistent pollutants in ground water. *Water Research*. <https://doi.org/10.1016/j.watres.2010.05.032>

13. Belfort, G. (1980). Artificial particulate fouling of hyperfiltration membranes IV. Dynamic protection from fouling. *Desalination*, 34(3), 159–169. [https://doi.org/10.1016/S0011-9164\(00\)88587-2](https://doi.org/10.1016/S0011-9164(00)88587-2)
14. Kagramanov, G. G., Farnosova, E. N., & Kandelaki, G. I. (2010). Heavy Metal Cationic Wastewater Treatment With Membrane Methods. *Water Treatment Technologies for the Removal of High-Toxicity Pollutants*, (September), 177–182.
15. Plakas, K. V., & Karabelas, A. J. (2012). Removal of pesticides from water by NF and RO membranes - A review. *Desalination*, 287, 255–265. <https://doi.org/10.1016/j.desal.2011.08.003>
16. Koyuncu, I. (2002). Effect of operating conditions on the separation of ammonium and nitrate ions with nanofiltration and reverse osmosis membranes. *Journal of Environmental Science and Health Part A-Toxic/Hazardous Substances & Environmental Engineering*, 37(7), 1347–1359. <https://doi.org/10.1081/Ese-120005991>
17. Van Der Bruggen, B., & Vandecasteele, C. (2003). Removal of pollutants from surface water and groundwater by nanofiltration: Overview of possible applications in the drinking water industry. *Environmental Pollution*, 122(3), 435–445. [https://doi.org/10.1016/S0269-7491\(02\)00308-1](https://doi.org/10.1016/S0269-7491(02)00308-1)
18. Hegazi, H. A. (2013). Removal of heavy metals from wastewater using agricultural and industrial wastes as adsorbents. *HBRC Journal*, 9(3), 276–282. <https://doi.org/10.1016/j.hbrcj.2013.08.004>
19. Yoon, Y., & Lueptow, R. M. (2005). Removal of organic contaminants by RO and NF membranes. *Journal of Membrane Science*, 261(1–2), 76–86. <https://doi.org/10.1016/j.memsci.2005.03.038>
20. Bilstad, T. (1995). Nitrogen separation from domestic wastewater by reverse osmosis. *Journal of Membrane Science*, 102(C), 93–102. [https://doi.org/10.1016/0376-7388\(94\)00279-8](https://doi.org/10.1016/0376-7388(94)00279-8)
21. Drazevic, E., Kosutic, K., Fingler, S., & Drevenkar, V. (2011). Removal of pesticides from the water and their adsorption on the reverse osmosis membranes of defined porous structure. *Desalination and Water Treatment*, 30(1–3), 161–170. <https://doi.org/10.5004/dwt.2011.1959>
22. Glater, J. (1998). The early history of reverse osmosis membrane development. *Desalination*, 117(1–3), 297–309. [https://doi.org/10.1016/S0011-9164\(98\)00122-2](https://doi.org/10.1016/S0011-9164(98)00122-2)
23. Bodzek, M., & Konieczny, K. (1998). Comparison of various membrane types and module configurations in the treatment of natural water by means of low-pressure membrane methods. *Separation and Purification Technology*, 14(1–3), 69–78. [https://doi.org/10.1016/S1383-5866\(98\)00061-6](https://doi.org/10.1016/S1383-5866(98)00061-6)
24. Van der Bruggen, B., Verliefde, A., Braeken, L., Cornelissen, E. R., Moons, K., Verberk, J. Q. J. C., ... Amy, G. (2006). Assessment of a semi-quantitative method for estimation of the rejection of organic compounds in aqueous solution in nanofiltration. *Journal of Chemical Technology and Biotechnology*, 81(7), 1166–1176. <https://doi.org/10.1002/jctb.1489>
25. Kim, D., Jung, S., Sohn, J., Kim, H., & Lee, S. (2009). Biocide application for controlling biofouling of SWRO membranes - an overview. *Desalination*, 238(1–3), 43–52. <https://doi.org/10.1016/j.desal.2008.01.034>
26. Vanysacker, L., Denis, C., Declerck, P., Piasecka, A., & Vankelecom, I. F. J. (2013). Microbial adhesion and biofilm formation on microfiltration membranes: A detailed

- characterization using model organisms with increasing complexity. *BioMed Research International*, 2013. <https://doi.org/10.1155/2013/470867>
27. Elzo, D., Huisman, I., Middelenk, E., & Gekas, V. (1998). Charge effects on inorganic membrane performance in a cross-flow microfiltration process. In *Colloids and Surfaces A: Physicochemical and Engineering Aspects* (Vol. 138, pp. 145–159). [https://doi.org/10.1016/S0927-7757\(96\)03957-X](https://doi.org/10.1016/S0927-7757(96)03957-X)
 28. Sheikholeslami, R. (2003). Mixed salts—scaling limits and propensity. *Desalination*, 154(2), 117–127. [https://doi.org/10.1016/S0011-9164\(03\)80012-7](https://doi.org/10.1016/S0011-9164(03)80012-7)
 29. van den Brink, P., Zwijnenburg, A., Smith, G., Temmink, H., & van Loosdrecht, M. (2009). Effect of free calcium concentration and ionic strength on alginate fouling in cross-flow membrane filtration. *Journal of Membrane Science*, 345(1–2), 207–216. <https://doi.org/10.1016/j.memsci.2009.08.046>
 30. Schäfer, A. J., Fane, A. G., & Waite, T. D. (2000). Fouling effects on rejection in the membrane filtration of natural waters. *Desalination*, 131(1–3), 215–224. [https://doi.org/10.1016/S0011-9164\(00\)90020-1](https://doi.org/10.1016/S0011-9164(00)90020-1)
 31. Alhadidi, A., Kemperman, A. J. B., Schippers, J. C., Wessling, M., & van der Meer, W. G. J. (2012). SDI: Is it a reliable fouling index? *Desalination and Water Treatment*, 42(1–3), 43–48. <https://doi.org/10.1080/19443994.2012.683102>
 32. Bellona, C. (2014). *Desalination. Desalination: Water from Water*. <https://doi.org/10.1002/9781118904855>
 33. Potts, D. E., Ahlert, R. C., & Wang, S. S. (1981). A critical review of fouling of reverse osmosis membranes. *Desalination*, 36, 235–264. [https://doi.org/10.1016/S0011-9164\(00\)88642-7](https://doi.org/10.1016/S0011-9164(00)88642-7)
 34. Goosen, M. F. A., Sablani, S. S., Al-Hinai, H., Al-Obeidani, S., Al-Belushi, R., & Jackson, D. (2004). Fouling of reverse osmosis and ultrafiltration membranes: A critical review. *Separation Science and Technology*. <https://doi.org/10.1081/SS-120039343>
 35. Kiso, Y., Nishimura, Y., Kitao, T., & Nishimura, K. (2000). Rejection properties of non-phenylic pesticides with nanofiltration membranes. *Journal of Membrane Science*, 171(2), 229–237. [https://doi.org/10.1016/S0376-7388\(00\)00305-7](https://doi.org/10.1016/S0376-7388(00)00305-7)
 36. Van Der Bruggen, B., Schaep, J., Maes, W., Wilms, D., & Vandecasteele, C. (1998). Nanofiltration as a treatment method for the removal of pesticides from ground waters. *Desalination*, 117(1–3), 139–147. [https://doi.org/10.1016/S0011-9164\(98\)00081-2](https://doi.org/10.1016/S0011-9164(98)00081-2)
 37. Košutić, K., & Kunst, B. (2002). Removal of organics from aqueous solutions by commercial RO and NF membranes of characterized porosities. *Desalination*, 142(1), 47–56. [https://doi.org/10.1016/S0011-9164\(01\)00424-6](https://doi.org/10.1016/S0011-9164(01)00424-6)
 38. Republic, C., Britain, G., & Republic, S. (2003). Less cost – more convenience : EU standard transfer ., 3–5.
 39. Bracco, G., & Holst, B. (2013). *Surface science techniques. Springer Series in Surface Sciences* (Vol. 51). <https://doi.org/10.1007/978-3-642-34243-1>
 40. Kim, S., Lee, S., Kim, C. H., & Cho, J. (2009). A new membrane performance index using flow-field flow fractionation (fl-FFF). *Desalination*, 247(1–3), 169–179. <https://doi.org/10.1016/j.desal.2008.12.022>
 41. Choi, J., Hwang, T., Lee, S., & Hong, S. (2009). A systematic approach to determine the fouling index for a RO / NF membrane process. *Des*, 238, 117–127. <https://doi.org/10.1016/j.desal.2008.01.042>
 42. Flux (transmembrane pressure). (n.d.), 241–250.

43. Sagle, A., & Freeman, B. (2004). Fundamentals of membranes for water treatment. *The Future of Desalination in Texas*, 1–17.
44. Alhadidi, A., Kemperman, A. J. B., Blankert, B., Schippers, J. C., Wessling, M., & van der Meer, W. G. J. (2011). Silt Density Index and Modified Fouling Index relation, and effect of pressure, temperature and membrane resistance. *Desalination*, 273(1), 48–56. <https://doi.org/10.1016/j.desal.2010.11.031>
45. Qurie, M., Abbad, J., Scranò, L., Mecca, G., Bufo, S. A., Khamis, M., & Karaman, R. (2013). Inland treatment of the brine generated from reverse osmosis advanced membrane wastewater treatment plant using epuvalisation system. *International Journal of Molecular Sciences*, 14(7), 13808–13825. <https://doi.org/10.3390/ijms140713808>
46. Ruiz-García, A., Melián-Martel, N., & Nuez, I. (2017). Short review on predicting fouling in RO desalination. *Membranes*, 7(4), 1–17. <https://doi.org/10.3390/membranes7040062>
47. Al-alawy, A. F., Al-alawy, A. F., & Salih, M. H. (2017). Theoretical and Experimental Study of Nanofiltration and Reverse Osmosis Membranes for Removal of Heavy Metals from Wastewater. *International Journal of Science and Research (IJSR)*, 6(12), 778–788. <https://doi.org/10.21275/ART20178885>
48. Andrade, L. H., Aguiar, A. O., Pires, W. L., Miranda, G. A., Teixeira, L. P. T., Almeida, G. C. C., & Amaral, M. C. S. (2017). Nanofiltration and reverse osmosis applied to gold mining effluent treatment and reuse. *Brazilian Journal of Chemical Engineering*, 34(1), 93–107. <https://doi.org/10.1590/0104-6632.20170341s20150082>
49. Salinas-Rodríguez, S. G., Amy, G. L., Schippers, J. C., & Kennedy, M. D. (2015). The Modified Fouling Index Ultrafiltration constant flux for assessing particulate/colloidal fouling of RO systems. *Desalination*, 365, 79–91. <https://doi.org/10.1016/j.desal.2015.02.018>
50. Sanches, S., Penetra, A., Granado, C., Cardoso, V. V., Ferreira, E., Benoliel, M. J., ... Crespo, J. G. (2011). Removal of pesticides and polycyclic aromatic hydrocarbons from different drinking water sources by nanofiltration. *Desalination and Water Treatment*, 27(1–3), 141–149. <https://doi.org/10.5004/dwt.2011.2087>
51. Safe Drinking Water Foundation. (2008). Ultrafiltration , Nanofiltration and Reverse osmosis. *Filtration*, 1–6.
52. Wilf, M. (2008). Membrane Types and Factors Affecting Membrane Performance. *Membrane Types and Factors Affecting Membrane Performance*, 1–92.
53. Bakalár, T., Búgel, M., & Gajdošová, L. (2009). Heavy metal removal using reverse osmosis. *Acta Montanistica Slovaca*, 14(3), 250–253.
54. Matin, A., Khan, Z., Zaidi, S. M. J., & Boyce, M. C. (2011). Biofouling in reverse osmosis membranes for seawater desalination: Phenomena and prevention. *Desalination*. <https://doi.org/10.1016/j.desal.2011.06.063>
55. Childress, A. E., & Elimelech, M. (1996). Effect of solution chemistry on the surface charge of polymeric reverse osmosis and nanofiltration membranes. *Journal of Membrane Science*. [https://doi.org/10.1016/0376-7388\(96\)00127-5](https://doi.org/10.1016/0376-7388(96)00127-5)

13. Appendix.

Fouling indexes derived from the BOKU instrument with filter with pore size 0.45 µm.

Ukrainian surface water trial.

Table 37 Fouling indexes of Ukrainian surface water trial

Sample	Concentration factor	SDI2	SDI5	SDI10	SDI15	MFI
Ukrainian surface water	7.5:1	10.23	8.78	6.70	4.75	1.11
	7.5:1	10.06	7.99	7.10	4.89	0.99
	7.5:1	10.80	7.23	7.30	4.45	0.98
	12.5:1	11.97	11.97	7.85	5.70	1.21
	12.5:1	14.53	14.53	8.35	6.03	1.72
	12.5:1	14.74	13.67	9.55	6.00	1.60
	17.5:1	31.17	16.13	8.75	6.00	3.13
	17.5:1	27.12	11.81	7.69	5.84	3.45
	17.5:1	25.00	15.44	8.57	5.94	3.80
	22.5:1	31.98	16.26	9.10	6.22	4.55
	22.5:1	27.78	15.77	7.96	6.01	4.32
	22.5:1	25.96	15.57	7.77	6.00	3.77

Correlation to the water quality parameter.

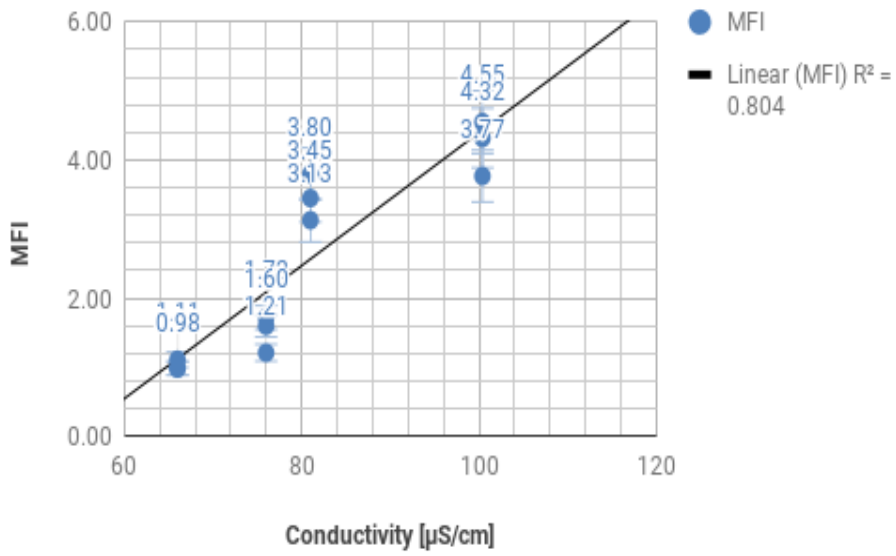


Figure 50. Correlation of MFI to conductivity.

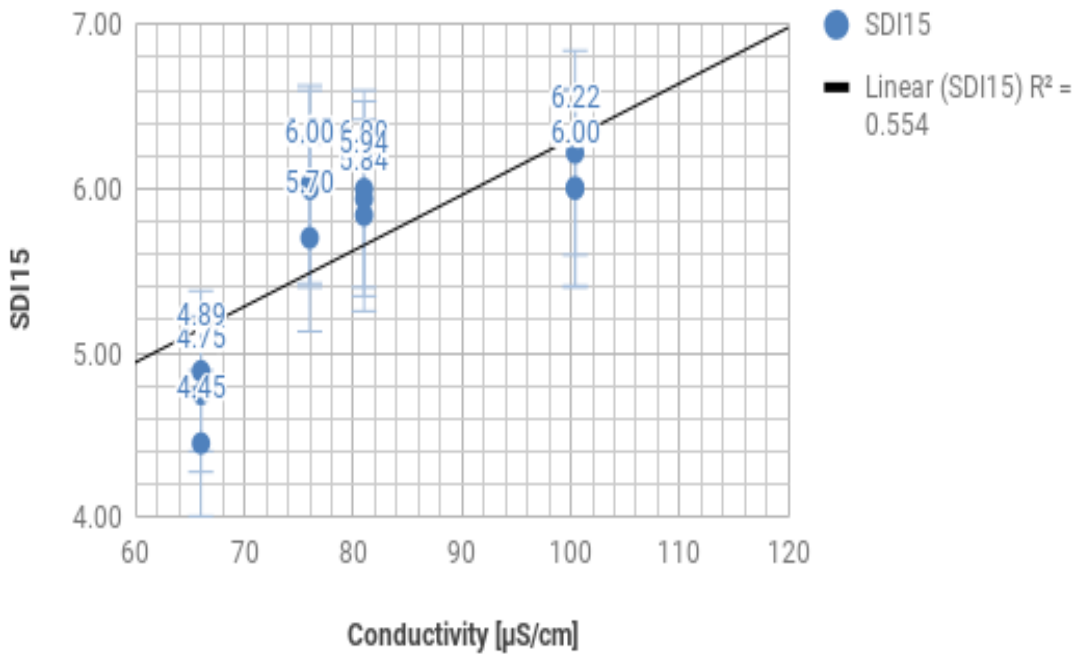


Figure 51. Correlation of MFI to Turbidity.

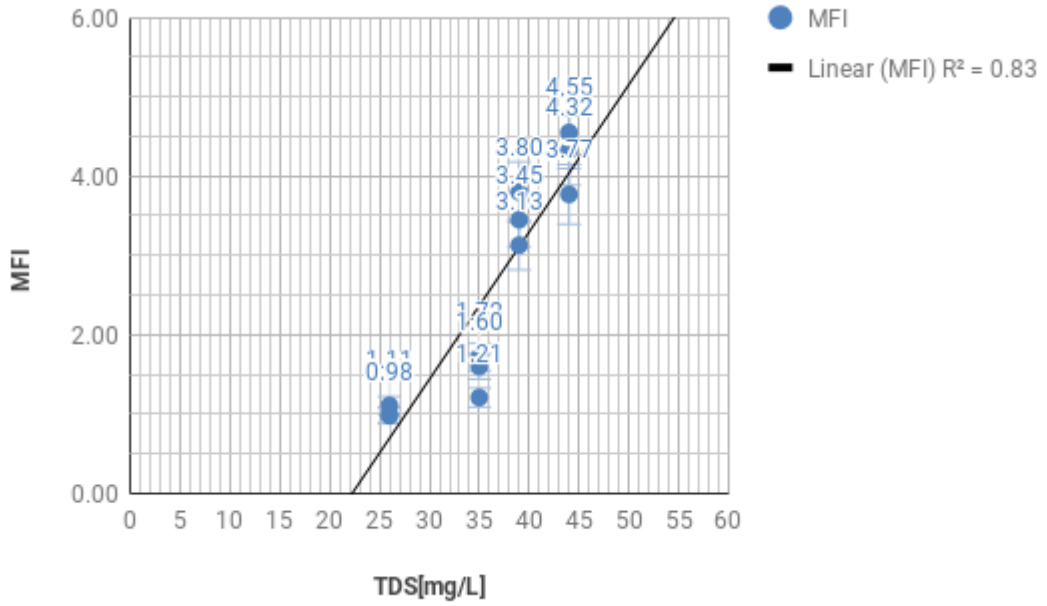


Figure 52. Correlation of MFI to TDS.

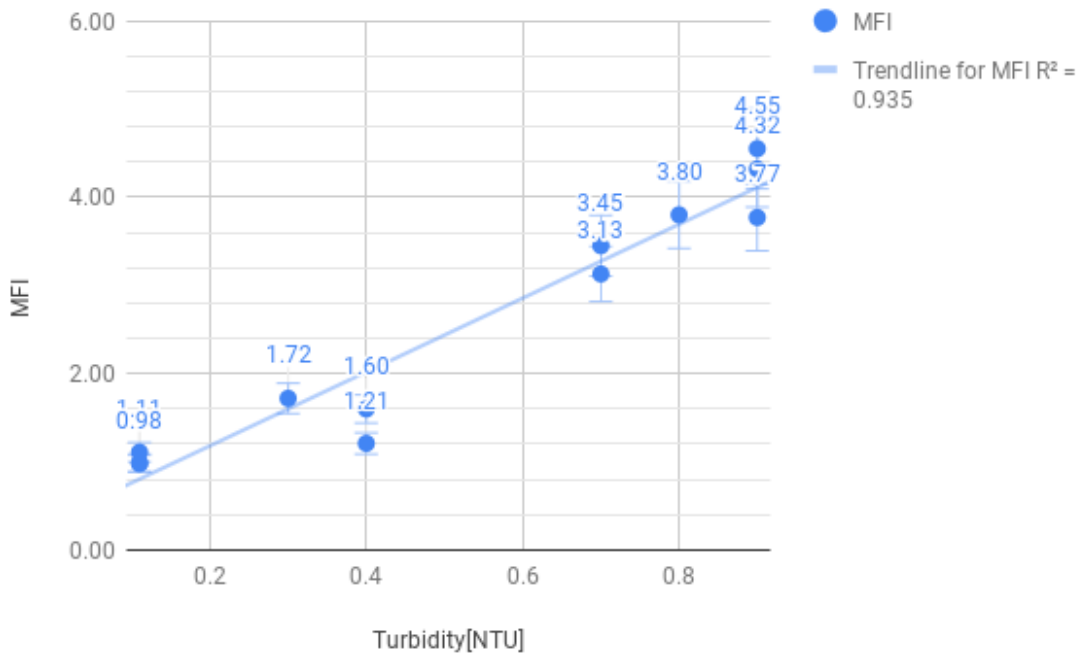


Figure 53. Correlation of SDI15 to conductivity.

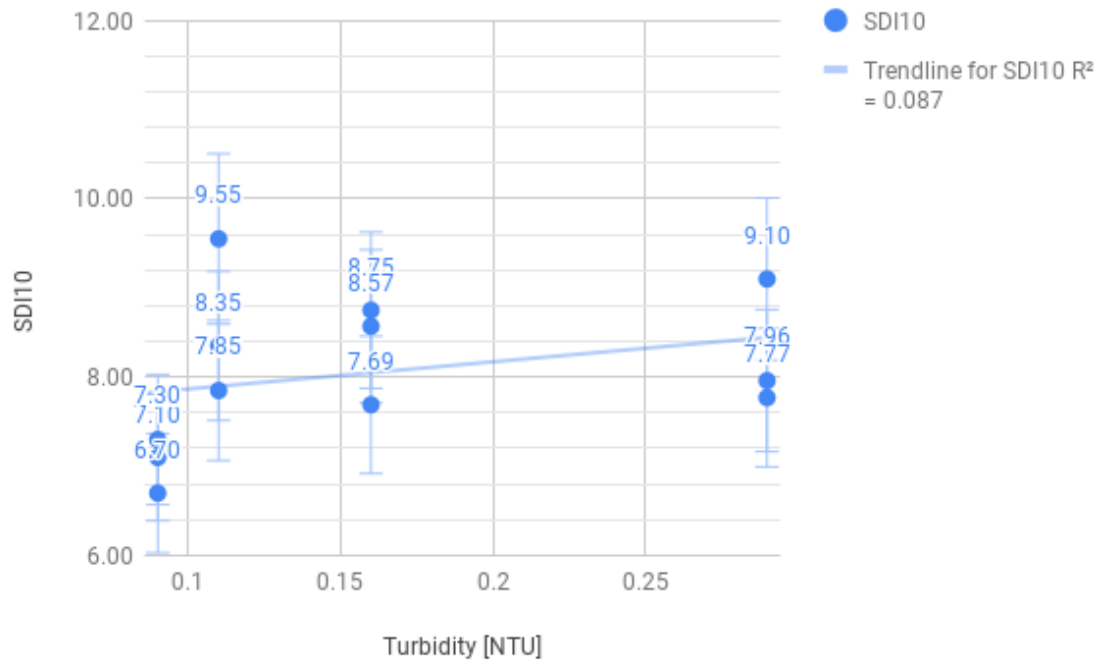


Figure 54. Correlation of SDI10 to Turbidity.

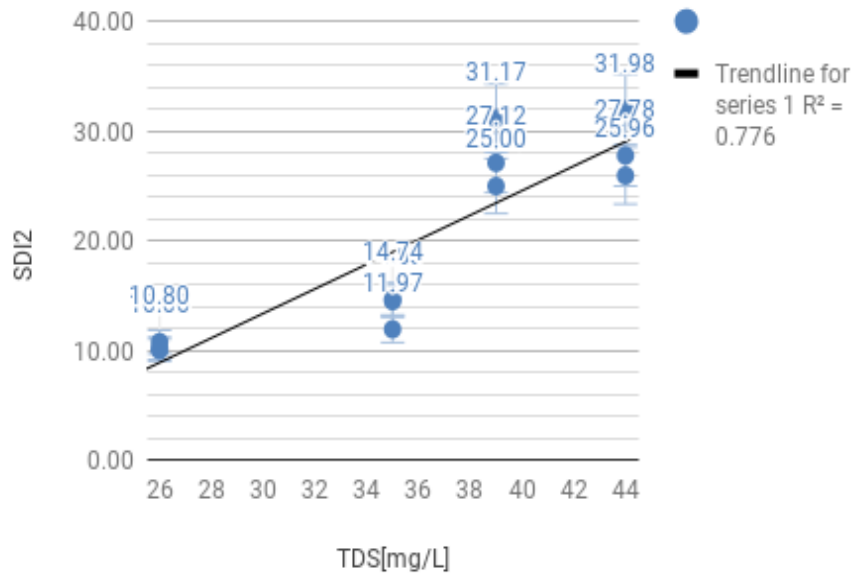


Figure 55. Correlation SDI2 to TDS.

Waste water trial.

Table 38. Fouling indexes of waste water trial.

Sample	SDI2	SDI5	SDI10	SDI15	MFI
2.5	42.23	17.79	9.45	6.36	2.65
2.5	42.30	18.46	9.41	6.27	2.69
2.5	42.19	18.50	9.33	6.25	2.70
5	46.08	19.17	9.65	6.43	3.59
5	48.06	19.43	9.79	6.54	3.20
5	47.60	19.37	9.75	6.50	3.22
7.5	45.75	19.61	9.44	6.43	3.87
7.5	46.90	19.18	9.38	6.61	4.07
7.5	46.03	18.69	9.99	6.39	3.67
10	46.47	18.84	9.53	6.58	4.03
10	45.35	18.38	9.33	6.25	4.10
10	46.02	18.90	9.64	6.69	4.11
12.5	47.74	19.01	10.01	6.99	3.87
12.5	47.84	19.11	9.66	6.87	4.00
12.5	48.01	19.23	9.77	7.01	4.77
17.5	46.42	18.85	9.34	6.50	4.56
17.5	47.34	19.03	8.99	6.51	4.99
17.5	47.71	19.12	9.56	7.47	4.61
22.5	47.60	19.34	9.66	7.79	4.77
22.5	47.80	19.11	9.59	8.12	4.81
22.5	47.99	19.32	9.61	8.22	4.74
25	47.91	19.42	9.72	8.35	5.64
25	48.01	19.21	9.65	8.65	5.71
25	49.00	20.01	9.71	8.95	5.67

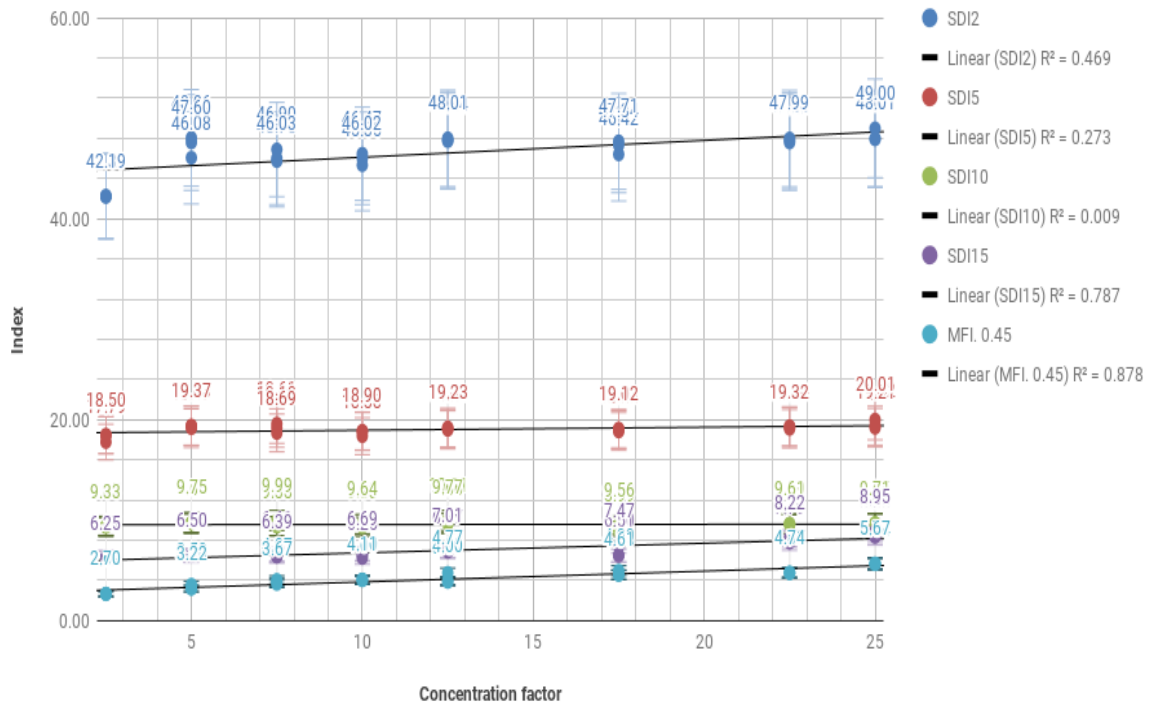


Figure 56. Correlation of the fouling indexes to the concentration factor.

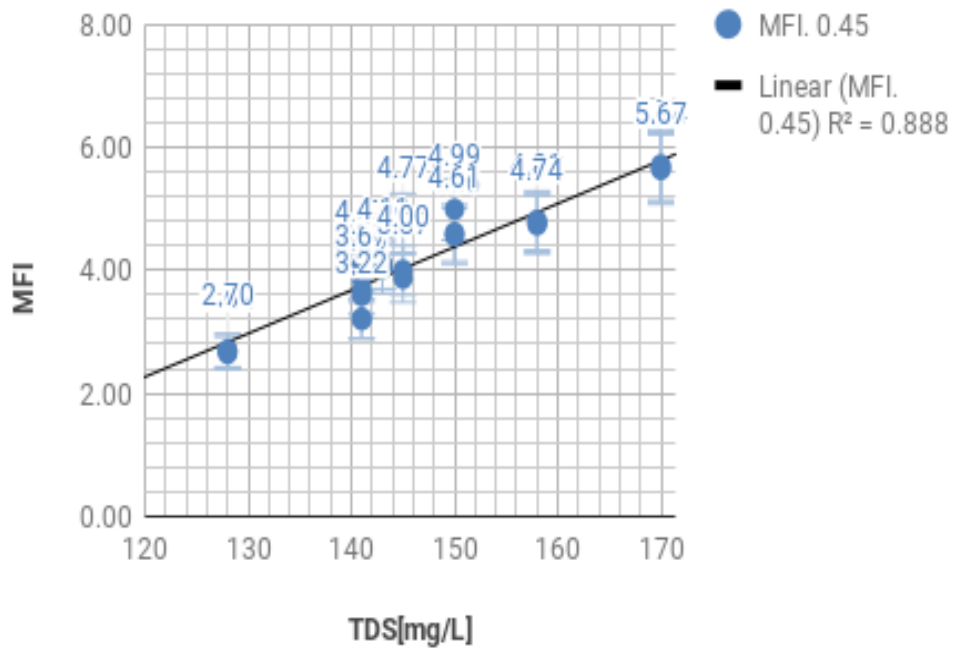


Figure 57. Correlation of MFI to TDS.

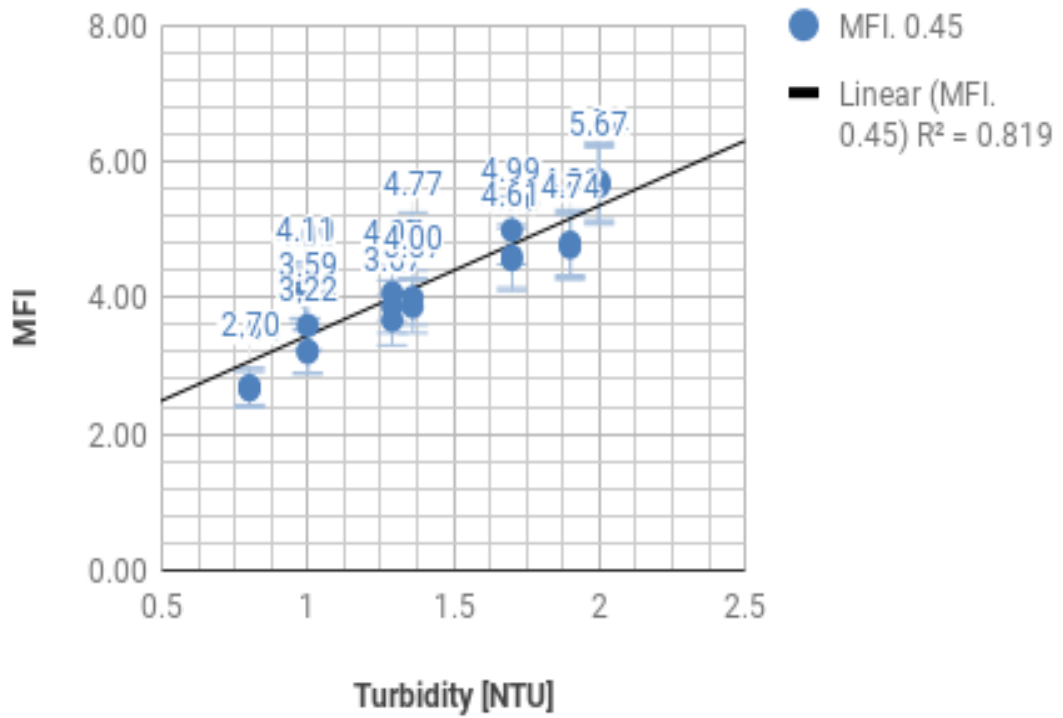


Figure 58. Correlation of MFI to Turbidity.

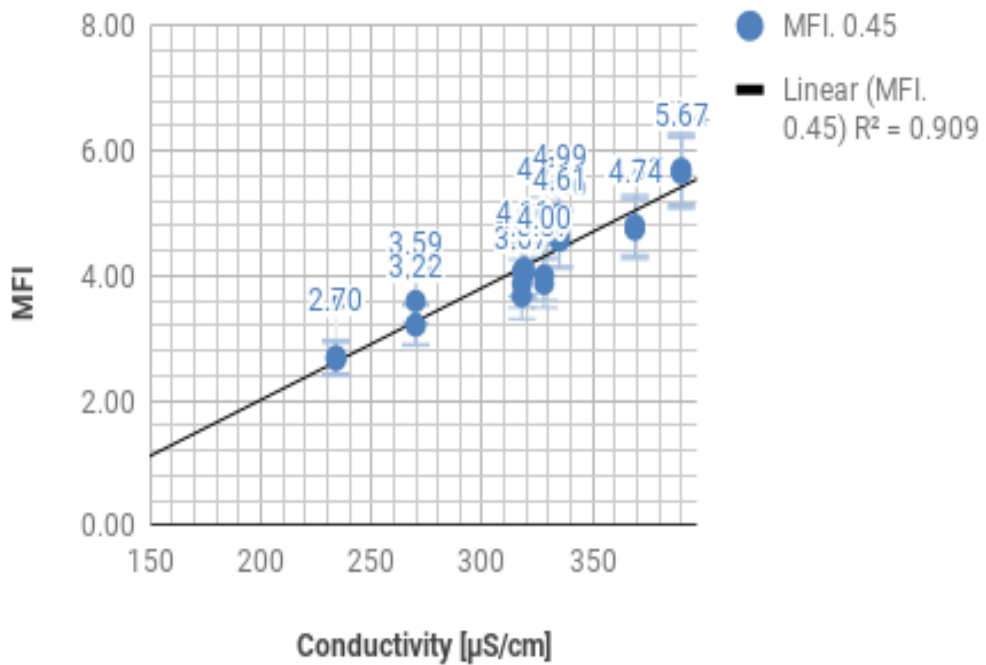


Figure 59. Correlation of MFI to Conductivity.

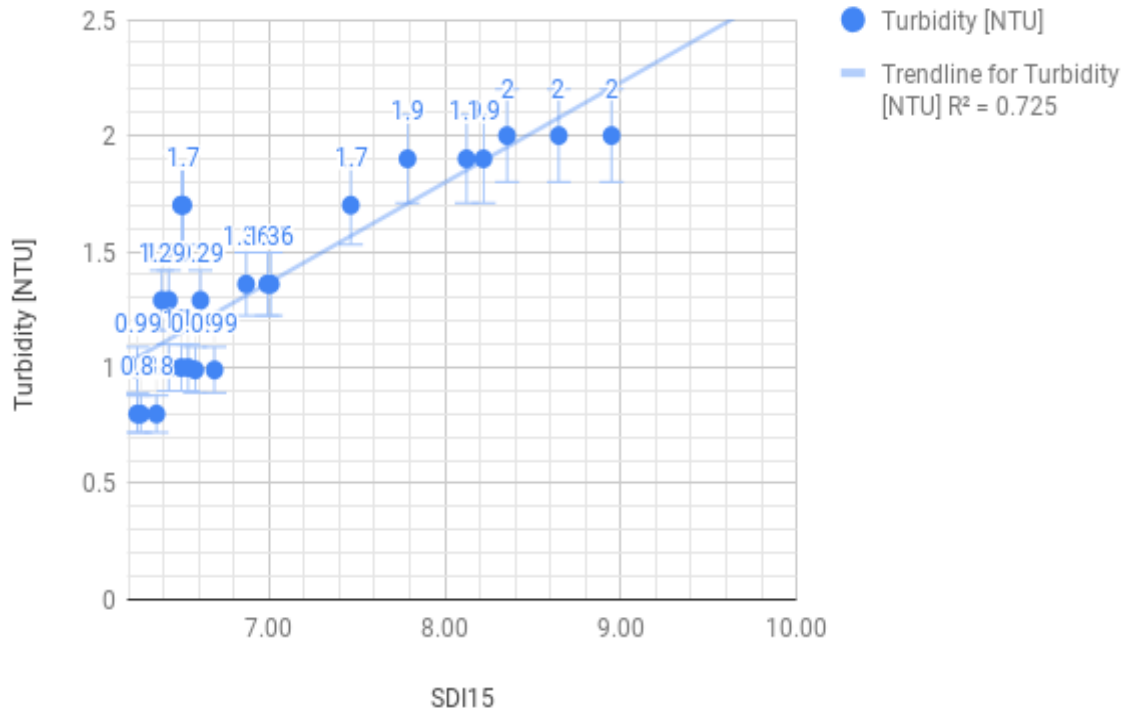


Figure 60. Correlation of SDI15 to Turbidity.

Commercial salt water trial.

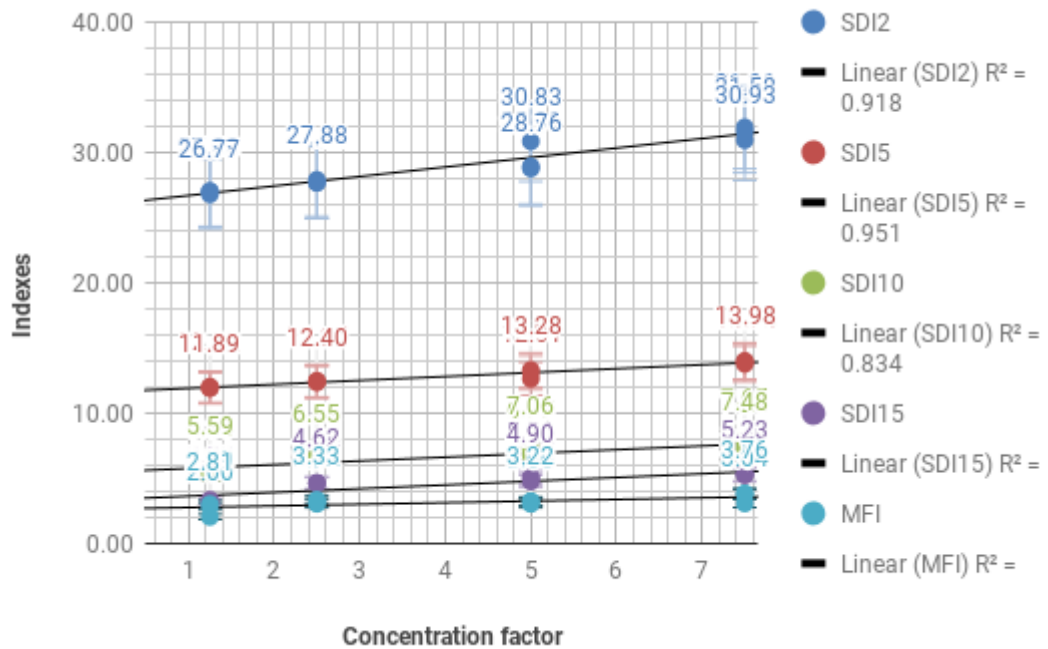


Figure 61. Correlation of fouling indexes to the concentration factor.

Table 39. Fouling indexes of salt trial

Sample	SDI2	SDI5	SDI10	SDI15	MFI
1.25	27.00	12.00	5.35	3.32	2.00
1.25	26.99	11.92	5.36	3.12	2.99
1.25	26.77	11.89	5.59	3.00	2.81
2.5	27.66	12.33	6.53	4.61	3.01
2.5	27.67	12.45	6.62	4.56	3.12
2.5	27.88	12.40	6.55	4.62	3.33
5	28.91	12.61	6.77	4.72	3.16
5	28.76	13.07	7.06	5.06	3.00
5	30.83	13.28	7.06	4.90	3.22
7.5	31.91	13.91	7.26	5.24	3.81
7.5	31.58	13.75	7.65	5.30	3.04
7.5	30.93	13.98	7.48	5.23	3.76

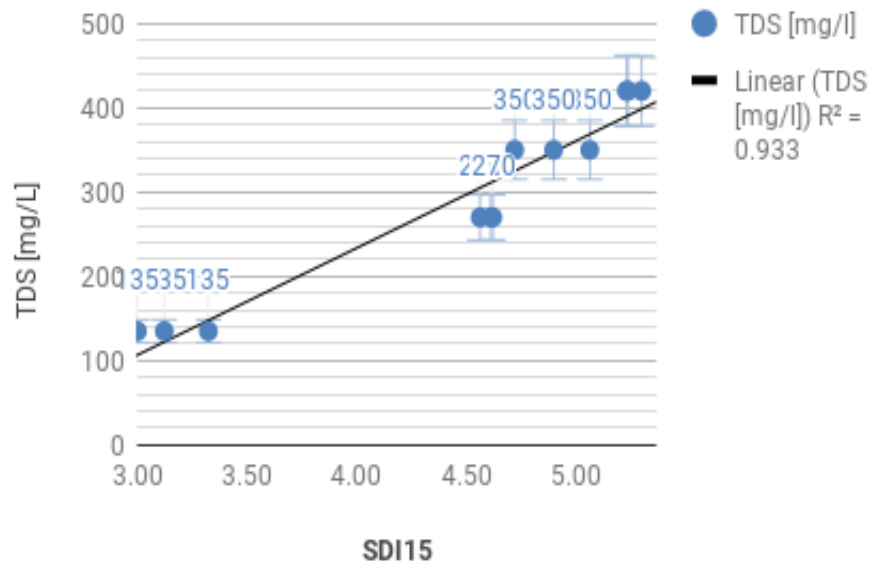


Figure 62. Correlation of SDI15 to TDS.

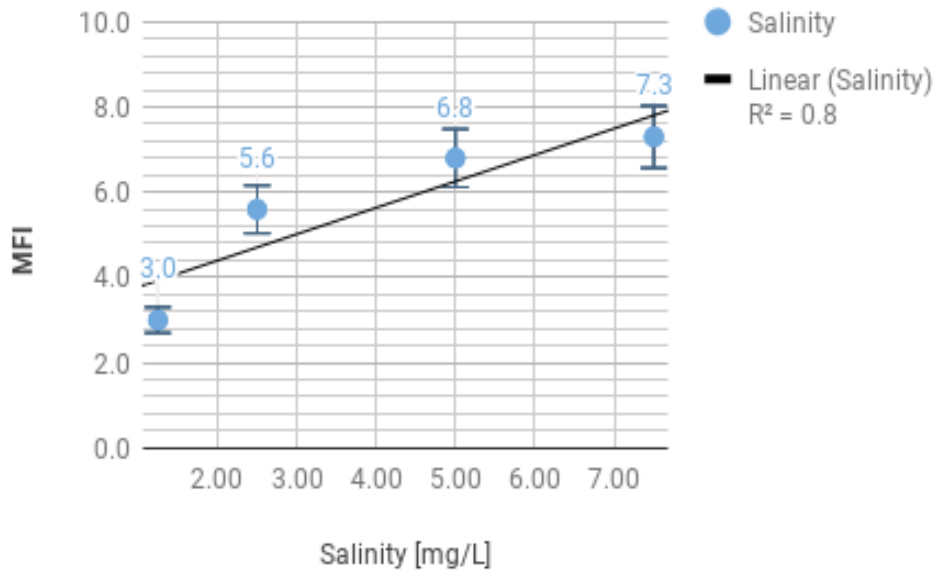


Figure 63. Correlation of salinity to the concentration factor.

Trial with a different filter with different pore size.

Waste water sample

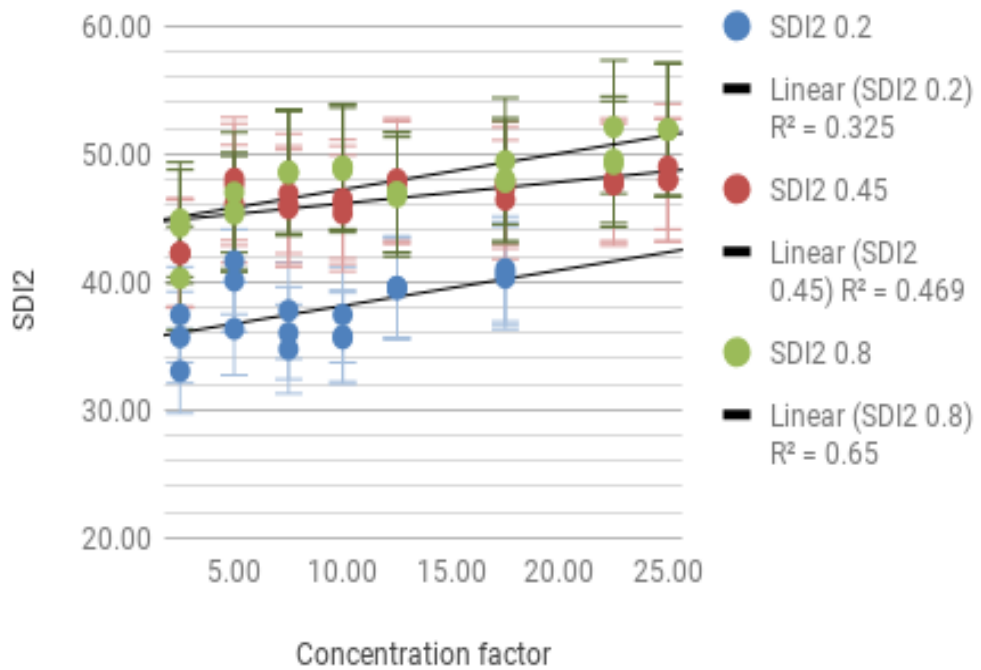


Figure 64. Correlation of SDI2 values derived from different the concentration factor.

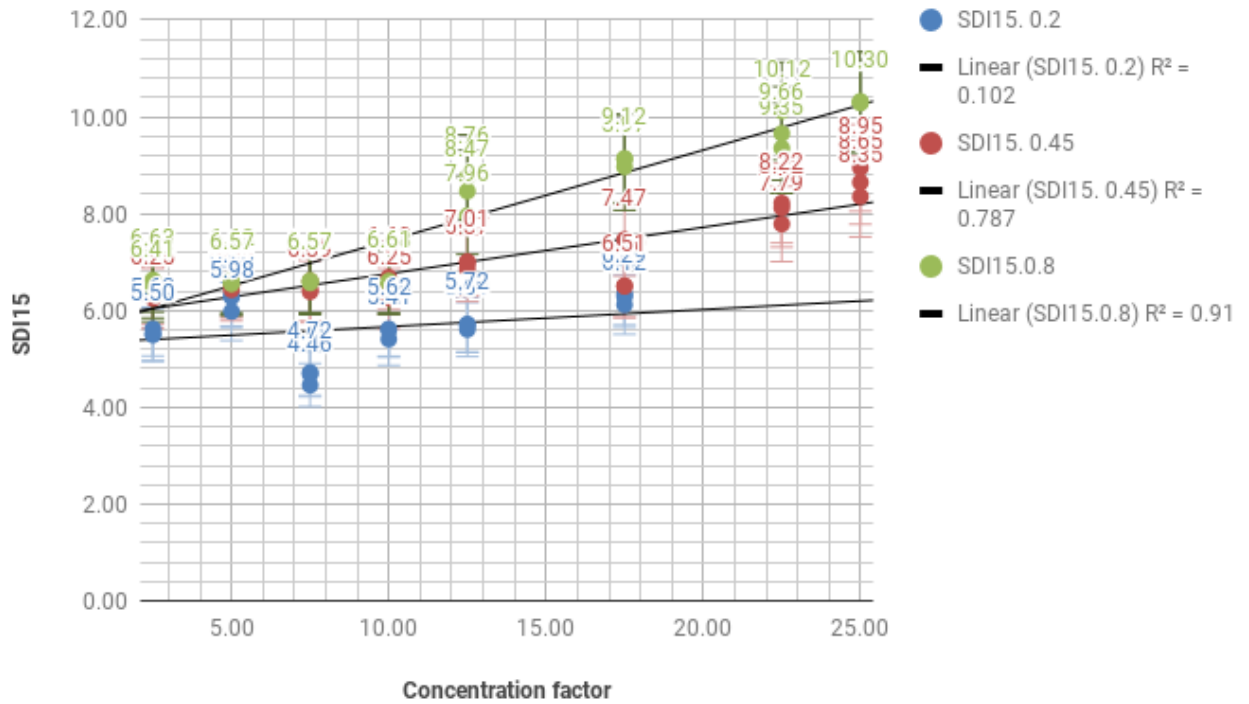


Figure 65. Correlation of SDI15 values to the concentration factor.

Sample from surface water from Ukraine.

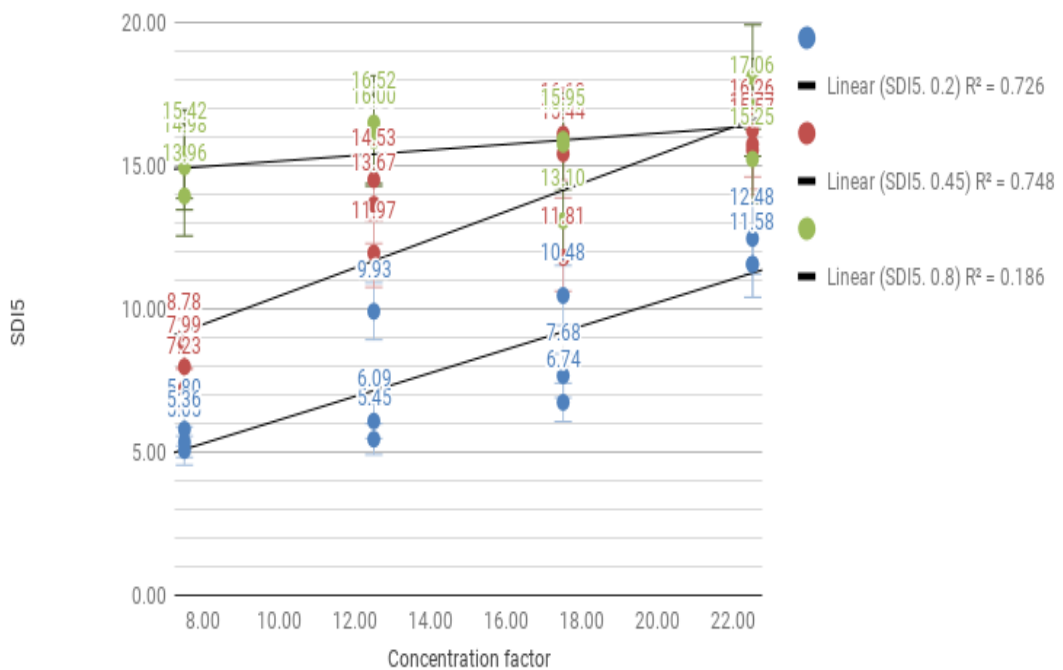


Figure 66. SDI5 correlate to concentration factor.

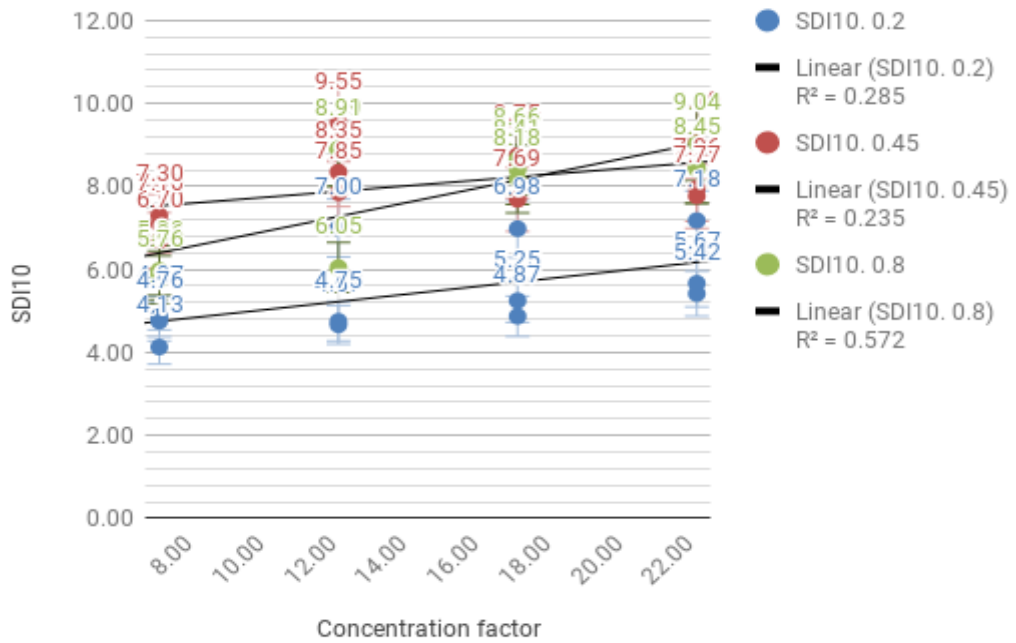


Figure 67. Correlation of SDI10 to concentration factor.

Reverse osmosis membrane separation experiment.

Tap water sample with new membrane

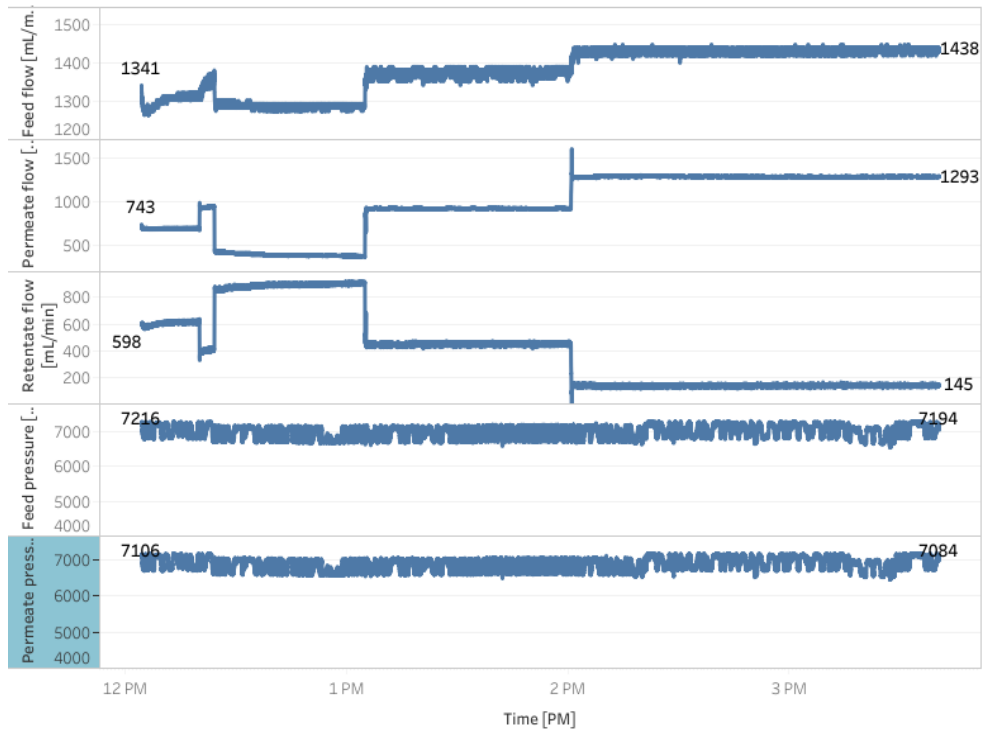


Figure 68. Tap water sample filtration by membrane (with pressure deviation).

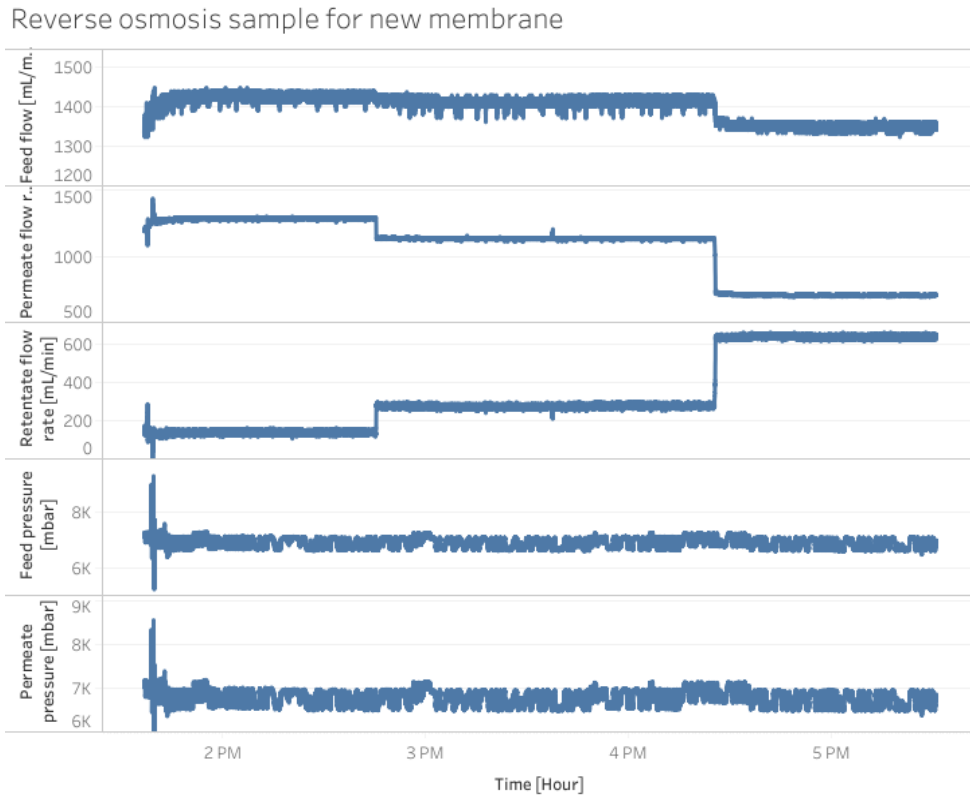


Figure 69. Reverse osmosis water sample filtration by new membrane (with pressure deviation).

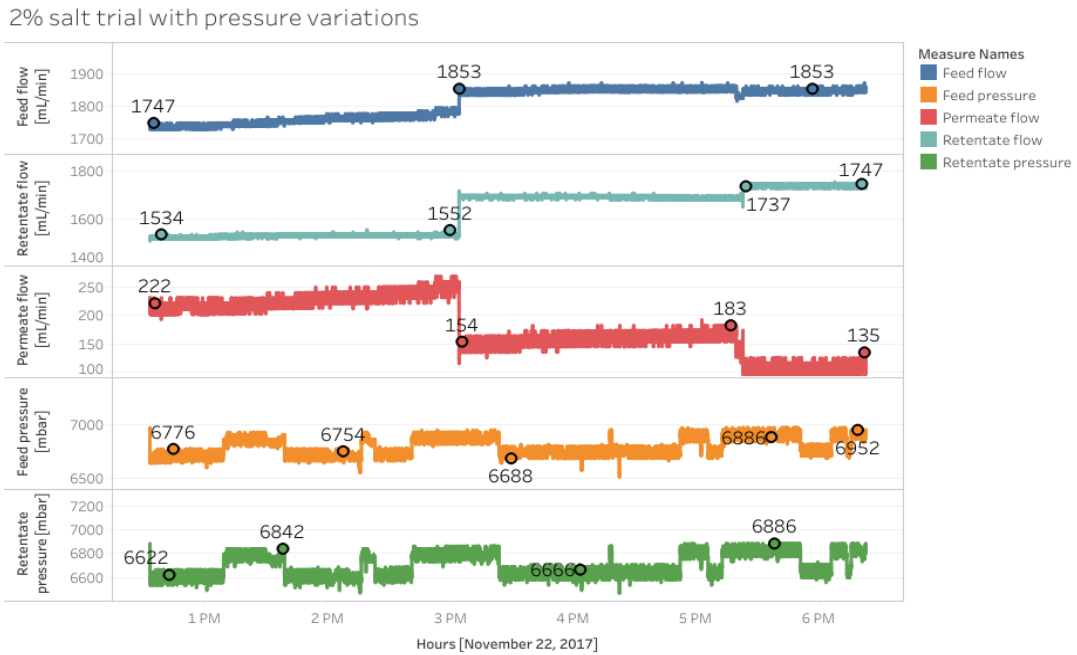


Figure 70. Commercial salt water filtration (2%) by old membrane (with pressure deviation).

4% salt trial with pressure variations

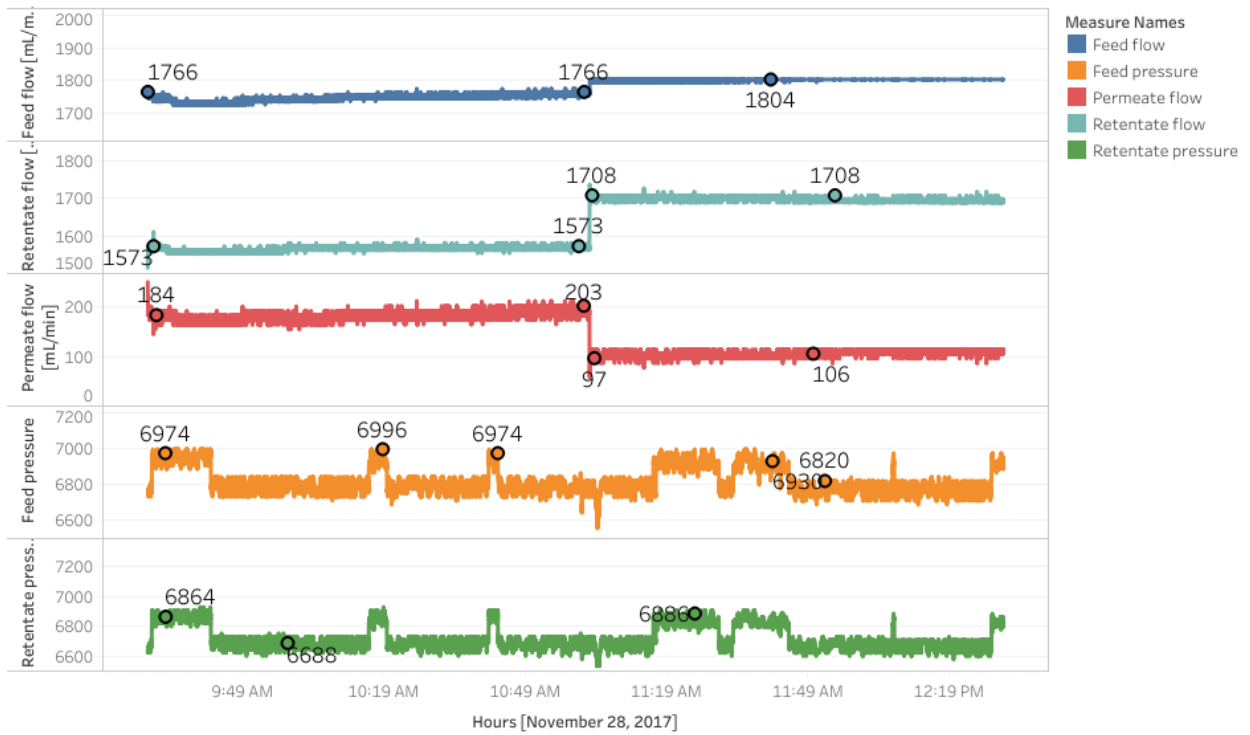


Figure 71. Commercial salt water filtration (4%) by old membrane (with pressure deviation).

2% salt trial with pressure variation, water quality indicators

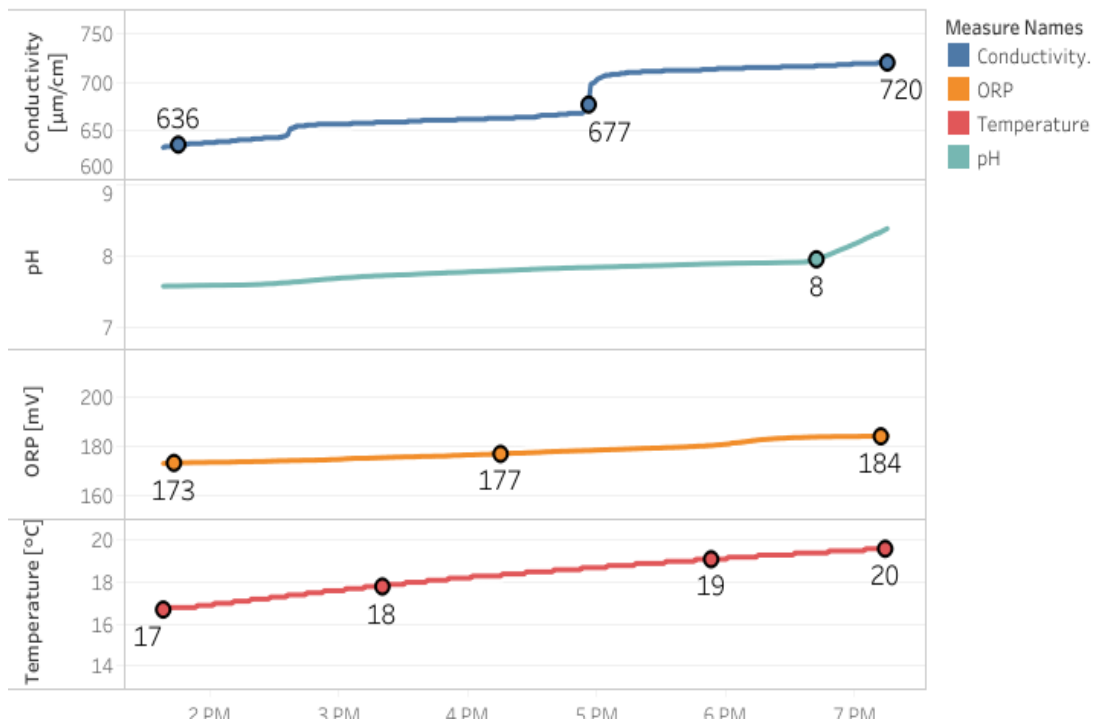


Figure 72. Water quality parameters throughout the filtration of salt sample (2%).

Sheet 1

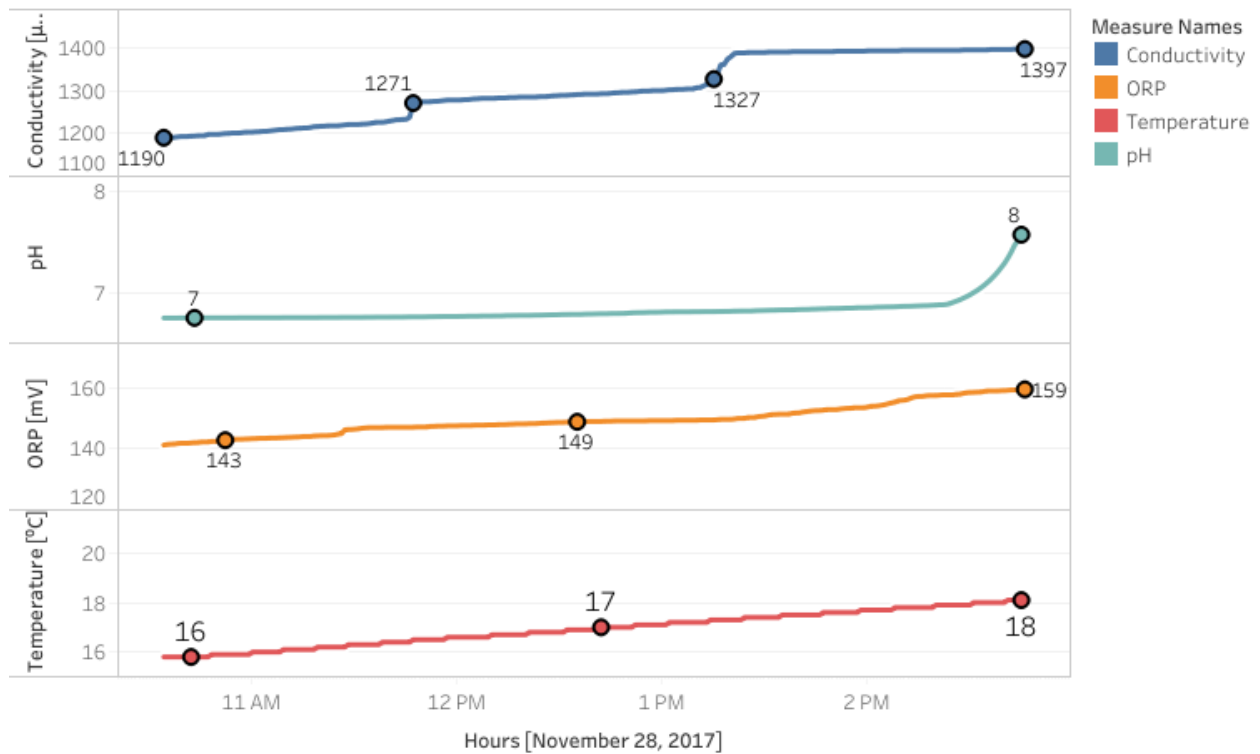


Figure 73. Water quality parameters throughout the filtration of salt sample (4%).

Table 40. Pollutant removal rate of the old and new membrane.

Old membrane		Atrazine		Diuron		Copper	
		Try 1	Try 2	Try 1	Try 2	Try 1	Try 2
RO+SS	tank	11,1	8,62	8,58	9,44	91,7	92,4
	10 min permeate	0,67	0,18	0,16	0,34	1,9	1,1
	5 hours permeate	1,36	0,73	0,71	0,71	<1.0	<1.0
	5 hours retentate	24,5	9,81	45,7	9,42	16	30,6
Tap water +	tank	8,56	8,67	8,4	8,49	97,7	96,8

Appendix

SS							
	10 min permeate	0,18	0,27	0,2	0,41	10	3,6
	5 hours permeate	0,3	0,11	0,63	0,61	<1	<1
	5 hours retentate	10,2	9,85	9,31	9,12	100	96,8
New membrane							
RO+SS	tank	8,71	8,59	8,4	8,38	91,6	97,4
	10 minute retentate	9,99	10,4	9,67	9,86	53,7	91,5
	5 hours retentate	9,84	10,9	8,88	9,67	69,5	97,3
	5 hours permeate	0,16	0,14	0,83	0,92	<1	<1
Tap water + SS	tank	8,55	8,41	8,19	7,78	91,5	97,3
	10 minute retentate	9,6	10,6	9,18	9,51	121	117
	5 hours retentate	9,9	11	8,7	9,53	112	115
	5 hours permeate	0,1	0,16	0,67	1,04	1,2	2,1

Old membrane		Nitrate		Simazine		Zink	
		Try 1	Try 2	Try 1	Try 2	Try 1	Try 2
RO+SS	tank	50	50	9,9	8,44	418	431
	10 min permeate	2,3	2,5	1,11	1,15	12	16,8
	5 hours permeate	2,7	2,2	1,22	0,97	5,8	8,2
	5 hours	74	59	43,5	9,67	483	521

	retentate						
Tap water + SS	tank	55	57	8,74	7,9	959	980
	10 min permeate	7,6	6	2,47	4,49	61,9	42,2
	5 hours permeate	5,6	5,5	0,67	0,65	14,9	15,6
	5 hours retentate	68	65	10,1	11	1040	1090
New membrane							
RO+SS	tank	52	52	8,82	8,03	443	439
	10 minute retentate	63	63	8,18	9,45	554	542
	5 hours retentate	64	67	9,57	10,7	610	585
	5 hours permeate	3	1,2	1,7	1,56	<3	<3
Tap water + SS	tank	54	58	8,41	8,34	627	854
	10 minute retentate	64	68	8,81	10,1	749	1050
	5 hours retentate	65	72	9,73	11,6	729	1050
	5 hours permeate	7,4	6,4	1,04	0,97	7,6	23,1

Table 41. The biocide experiment.

Live cells	Permeate	Retentate	RO
	Cell number 50 µl	Cell number 50 µl	Cell number 50 µl
New membrane	38	2524	12684
	32	2688	12647
	45	2599	12563

	148	8201	23106
	144	8281	23331
	142	8367	24069
Old membrane	353	4565	3588
	368	4520	3420
	427	4611	3427
	913	9810	7043
	884	9996	6779
	844	10023	7122
All cells	Permeate	Retentate	RO
	Cell number in ml	Cell number in ml	Cell number in ml
New membrane	2880	165620	466620
Old membrane	17680	199920	140860

Table 42. Removal rate of live cells per 50 µl sample in percentage.

	Removal rate [%].
New membrane.	99,7
	99,7
	99,6
	99,4
	99,4
	99,4
Old membrane.	90,2
	89,2
	87,5
	87,0
	87,0
	88,1

Arduino code for the pressure and flow sensor.

```
Code for the Arduino board
bytestatusLed = 13;
bytesensorInterruptkonz = 0;// 0 = digital pin 2
bytesensorInterruptper = 1;
```

```

bytesensorInterruptrezi = 2;
bytesensorPinkonz = 5;
bytesensorPinper = 3;
bytesensorPinrezi = 7;
bytehp1pin = 8;
// The hall-effect flow sensor outputs approximately 113 pulses per second per
// litre/minuteofflow.
floatcalibration Factor = 103;
volatile bytepulseCountkonz;
volatilebytepulseCountperpart
volatile bytepulseCountrezi;
floatflowRatekonz;
unsignedintflowMilliLitreskonz;
unsignedlongtotalMilliLitreskonz;
floatflowRateper;
unsignedintflowMilliLitresper;
unsignedlongtotalMilliLitresper;
floatflowRaterezi;
unsignedintflowMilliLitresrezi;
unsignedlongtotalMilliLitresrezi;
unsignedlongoldTime;
int ADC5=5;
int pbm2,pbm1; //pressurebeforemembrane
int ADC4=4;
int pam2,pam1; //pressure after membrane
intpbm;
intpam;// for analog valuesofpressuresensors
byte hp1;
voidsetup()
{
  // Initialize a serialconnectionforreportingvaluestothe host
  Serial.begin(38400);
  // Set upthestatus LED lineas an output
  pinMode(statusLed, OUTPUT);
  digitalWrite(statusLed, HIGH); // Wehave an active-low LED attached
  pinMode(sensorPinkonz, INPUT);
  digitalWrite(sensorPinkonz, HIGH);
  pinMode(sensorPinper, INPUT);
  digitalWrite(sensorPinper, HIGH);
  pinMode(sensorPinrezi, INPUT);
  digitalWrite(sensorPinrezi, HIGH);
  pinMode(hp1pin, OUTPUT);
  digitalWrite(hp1pin, LOW);
  pulseCountkonz = 0;
  flowRatekonz = 0.0;
  flowMilliLitreskonz = 0;
  totalMilliLitreskonz = 0;
  pulseCountper = 0;

```

```

flowRateper      = 0.0;
flowMilliLitresper = 0;
totalMilliLitresper = 0;
pulseCountrezi   = 0;
flowRaterezi     = 0.0;
flowMilliLitresrezi = 0;
totalMilliLitresrezi = 0;
oldTime          = 0;
  pam1=0;
  pam2=0;
pam=0.0;
  pbm1=0;
  pbm2=0;
pbm=0.0;
  hp1=0;
  // The Hall-effectsensorisconnectedtopin 3 whichusesinterrupt 0.
  // Configuredtotrigger on a FALLING statechange (transitionfrom HIGH
  // stateto LOW state)
attachInterrupt(sensorInterruptkonz, pulseCounterkonz, FALLING);
attachInterrupt(sensorInterruptper, pulseCounterper, FALLING);
attachInterrupt(sensorInterruptrezi, pulseCounterrezi, FALLING);
}
/**
 * Main programloop
 */
voidloop()
{
if((millis() - oldTime) >1000) // Onlyprocesscountersonce per 10 second
{
  // Disabletheinterruptwhilecalculatingflow rate andsendingthevalueto
  // the host
detachInterrupt(sensorInterruptkonz);
detachInterrupt(sensorInterruptper);
detachInterrupt(sensorInterruptrezi);
  // Becausethisloopmay not complete in exactly 10 secondintervalswecalculate
  // thenumberofmillisecondsthathavepassedsince the last executionanduse
  // thattoscaletheoutput. We also applythecalibrationFactortoscaletheoutput
  // based on thenumberofpulses per second per unitsofmeasure (litres/minute in
  // thiscase) comingfromthesensor.
flowRatekonz = ((1000.0 / (millis() - oldTime)) * pulseCountkonz) / calibrationFactor;
flowRateper = ((1000.0 / (millis() - oldTime)) * pulseCountper) / calibrationFactor;
flowRaterezi = ((1000.0 / (millis() - oldTime)) * pulseCountrezi) / calibrationFactor;
  //Read of analog valuesof 0-5V of pressuresensore at port ADC4 and ADC5
  pbm1=analogRead(ADC4);
  pam1=analogRead(ADC5);
  //pbm2=map(pbm1,0,1023,0,160);
  //pam2=map(pam1,0,1023,0,160);
  pbm=pbm1*15,640; //converts analog Volt values 0-5V topressurevalue 0-16bar to mbar

```

```

pam=pam1*15,640;
// Note the time this processing pass was executed. Note that because we've
// disabled interrupts the millis() function won't actually be incrementing right
// at this point, but it will still return the value it was set to just before
// interrupts went away.
oldTime = millis();
// Divide the flow rate in litres/minute by 60 to determine how many litres have
// passed through the sensor in this 1 second interval, then multiply by 1000 to
// convert to millilitres.
flowMilliLitreskonz = (flowRatekonz ) * 1000;
flowMilliLitresper = (flowRateper ) * 1000;
flowMilliLitresrezi = (flowRaterezi ) * 1000;
// Add the millilitres passed in this second to the cumulative total
totalMilliLitreskonz += (flowMilliLitreskonz / 60);
totalMilliLitresper += (flowMilliLitresper / 60);
totalMilliLitresrezi += (flowMilliLitresrezi / 60);
unsigned int frac;
// Print the number of litres flowed in this second
//Serial.print(""); // Output separator
Serial.print(flowMilliLitreskonz);
//Serial.print(";mL/min");
Serial.print(""); // Output separator
Serial.print(flowMilliLitresper);
//Serial.print(";mL/min;");
Serial.print(""); // Output separator
Serial.print(flowMilliLitresrezi);
//Serial.print(";mL/min;")
Serial.print("");
// Print the cumulative total of litres flowed since starting
Serial.print(""); // Output separator
Serial.print(totalMilliLitreskonz);
//Serial.print(";mL;");
Serial.print(""); // Output separator
Serial.print(totalMilliLitresper);
Serial.print("");
Serial.print(totalMilliLitresrezi);
Serial.print("");
//Serial.print("Relativdruck_");
//Serial.print("pbm=");
//Serial.print(pbm);
//Serial.print(";mbar;");
//Serial.print("pam=");
// Serial.print("");
//Serial.print(pam);
//Serial.println("");
// Reset the pulse counter so we can start incrementing again
pulseCountkonz = 0;
pulseCountper = 0;

```

```

pulseCountrezi = 0;
  // Enabletheinterruptagainnowthatwe'vefinishedsendingoutput
attachInterrupt(sensorInterruptkonz, pulseCounterkonz, FALLING);
attachInterrupt(sensorInterruptper, pulseCounterper, FALLING);
attachInterrupt(sensorInterruptrezi, pulseCounterrezi, FALLING);
  }
if(pam>8000)
  {
digitalWrite(hp1pin, HIGH);
oldTime=4000000000;
  }
}
/*
Insterrupt Service Routine
*/
voidpulseCounterkonz()
{
  //Incrementthe           pulse           counter
pulseCountkonz++;

}
voidpulseCounterper()
{
  // Incrementthe pulse counter
pulseCountper++;
}
voidpulseCounterrezi()
{
  // Incrementthe pulse counter
pulseCountrezi++;
}

```

Code for Rstudio for the illustration of mfi with different filter.

```

MFI
MFI$Dillution.factor <- as.factor(MFI$Dillution.factor)
melt(MFI)
MFI <- reshape2 :: melt(MFI, id.vars ="Dillution.factor")
MFI$value <- as.numeric(MFI$value)
ggboxplot(MFI, x = "Dillution.factor", y = "value", fill = "variable")
p <- ggpaired(MFI, x = "Dillution.factor", y = "value",
              color = "variable", palette = "jco",
              add = "jitter") + facet_grid(variable~.) + stat_compare_means(method =
"anova")
c <- p + xlab("Concentration factor") + ylab("MFI")

```

Curriculum Vitae

Private Information:

Kriemhildpl. 8, Wien, 1150, Austria
+436606322622 ernomundari@gmail.com

DATE / PLACE OF BIRTH

1993-06-01

Mongolia

NATIONALITY

Mongolian

Employment History

Former head of International Relations Department,

Humanitarian activities for welfare of the society

[February 2012 – September 2015](#)

Private Assistant for the head of the Microbiology department of National University of Mongolia

[September 2012 – May 2015](#)

Education

Bachelor of Science, Microbiology, National University of Mongolia, Ulaanbaatar

[September 2011 – June 2015](#)

Masters in Science, University of Life Science and Natural Resources, Vienna

[October 2015 – Present](#)

Specialised in Natural Resource Management and Ecological Engineering (Master thesis topic covering the drinking water treatment by means of membrane systems)

International joint degree

Masters in Science, Czech University of Life Science, Prague

[October 2016 – January 2017](#)

Specialised in Natural Resource Management and Ecological Engineering (Exchange semester, as the study is international double degree)

Extra-curricular activities

United Nations Youth and Student Association of Austria - Academic Forum for Foreign Affairs (UNYSA-AUSTRIA-AFA), at United Nations, Vienna

[March 2016 – Present](#)

Business Negotiation Club

UNESCO, World Heritage Center, Wild Life Management Mongolia at UNESCO, Ulaanbaatar

[December 2017](#)

Voluntary contribution, Translation of Interviews



Affirmation

I certify, that the master thesis was written by me, not using sources and tools other than quoted and without use of any other illegitimate support.

Furthermore, I confirm that I have not submitted this master thesis either nationally or internationally in any form.

Place, date, name surname

signature